Enhanced Distributed Space Systems with Miniature Spacecraft
Spatial Distribution, Collision Analysis and Cooperative Communication

Sandaramoorthy, Prem

DOI
10.4233/uuid:517fdbaf-0102-4f22-88bc-9883e66b7dca

Publication date
2018

Document Version
Final published version

Important note
To cite this publication, please use the final published version (if applicable).
Please check the document version above.

Enhanced Distributed Space Systems with Miniature Spacecraft

Spatial Distribution, Collision Analysis and Cooperative Communication

Prem Prasad SUNDARAMOORTHY

Enhanced Distributed Space Systems
with Miniature Spacecraft

Spatial Distribution, Collision Analysis and Cooperative Communication

Dissertation

for the purpose of obtaining the degree of doctor at

Delft University of Technology,

by the authority of the Rector Magnificus, prof.dr.ir. T.H.J.J. van der Hagen,

Chair of the Board for Doctorates, to be defended publicly on

Friday, 14 December 2018 at 15:00 o'clock

by

Prem Prasad SUNDARAMOORTHY

Master of Science in Aerospace Engineering,

Delft University of Technology, The Netherlands

born in Chennai, India

This dissertation has been approved by the
promotor: Prof.dr. E.K.A. Gill
copromotor: Dr.ir. C.J.M. Verhoeven

Composition of the doctoral committee:
Rector Magnificus   chairperson
Prof. dr. E. K. A. Gill   Delft University of Technology, promotor
Dr.ir. C.J.M. Verhoeven   Delft University of Technology, copromotor

Independent members:
Prof. dr.ir. M. Bentum   Eindhoven University of Technology
Prof. ir. P. Hoogeboom   Delft University of Technology
Prof. dr. K. Schilling   University of Wuerzburg
Prof. dr.ir. P. Visser   Delft University of Technology
Prof. dr. T. Vladimirova   University of Leicester

An electronic version of this dissertation is available at http://repository.tudelft.nl/.

பெரியோரை வியத்தலும் இலமே,
சிறியோரை இகழ்தல் அதனினும் இலமே.

translated from Tamil as

Neither be in awe of the Big,
nor belittle the Small.
— Kaniyan Pungundranar, *Purananuru* — 192

To Delft and the memories thereof.

Contents

Acknowledgments

First and foremost, thanks to my parents for their love, support and understanding. The first credit for all positive things in me goes to them. I would also like to thank my brother, my sister-in-law and my nephews for all the love.

I thank my promotor Prof. Eberhard Gill for the opportunity to pursue a PhD at the Space Systems Engineering Group. Prof. Gill's support and guidance through regular meetings and reviews is highly appreciated. I extend my gratitude to my co-promotor Dr. Chris Verhoeven for his support and motivation and for toggling between the roles of a friend, philosopher and guide. I would like to acknowledge the committee members for their time and their reviews. This is a great opportunity to thank Marion de Vlieger for making things smooth and easy during the time I was a PhD candidate.

I would very sincerely like to thank the late Prof. Gunnar Stette for being one of the first reviewers of my work on phase synchronization, which is an integral part of this thesis. Prof. Stette readily accepted my request to review my work with the following message "*Since I send you this message before opening the attached document I can state, without offending you, that I will do the reading with a critical mind, believing that this would be my most useful contribution.*" He also added that the Hungarian Nobel laureate, von Békésy, stated in the foreword of his famous book on hearing, that it is useful to have friends to review papers, but it is even more useful to have enemies, since they will devote much time and effort to find weaknesses. Prof. Stette's critical remarks and encouraging feedback continues to reinforce my conviction and enthusiasm in the topic.

Thank you, Piotr Perczynski and Christina Aas, for accepting and allowing me to share the Room when I started my PhD. They proved to be the best company to begin anything. With the variety of conversations – technical, political, spiritual and everything in between, the transition from acquaintances to amazing friends did not take long. Thank you for all the great times and the ones to follow. I would also like to thank Nicoletta, Mathias, Federica and Stef for all the fun times. I must thank Pooja Mahapatra for the nice coffee chats and making me look forward to the LR coffee.

There were several people when I started my PhD who made life easier for me by sharing their experiences. I would very much like to acknowledge the support of my fellow PhDs – Daan, Steven and Rouzbeh. Special thanks to Arash Noroozi, who has been a co-PhD, co-TA, co-director, co-founder and a constant friend. To the ever optimistic and cheerful Rui Sun, my dear friend I thank you for all the support and kindness.

During the time I was a PhD candidate and subsequent to that, I have been surrounded by intelligent, interesting and friendly colleagues. They have made my stay at the Faculty of Aerospace Engineering

a memorable one. Thank you, Debby, Marielle, Hans, Jasper, Jian and Robert. Special thanks to my colleague, roommate and friend Angelo, for putting up with me and my chaotic desk for close to 6 years. Thank you, Angelo, for all the inspiration, support and the dropjes. The interactions with my colleagues from the 9th floor – Bart, Dominic, Joao, Wouter, Erwin, Pieter, Bert, Relly, Marc, Jose, Daphne, Jeanette, Eelco and Ejo, will be remembered fondly and I thank them for all the interesting discussions. To the relatively new colleagues who have very quickly extended me their friendship – Stephanie, Alessandra, Stefano, Samiksha, Sevket, Silvana and Vidhya, I thank you for all the good times.

This is a great opportunity to also thank two very special people, Ron and Barry. They have always made me feel very welcome at the department and have continuously inspired and motivated me. Thank you and it has been a pleasure and a privilege to work with you.

I would like to thank all the students I have interacted with in the past years. I have learnt a lot from them. Special thanks to these students who did their MSC. thesis with me – Chetan Angadi, Diederik Florijn, Daniel Djordjevski and Heiko Engwerda.

In the last years, when I have sometimes been overwhelmed by the drudgery of writing the dissertation, several colleagues have helped restore my hope and sanity. Crucial amongst them have been fellow PhDs – Johan, Adoflo, Dennis, Kartik, Svenja, Linyu, Jing, Minghe, Mario, Zixuan, Mao, Tatiana, Nikos and Megan. A very special thanks to Fiona and Kirsty, Marsil and Carina, Dadui, Fernanda and Zoe, for the wonderful times. Lord Limitless would also like to show his appreciation and gratitude to Doctor Brilliant, for his humour and his poses, Sergeant Longbeard, for the beer and politically correct statements, and Prof. Heartbreaker, for skipping the acquaintance part before becoming a friend. The other set of crucial people who ensured that I stayed sane and happy are the folks at Locus – Jim, Thijs, Nikos and Tjeerd. Thank you.

There were already many reasons to thank Kevin, his morale raising wit, adrenalin boosting coffee, or just lively company, but then he also translated, a not very concise summary of this work into Dutch. Thank you, Kevin, and looking forward to more good times.

I raise a glass to my friends who made sure my evenings and weekends were packed with fun and entertainment. Gunjan, Shreyas, Laia, Sidd, Niky, Bob, Mariam and Joe – HappYness IS everything! I also eagerly look forward to the friendship of Dhruv, Kira, Thomas,. Thanks to my Columbian friends, Andrea and Flavia for the many funny and memorable moments we have shared. Many thanks to my Italian friends – Alessandro, Angelo, Peppe , Gianni and almost Italian Frederique for their friendship and persistence in inviting me to their parties, despite my very poor turn-up ratio. The Leviosers – Olga, Jetze, Ysbrand, Sabine, Martijn, Emily, Steven and Etienne, thank you for the awesome and fun-filled Christmas parties, Eurovision, Sinterklaas dinners and much more.

For the always high-spirited, fun-filled times, I thank Rajeev, Fabian, Jason, Joanna, Alina and Paul. Thanks to Shiva and Venkat, especially for the coffee discussions at EWI. Thanks to Ranjita, for her

company and deep conversations, and Hari for the fun times. Thanks to the AVS gang, with whom I have had many a great time – Raghu, Suresh, Muru, Maruti, Saravanan, Arvind, Priti, Arpita, Sampath, Naveen, Rajitha, Ranadeep and Kanag. And frankly, how do you really thank a problem like Maria?

I also owe my friends who have continuously supported me despite living thousands of miles away. Thanks to my dear friend Sneha, whose circle is a straight line, for always being there for me and introducing me as a rocket scientist whenever she got the chance. Thank you, Nrutya, for all the confidence and being a great friend and please continue to visit me more often. My friends, Selvan and Rikhab, who always consider me a better friend than I deserve to be and never give up on me, I thank them for their overestimation and will try to live up to it someday. I thank the Baldwinian boys, Tarun and Manish for making my trips to Bangalore more exciting.

I should admit and acknowledge that this thesis would not have been completed in this time if not for my dear wife Sruti. She made sure I had no other concerns than the PhD, but also made me realize there were more things to life. She had to put up with some eccentric behaviour, scrambled priorities and dark humour. I thank her for all the love and support and for reviewing and refining this acknowledgement. Thanks, also to my mother-in-law for the support and kindness. A special thanks to Thathi, Sai, Shanthi, Sabita Mam, Sarang and my favourite niece Sahana for all the love. On a sad note, during this period, I lost my grandfather V.C. Sekaran. He was a great source of inspiration and support. I will continue to miss him.

As I near the end of this acknowledgment, I very humbly realize that it was presumptuous to think that I would know and could recollect all the support I have received in the process of getting here. I thank everyone who has supported me during this work and who have contributed to improving the quality of this work.

Prem Sundaramoorthy
Delft, December 2018

SUMMARY

The repertoire of words in the English language to refer to groups of animals is quite fascinating to say the least – a congregation of alligators, an army of ants, a troop of baboons, a pride of lions, a train of camels, a destruction of cats, an intrusion of cockroaches, a mob of emus, a plague of insects, a drift of pigs, and so on. The intention of using such a wide range of terms is to associate an underlying emotion or meaning to the different kinds of groups. Therefore, without knowing much about choughs or goldfinches, one is more likely to appreciate a charm of goldfinches rather than a clattering of choughs. This thesis is about groups of small spacecraft – characterizing them and enhancing them. The aim of this thesis is to enable charms of CubeSats and prides of PocketQubes.

The context of this thesis is based on two aspects of scaling – scaling down in size and scaling up in number. This gives rise to a system with multiple entities, with each individual entity characterized by a small size and thus limited capability. In this thesis we address a distributed system in space with multiple small spacecraft. Small, of course, is a relative term, and the definition of small changes with time. The capability of a system, for a fixed mass and volume, tends to continuously increase with advances in technology. With advances in semi-conductor technology, described by the ubiquitous Moore's law, electronic systems have been getting smaller and smarter. This coupled with Commercial-Off-The-Shelf (COTS) technology in space, has translated this benefit to the space industry. Experience, heritage and standardization have also improved packing efficiency in a spacecraft. Therefore, today, at a fraction of the cost and effort, CubeSats can be built that can pretty much 'technically' do what Sputnik did.

This paradigm shift towards a fast and low-cost approach in building small spacecraft has also enabled the entry of private players into the space market as now the entry barrier, with respect to initial investment and resources, has been lowered. All these have led to a vibrant small satellite landscape – leading to many exciting and innovative applications with small satellites. Small spacecraft by themselves are already becoming popular and are slowly finding a niche for certain application such as technology demonstration missions . However, for more exciting missions, we need many of them working together. Once spacecraft are low-mass and low-cost, a system with many of them can be envisioned. There has been a recent deployment of more than 100 spacecraft from a single launch showing that the launcher industry is also getting prepared for massive distributed systems in space. There are many space applications that need and benefit from aspects such as simultaneous multipoint sensing and high revisit times that can only be provided through a Distributed Space System (DSS). This is the calling for DSS, and what enables it, is affordable realization and access of multiple entities to space.

Now, when we concern ourselves with systems and groups with many simplistic entities, and add to this quirky space dynamics, then the problem gets even more interesting. A standard terminology that serves as an umbrella to cover all configurations involving multiple spacecraft in space is the Distributed Space System. It can, however, take on different avatars such as constellations, fractionated systems, swarms and more. There is a multitude of challenges when you want to realize a system in space and more so when this system comprises multiple entities. Characterising dynamics and realizing cooperation are two key elements that can enable and enhance DSS. To this end, in this thesis, these two distinct aspects are investigated – dynamics, where the spatial evolution of the system and collision probability between elements of the system is addressed, and cooperation between elements to enhance the system.

This thesis addresses questions that arise with respect to the characteristics and dynamics of distributed system in space. How fast is the system spreading? How are the elements within the system distributed? Is it tightly or loosely packed? What is the effect of perturbations on its absolute and relative dynamics? What are the chances of a collision within the system? In this thesis, quantitative metrics are established that nable characterizing DSS and answering the above questions.

Two distinct metrics to characterize a DSS have been developed and discussed: a cluster distribution index (CDI) and a measure for collision probability using the line-integral method (CALM). The metrics can be used either as an optimization variable in the mission design process for a DSS or as a control variable during operations.The distribution index can be used to assess the effectiveness of DSS in meeting system requirements such as coverage and resolution. An n-dimensional grid-based method has been developed to evaluate the CDI. The applicability of CDI for a cluster of spacecraft under the influence of differential drag has been analyzed. It has been shown that the CDI can be effective in capturing the influence of perturbations on spatial distribution of DSS.

The collision probability within a network is an important measure for DSS, especially when the number of spacecraft is large. The collision analysis using line-integral method (CALM) is proposed as a computationally efficient approach for collision analysis. The validity of the method is assessed by comparing results with existing non-linear methods which demonstrated an approximation better than one percent at a much lower computational load. The method for collision analysis has been developed in particular for DSS comprising of small spacecraft that are intended to be launched from a single deployment mechanism. The CALM approach is three orders of magnitude faster than existing approaches that evaluate collision probability for non-linear motion.

To pursue the aspect of cooperation, methods to enhance the communication capability of the distributed system were explored. Different communication scenarios were investigated that can enhance the communication link between the distributed system and ground. Key and almost prohibitive challenges were estimating the position of the spacecraft with required levels of accuracy and having high accuracy clocks on such resource-limited platforms. A novel phase synchronization

approach has been developed which uses an external beacon to enable beam forming with much reduced clock constraints on localization accuracy. This will allow resource-limited platforms to cooperatively enhance their communication capability. Results show sub-centimeter level phase synchronization with a localization accuracy in the order of meters.

In conclusion, a distributed network of miniature systems will ideally combine the advantages of miniaturization and distributed systems to realize an efficient and effective system. There, however exists, significant gaps and hurdles in achieving this vision. The aim of this thesis is to identify and bridge these gaps. The findings in this thesis should eventually pave the way towards building a pride of ants in space.

Samenvatting

Het scala aan verzamelwoorden in de Nederlandse taal voor het aanduiden van groepen van dieren is op zijn minst fascinerend - een leger mieren, een troep bavianen, een groep leeuwen, een roedel wolven, een meute jachthonden, een kolonie kakkerlakken, een vlucht spreeuwen, een zwerm insecten, een kudde koeien, een span paarden en zo voort. De bedoeling van het gebruiken van een zoveel verschillende termen is om een onderliggende emotie of betekenis met deze verschillende soorten groepen te associëren. Zonder dus al te veel te weten over paarden of honden is men toch meer geneigd om een span paarden als georganiseerder te zien dan een zwerm vliegen. Dit proefschrift is gericht op groepen van kleine satellieten - met name het karakteriseren en optimaliseren daarvan.

De context van dit proefschrift berust op twee aspecten van het schalen - omlaag schalen in grootte en opschalen in aantal. Hieruit ontstaat een systeem van meerdere objecten, waarbij elk object gekenmerkt wordt door een kleine afmeting en daarmee beperkte capaciteiten. In dit proefschrift behandelen we een systeem met meerdere kleine satellieten verspreid in de ruimte. "Klein" is natuurlijk een relatief begrip en de definitie van "klein" verandert voortdurend. De prestaties van een systeem, bij een gelijk gehouden massa en volume, groeit in het algemeen continu met vooruitgang in technologie. Met de vorderingen in semi-conductor technologie, zoals voorspeld door de bekende wet van Moore, zijn elektronische systemen steeds kleiner en slimmer geworden. Door het toenemende gebruik van Commercial-Off-The-Shelf (COTS) technologie in de ruimte bereikt deze vooruitgang nu ook de ruimtevaartindustrie. Met ervaring, verworven uit de praktijk, en standaardisatie is de productie van kleine satellieten efficiënter geworden. Vandaag kunnen CubeSats vervaardigd worden die voor maar een fractie van de kosten en inspanning, de 'technische' prestaties van Sputnik eenvoudig kunnen evenaren.

Deze aardverschuiving naar een snelle, goedkope manier om kleine satellieten te produceren heeft er ook voor gezorgd dat private bedrijven het speelveld kunnen betreden in de ruimtevaartsector omdat de barrières tot toetreden, zoals hoge startinvesteringen en complexe productiemethoden, afnemen. Al deze factoren hebben een bruisende markt voor kleine satellieten gecreëerd - waardoor ook interessante en innovatieve toepassingen met kleine satellieten zijn ontstaan. Kleine satellieten zijn op zichzelf al populair aan het worden en er is een eigen niche voor bepaalde toepassingen aan het ontstaan zoals missies gericht op de technologie demonstraties. Nóg interessantere missies kunnen gerealiseerd worden met behulp van meerdere, samenwerkende kleine satellieten. Als deze satellieten eenmaal een lage massa en laag kostenplaatje hebben, dan kunnen we aan een systeem denken van zeer grote aantallen satellieten. Recentelijk zijn bijvoorbeeld meer dan 100 satellieten de ruimte in gebracht via één enkele raketlancering. Dit toont aan dat de lanceerindustrie zich ook voorbereidt op het lanceren van massale, gedistribueerde satellietsystemen. Veel

ruimtetoepassingen zullen profijt hebben van, of worden uitsluitend mogelijk gemaakt door, een Distributed Space System (DSS), zoals gelijktijdig, multipoint sensing en hoge temporale frequentie. Dit is de oproep voor DSS, en betaalbare realisatie alsook toegang tot de ruimte via verschillende partijen maakt het mogelijk.

Als we nu systemen en verzamelingen van meerdere, eenvoudige ruimteobjecten beschouwen, en de eigenaardigheden van ruimtedynamica meenemen, dan wordt het probleem des te intrigerender. Een standaard naamgeving, die de lading dekt voor alle configuraties van meerdere satellieten, is de Distributed Space System. Het gaat wel schuil onder meerdere avatars, zoals constellaties, fractionated systemen, zwermen, en zo zijn er nog meer. Er is een verscheidenheid aan uitdagingen om een systeem in de ruimte te realiseren, en deze worden alleen meer als het systeem meerdere objecten bevat. Het karakteriseren van de dynamica en het implementeren van samenwerking zijn twee belangrijke onderdelen voor het realiseren en verbeteren van DSS. Beide van deze aspecten worden in dit proefschrift onderzocht - dynamica, waar de ruimtelijke evolutie van het systeem en de kans op botsingen tussen de objecten van het systeem wordt behandeld, alsook de samenwerking tussen de objecten om het systeem te verbeteren.

Deze dissertatie behandelt vraagstukken met betrekking tot karakteristieken en dynamica van gespreide systemen in de ruimte, van DSS dus. Hoe snel spreid het systeem zich uit? Hoe zijn de objecten van het systeem verdeeld? Is het dicht of open verpakt? Wat is het effect van stoorkrachten op de absolute of relatieve dynamica? Wat zijn de kansen op botsingen binnen het systeem? In dit proefschrift worden kwantitatieve maatstaven vastgesteld voor het karakteriseren van een DSS en voor het beantwoorden van de bovenstaande vraagstukken.

Twee afzonderlijke maatstaven zijn ontwikkeld en besproken om een DSS te karakteriseren: een Cluster Distribution Index (CDI) en een maatstaf voor de kans op botsingen met gebruik van de lijnintegraal methode (CALM). Deze maatstaven kunnen als optimalisatievariabel in het missieontwerpproces van een DSS of als regelvariabel gedurende missieuitvoering dienen. De CDI kan gebruikt worden om te beoordelen in hoeverre een DSS aan de systeemvoorwaarden, zoals dekking en resolutie, voldoet. Een n-dimensionale, rooster-gebaseerde methode is ontwikkeld om de CDI te evalueren. De toepasbaarheid van de CDI op een cluster van satellieten onder de invloed van differentieelweerstand is geanalyseerd. Het is aangetoond dat de CDI effectief kan zijn in het identificeren van de invloed van stoorkrachten op de ruimtelijke verdeling van een DSS.

De kans op botsingen binnen een netwerk is een belangrijke maat voor DSS, in het bijzonder als het aantal objecten groot is. De botsingsanalyse met de lijnintegraalmethode (CALM) wordt voorgesteld als een efficiënte rekenmethode voor botsingsanalyse. De geldigheid van deze methode is beoordeeld door de resultaten met bestaande niet-lineaire methodes te vergelijken, en deze heeft aangetoond dat een schatting van beter dan een procent mogelijk is met een veel lagere rekenlast. De methode voor botsingsanalyse is in het bijzonder ontwikkeld voor DSS van kleine satellieten die bestemd zijn voor lancering door middel van een enkele deployment mechanisme. De CALM

aanpak is drie ordes van grootte sneller dan bestaande methodes om de botsingskansen van niet-lineaire beweging te evalueren.

Om het aspect van samenwerking te bestuderen zijn methodes verkend om het communicatie-vermogen van het DSS te verbeteren. Verschillende communicatiescenario's zijn onderzocht om de communicatielink tussen DSS en grondstations te verbeteren. Het schatten van de positie van een ruimtevoertuig met de vereiste nauwkeurigheid en de aanwezigheid van hoog-nauwkeurige klokken op dergelijke platforms met beperkte vermogen vormden belangrijke, bijna onoverkomelijke, uitdagingen. Een nieuw fasesynchronisatie benadering is ontwikkeld die een externe baken gebruikt om beamforming mogelijke te maken met gereduceerde klokvoorwaarden op localisatienauwkeurigheid. Dit zorgt ervoor dat platforms met beperkte vermogen samen kunnen werken om hun gezamenlijke communicatievermogen te verhogen. Het resultaat is fasesynchronisatie onder het centimeter niveau met een localisatienauwkeurigheid van een orde van grootte van enkele meters.

In samenvatting, een gespreide netwerk van geminiaturiseerde systemen combineert idealiter de voordelen van miniaturisatie met die van gespreide systemen om een efficiënt en effectief systeem te realiseren. Wel zijn er nog significante leemtes en obstakels die uit de wereld geholpen moeten worden om deze visie waar te maken. Het doel van dit proefschrift is om deze leemtes te identificeren. De bevindingen in deze dissertatie zullen het uiteindelijk mogelijk moeten maken om verschillende ruimtetoepassingen te realiseren met een systeem van kleine satellieten.

Contents

Chapter 1
Introduction

Where there is righteousness in the heart, there is beauty in the character.
When there is beauty in the character, there is harmony in the home.
When there is harmony in the home, there is an order in the nation.
When there is order in the nation, there is peace in the world.

An anonymous Indian saying requoted by Dr. Abdul Kalam,
an Indian statesman, scientist and poet, while addressing the
European Union Parliament in 2007. A bottom-up approach to World Peace.

sgrìob /ˈskriː-ʌp/

noun the itchiness that overcomes the upper lip just before taking a sip of whisky.
Language: Gaelic

At the beginning of each chapter, a quotation and a definition of a word have been added as an epigraph. The reason for including a particular quote ranges from setting the context of the chapter, to admiration for the author of the quote, to humour in the saying. The words have been chosen from different languages, and the author has been impressed by the fact that there exists single words or short phrases to describe elaborate thoughts, actions and feelings in certain languages.

The aim of this thesis is to advance the research in the field of Distributed Space Systems (DSS) composed of miniature spacecraft in order to enhance and enable space applications with such systems. DSS composed of miniature spacecraft is seen as an enabler of next-generation innovative mission concepts that will enhance mission return of future space applications. This chapter introduces the context and scope of this study. On DSS, a brief history of space applications is provided followed by an introduction to conventional classification of different DSS configuration. On miniaturization, the impact of Moore's law, standardization and COTS adoption in space on the small satellite industry is discussed. Key challenges of realizing DSS with miniature spacecraft is explored and constitutes the motivation for the research questions that are subsequently discussed. A final section provides an outline of the rest of the chapters to acquaint the reader with the structure of this dissertation.

1.1 Background and Motivation

New and exciting application areas are envisaged with low cost miniature spacecraft that can be deployed as massively distributed systems in space. In particular femto-satellites with a mass of less than 0.1 kg could in the future be mass produced and hundreds to thousands of femto-satellites could be deployed as a swarm for example to enhance the monitoring capability of the Earth's environment [1,2,3].

1.1.1 Multiple spacecraft

The concept of using multiple miniature satellites was explored in the West Ford project in the late 1950s and the West Ford space experiment [4] in 1963 is credited with the first realization of a distributed system in space. Millions of copper needles were dispensed from a single launcher to build a cloud of resonant dipoles around the Earth to test a novel concept for global communication. The dipoles were intended to form a virtual ionosphere that could reflect radio waves enabling communication between two distant points on Earth. The individual "satellites" were 40 μg, and 20 kg of these copper dipoles were deployed into orbit making it the first massively distributed system in space, albeit a passive one.

Over the years, the application potential of DSS has been showcased through constellations such as GPS [5], GLONASS [6], Iridium [7] and the A-train [8] where a number of high performing spacecraft work together to enable applications in diverse areas such as navigation, communication and Earth observation. These are all, however, extremely high budget projects. The recent advent and growth of the small satellite industry has led to the exploration of space missions involving multiple low-cost spacecraft. Such missions aim to enable novel applications and enhance mission return at low project costs. The different configurations of DSS and related space missions will be further addressed in the next sections.

1.1.2 Miniaturization and COTS

In the mid 1960s, Gordon Moore, co-founder and chairman emeritus of Intel Corporation, (who was then the director of research and development (R&D) at Fairchild Semiconductor) made a prediction that set the pace for semi-conductor technology development. Moore extrapolated an emerging trend and postulated that computing capability would increase in power and decrease in relative cost, at an exponential rate. "The insight, known as Moore's Law, became the golden rule for the electronics industry, and a springboard for innovation. " As more transistors fit into a smaller area, the processing capability increased, with a simultaneous decrease in relative cost. The trend in transistor price and volume over the last decades is shown in Figure 1-1.
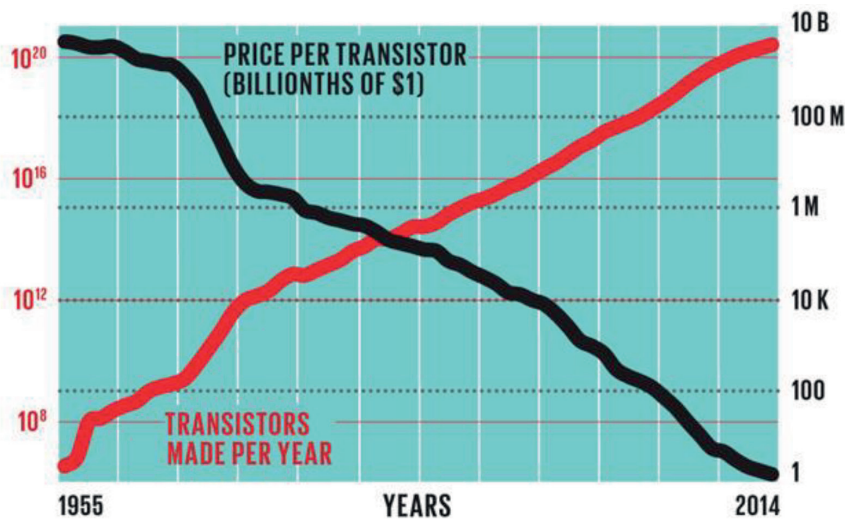
Figure 1-1 | Transistor price and volume over the years [9].

Through the adoption of COTS in spacecraft design and manufacturing, the benefits from the semi-conductor industry have also steadily seeped into the space industry [10,11,12]. By way of example, the TU Delft CubeSats Delfi-C3, launched in 2007, and Delfi-n3xt launched in 2013, incorporated components such as COTS resistors as thermal knives and COTS magnetometers for attitude determination, respectively [13].

1.2 Nanosatellites, CubeSats and Femto-satellites

Although nanosatellite class missions were experimented as early as in the late 1950s in programs such as Vanguard TV3 and OSCAR, it was only after the introduction of the CubeSat standard that nano and pico-satellite missions really took off [14]. An example of the different form factors these CubeSats can take is shown in Figure 1-2. Embracing relaxed requirements, leveraging Commercial-

Off-The-Shelf (COTS) technology and adopting the KISS (Keep it Simple and Stupid) design philosophy has led to a fast growing small satellite industry. CubeSat missions, promoted by the constraints of an academic environment, have demonstrated the successful use of COTS products in space. The first CubeSats were launched in 2003 and over the next ten years more than 100 of them were launched. In recent years a number of missions with multiple CubeSats have been proposed and flown.
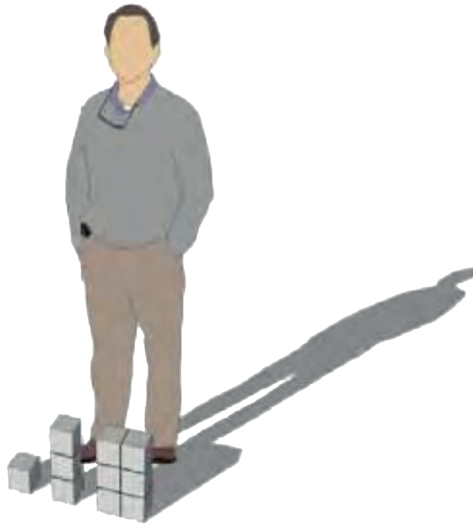
Figure 1-2 | CubeSats with form factors of 1U, 3U, and 6U, respectively. The volume of the 1U base unit is 100×100×100 mm [15]

Figure 1-3 | Announced launch years and actual nano-satellite launches between 1998 and 2022 [16]

Planet, a private start-up company , has built a flock of 28 CubeSats (FLOCK-1), spacecraft referred to as Doves, to image the Earth with an unprecedented resolution [17,18]. The QB50 mission initiated by the Von Karman Institute initially proposed around 50 CubeSats developed from institutes spread all over the globe for profiling the Earth's lower thermosphere [19]. The Dutch Orbiting Low Frequency Antennas for Radio Astronomy (OLFAR) project proposes a space mission around the moon to create a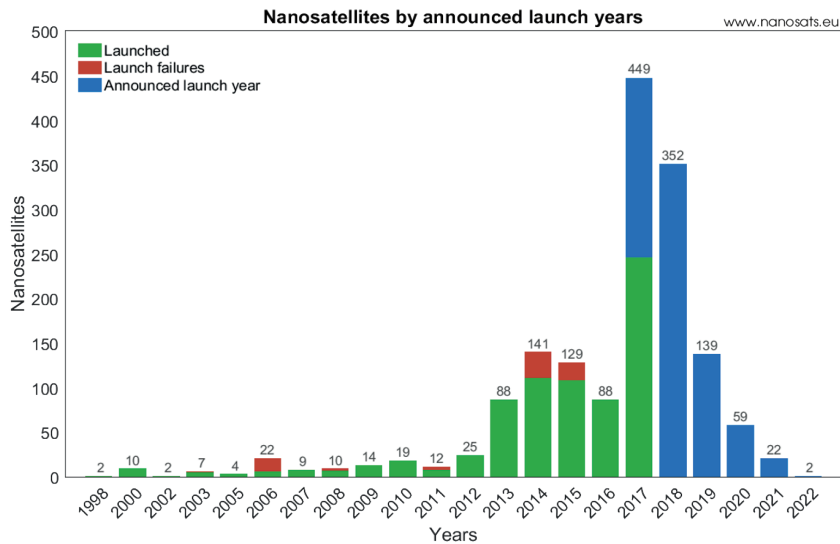 virtual radio telescope with distributed CubeSats. As seen in Figure 1-3, the year 2017 witnessed close to 250 nanosatellite launches. The PSLV-C37 put a record 103 of these nanosatellites into space in a single launch. Table 1-1 lists the nanosatellite and CubeSat launch statistics as of July 30, 2017 and Figure 1-4 provides a classification of these spacecraft on the basis of form factor.

Table 1-1 | Nanosats and CubeSats statistics as of July 30, 2017 [16]

Facts as of 2017 July 30
Nanosats launched in total: **829**
CubeSats launched in total: **764**
Nanosatellites in orbit: **535**
Nanosats destroyed on launch: **71**
Most nanosats on a rocket: **103**

Advances in miniaturization, standardization such as the CubeSat standard, reduction of cost and time schedules through adoption of COTS components and processes, and a mind-set change from risk avoidance to risk management have all contributed to a vibrant small satellite landscape.

Although most interest in small satellites has hovered around the micro-satellites (10 to 100 kg) through to the pico-satellites (100 g to 1 kg), there has been considerable interest in the sub 100 g range of satellites as well [20,21]. Femto-satellite is seen as the next class of extremely miniaturized satellites which will embrace disruptive spacecraft engineering, swarm science and mission design to realize new space missions. Consequently, there has been considerable research interest in the sub 100 g range of satellites and the advantage of using them in a distributed space network [22].

Femto-satellites have been proposed as a satellite inspector in projects such as the Co-orbiting Satellite Assistant (COSA) [23]. The N-Prize inspired WikiSat is a 20 g spacecraft. PCBSat [2] developed at Surrey and the crowd-funded KickSat project initiated at Cornell [24], where a number of 'Sprites' are deployed from a CubeSat, are other examples of proposed architectures and mission concepts for femto-satellites. Space missions employing very small spacecraft have been proposed for applications such as in-situ measurement and remote sensing based on system on chip architectures (Smart Dust [25], WiseNET [26]) , for technology demonstration (MiTEE – Miniature Tether Electrodynamics Experiment [27]) and much more.
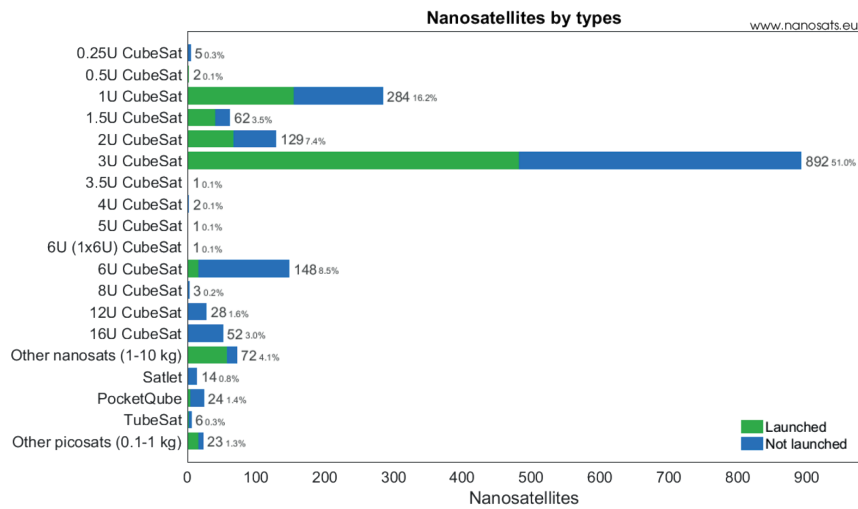
Figure 1-4 | Nano-satellites, listed in Table 1-1, classified by form factor [16]

1.3 Distributed Space Systems

A Distributed Space System (DSS) is defined as *an end-to-end system including two or more space vehicles and a cooperative infrastructure for science measurement, data acquisition, processing, analysis and distribution* [28].

The Stanford website [29] gives a working definition of DSS as "*Distributed Space Systems (DSS) consist of two or more satellites that interact to accomplish scientific, commercial or technological objectives that are otherwise very difficult if not impossible to achieve using a traditional monolithic spacecraft*".

Under the DSS umbrella, there are a number of multi-satellite architectures like formation flying satellites, constellations, fractionated spacecraft, and satellite swarms that can be realised in space. Each of these architectures can be considered as subsets of distributed systems in space and are characterized by certain unique features [3]. In this section we define these configurations and highlight their features. The term 'cluster' is used to refer to a group of satellites without reference to any particular topology or realisation of the distributed system. The aim is not to provide rigid definitions, but rather to provide prevailing perceptions of these architectures.

1.3.1 Constellation

A constellation is a set of satellites distributed over space intended to work together to achieve common objectives [30]. A constellation is a set of satellites that aim for a coordinated ground coverage with the help of a common ground control that tries to optimise the coverage of the entire constellation so that the individual satellites complement each other. There exist no explicit rules or conditions of interdependency between the satellites. Examples include the GPS, GLONASS, and IRIDIUM satellite constellations.

1

Figure 1-5 | Illustration of ESA's 30 satellite Galileo constellation (Photo: ESA)

The proposed Galileo constellation for satellite enabled navigation is shown in Figure 1-5. Planners and engineers at ESA have proposed this 30 satellite configuration that ensures a very high probability (> 90%) that users around the world will have visibility of at least four satellites to determine their position from the ranging signal transmitted by these satellites. The orbital arrangement also ensures good coverage of polar regions, which are poorly served by the GPS system [31].

1.3.2 Formation Flying

An engineering definition of formation flying is *the tracking or maintenance of a desired relative separation, orientation or position between or among spacecraft* [30]. Another definition, from the control perspective, defines formation flying *as a set of more than one spacecraft whose states are coupled through a common control law* [32]. This coupling can be in translational and/or rotational degrees of freedom and in position and/or velocity.

Depending on the application, the engineering requirements for formation flying can vary substantially. Missions such as EO-1 Landsat -7, Magnetospheric Multi-Scale (MMS) mission, Solar Imaging Radio Array (SIRA) represent a loose and less collaborative form of formation flying. The formation flying for EO-1 Landsat-7 was implemented through the ground, the MMS mission required only control of the geometry between the spacecraft, and SIRA required a loose control window for the spacecraft. These missions are classified as loose formations as there is much flexibility in controlling the inter-satellite distances and the control frequency is minimal. However, they are still formation flying as the relative positions need to be controlled. Readers are referred to the work of Leitner for a more elaborate exposition on the future of remote sensing in space with formation flying missions [33].

A class of the formation flying missions that push current technological capabilities are the proposed distributed interferometry missions such as the Laser Interferometry Space Antenna (LISA) [34], the

DARWIN mission [35], and the Terrestrial Planet Finder (TPF) [36]. These missions demand precise and continuous control.

Formation flying technology has progressed immensely from the first formation flying demonstration in 1965, where Gemini 6A was manually piloted to as close as 0.3 m to Gemini 7. Applications and demonstrations have progressed from short mission durations with extensive ground control towards continuous operation with autonomous control. ESA's PROBA-3 expected to be launched in end of 2018 aims to demonstrate, a first of its kind, highly precise autonomous formation flying. Two spacecraft will autonomously maintain a 150 m separated formation with accuracies in the order of millimeters and arc seconds [37]. The projected capabilities allow formations of more than 30 spacecraft controlled with nanometer level precision by 2025 [33].

1.3.3 Fractionated spacecraft

A fractionated spacecraft is a new architectural model whereby a satellite is decomposed into a set of similar or dissimilar component modules which interact wirelessly while in cluster orbits [38]. Cluster flying is used to refer to persistently proximate orbital positioning of multiple satellite modules in passively stable, Keplerian orbits. This approach to spacecraft design is expected to enhance responsiveness by making the spacecraft architecture flexible and robust, along with reducing spacecraft development time and launch constraints.

The Defense Advanced Research Projects Agency (DARPA) has initiated System F6 to demonstrate the feasibility and benefits of a fractionated spacecraft architecture wherein the functionality of a traditional monolithic spacecraft is delivered by a cluster of wirelessly-interconnected modules. The fractionated concept of System F6 is shown in Figure 1-6. Such architectures are expected to enhance the adaptability and survivability of space systems, while reducing development timelines [39].

1.3.4 Swarms

A Swarm is defined as a set of agents which are liable to communicate directly or indirectly with each other and which collectively carry out a distributed problem solving [40]. In this context, a satellite swarm is a group of identical, minimal, self-organised (self-functioning) satellites in space that achieve a common objective with their collective behaviour. They form loosely coherent groups or clusters based on simple opportunistic rules [41].

Figure 1-6 | Illustration of SYSTEM F6: DARPA's Fractionated spacecraft concept (Photo: DARPA) [39])

1.3.5 Other configurations

Rendezvous and docking, and Space tethers are two additional configurations that fall under the DSS umbrella. In 1966, astronauts Neil Armstrong and David Scott successfully docked their Gemini VIII spacecraft with the Agena target vehicle, the first docking demonstration in space [42]. The first demonstration of automated docking was through the Kosmos 186 and 188 in 1967. A search and approach phase was followed by mooring and docking [43,44]. Since then, through the Apollo program and up to present day operations with the International Space Station, rendezvous and docking missions have been an integral part of space exploration. There is an increasing interest in space missions that not only rely on rendezvous and docking, but also on the capability to manoeuvre the spacecraft once docked, for example in applications such as active debris removal, on-orbit assembly, and on-orbit servicing and repair [45].

The earliest experiments with tethers can be traced back to the 1960s. In two separate experiments in 1966, the Gemini 11 and 12 manned capsules were connected by a cable around 30 m long to their respective Agena upper stage [46]. The astronauts manually controlled the coupled system to first establish a gravity gradient stabilization and then rotation. The complex dynamics encountered with short tethers in these trails may have been the reason it took another 14 years before tethers were deployed in space again [47]. More recently in 2010, JAXA demonstrated the T-REX mission (Tether Technologies Rocket Experiment) by launching a sounding rocket to perform sub-orbital tether experiments [48]. The interested reader is referred to a comprehensive review on space tethers by Cartmell and Mckenzie [49] and the handbook on space tethers edited by Cosmo and Lorenzini [50] for more applications and potential of tethers in space.

1.4 Research Gaps for DSS

The convergence and development of these two domains – miniaturization of space systems and distributed systems in space, forecasts an array of innovative space missions. Distributed systems enjoy features such as redundancy, robustness, reliability, ability for incremental growth but also suffer from security issues, network problems and operating software. Miniature systems are advantageous by virtue of their small size (packaging of more functional components), low mass and hence low mechanical inertia (precision movements and rapid actuation), ability to be mass produced and less material requirements among others [51]. Miniature spacecraft will enjoy all these benefits and add more aspects like low spacecraft cost, low launch cost, and fast development time. A distributed network of miniature systems will ideally combine the advantages of miniaturization and distributed systems to realize an efficient and effective system.

Some key issues need to be addressed before we can enable the above discussed convergence and build massively distributed space systems. The rest of this sub-section highlights the main concerns in the existing body of knowledge to enable this convergence, and the research approach established to tackle these concerns.

1.4.1 Mapping Applications to Capabilities

On a programmatic level, approaches to map the performance requirements of a DSS mission with the capabilities of the individual spacecraft in that system has not been well addressed [52]. Most of the research work on DSS with miniature spacecraft has been limited to designing and prototyping miniature spacecraft [21,53] and not much on characterizing DSS. An in-depth investigation into the scaling factor for swarms was recommended as a key finding before satellite swarms can be realized [54]. A first attempt at systematically identifying applications was explored through a qualitative analysis which matched the functional requirements of a space mission to the individual capability of a spacecraft in a DSS [52]. Here, it was established that a more quantitative approach to scale the capabilities is essential.

1.4.2 Spatial Distribution

Missions with multiple spacecraft are envisioned as key enablers for innovative space applications ranging from constellations for earth imaging to interferometric missions for building virtual telescopes. Depending on the particular space application we may want the network or cluster of spacecraft to evolve into specific configurations. For an earth monitoring mission that requires global coverage, the cluster would ideally spread in space in such a way so as to maximize spatial coverage, while for an application such as interferometry the cluster ideally maintains a tight configuration with the spacecraft relatively closer to each other. Either way, we need tools to analyse how these networks will evolve in time so that we can optimize mission design to enhance mission return.

For spacecraft dynamics, research on analysis and representation of relative dynamics has been restricted to, mainly dual spacecraft configurations [55,56]. Representations involving the Hill's frame,

1

Eccentricity- Inclinations vectors and Analemmas are also primarily suited for dual spacecraft [57]. Although some of these methods can be extended to a larger number of spacecraft, the methods do not naturally scale and become extremely cumbersome when the number of spacecraft increase even moderately. Recent literature on DSS has focussed on applications and missions concepts involving multiple spacecraft, for example in the form of fractionated systems [58] and swarms [59], and not on representation or characterization of DSS. Therefore, new approaches need to be investigated and new metrics need to be developed that are suitable and insightful for DSS design and characterization.

1.4.3 Collision Between Spacecraft

Space debris is one of the fundamental challenges of contemporary and future spaceflight. The number of spacecraft launched has been increasing steadily and a record 214 spacecraft were launched in 2013 alone [60] and in 2017 more than 100 spacecraft were deployed from a single launch [61]. Therefore, collisions not only with debris but between spacecraft has become a real and immediate concern. The collision probability analysis is, however, not straightforward and involves computationally intensive calculations. Most works on collision analysis is restricted to a linear analysis involving a spacecraft and debris, where a number of assumptions are introduced to simplify collision probability analysis [62-64]. This, however, cannot be applied for collision between spacecraft that are close to each other for significant periods of time [65]. Therefore, efficient and effective methods to analyse collisions between spacecraft need to be developed.

1.4.4 Cooperation and Synergy

Synergy is not a new idea for distributed systems and the concept is not a new proposition for DSS. The Oxford English dictionary defines synergy as *"the interaction or cooperation of two or more organizations, substances, or other agents to produce a combined effect greater than the sum of their separate effects"* [66]. Although, a number of concepts have been proposed, there have been very limited demonstrations of synergetic DSS [16]. Until now, the benefit of distributed systems in space has been limited to enhancing coverage, multipoint sensing, typically for creating virtual baselines (e.g. interferometry) or to enhance redundancy. Further benefits can be identified by understanding the nature of distributed systems and by productively incorporating it into mission and spacecraft design [1]. For example, prior knowledge of the spatial evolution of such systems can lead to innovative communication architectures for these distributed systems. Therefore, establishing scenarios for synergy and mechanisms to implement such scenarios with simplistic spacecraft is essential [67].

1.5 Research Questions and Methodology

The aim of this thesis is to advance the research in the field of DSS with miniature spacecraft to enhance and enable space applications with such systems. To this end, specific research questions (RQ) have been identified and formulated. The RQs and the associated methodologies that have been employed in this thesis are introduced in this section.

RQ1: **When is scaling in spacecraft size and number beneficial for a DSS?**

Distributed systems and miniature systems are essentially systems that are scaled. While distributed space systems are scaled up in quantity or units of individual spacecraft, miniature systems are scaled down with respect to the size or form factor of the spacecraft. An important part of this thesis is a discussion on scalable systems and identifying systems and scenarios that favour miniaturization and a distributed nature.

A novel classification system is introduced and scalable systems are divided into three kinds – systems that scale linearly; systems that scale sub-linearly; and ones that scale super-linearly with the dimension of interest. Methods to quantify coefficients that can identify the scaling category, to which a particular system belongs to, are outlined and discussed. The downlink communication capability is taken as a case study to explore scenarios and bounds where scaling in number will enhance data throughput. This is followed by a feasibility study of a phased array in space to enhance the downlink communication capability of a DSS. Requirements on spacecraft on-board capabilities to achieve different accuracy levels are derived and highlighted.

RQ2: Are there quantifiable global metrics for a DSS that can aid in mission design and analysis? How can such metrics be defined, developed and used?

While a collision free and safe configuration is a prime concern, deriving parameters that can provide insight into the spatial and temporal evolution of these distributed systems in space can add additional value in mission design and operations. This question seeks a solution with respect to the characterization of cluster evolution through quantitative parameters such as cluster distribution index (CDI) and overall collision probability. The distribution index can be used to assess the effectiveness of DSS in meeting system requirements such as coverage and resolution. The Collisions Analysis using Line-Integral method (CALM) is proposed as an effective and efficient approach to analysing collision probability within DSS.

An n-dimensional grid-based numerical approach is used to evaluate CDI. The discrepancy with respect to a uniform distribution is used as an intermediate variable to derive the CDI. The entire set of spacecraft orbits is numerically propagated in the presence of relevant perturbations. The spatial distribution is then transformed into the required reference frame to contrast with a uniform distribution and then yield a spatial discrepancy. An analytical framework has been established to convert this discrepancy into the cluster distribution index.

Determining the probability of collision is not straightforward and requires the integration of overlapping multi-dimensional probability distribution functions. This is a tedious and cumbersome process. An analytical method has been developed , with scenario based assumptions, that allows the volume integral to be reduced to a scalar multiplication to evaluate the instantaneous collision probability. This simplified line-integral method is computationally much faster than conventional methods of calculating collision probability. The results are validated by comparing with other methods for determining collision probability.

RQ3: How can beamforming be achieved with highly resource constrained miniature spacecraft?
Beamforming is a technique, developed originally for terrestrial sensor networks, for directional signal transmission or reception. Distributed beamforming can be an enabling technique for enhancing communication in distributed nodes with transmission capability. The concept of distributed beamforming can be extended and applied to distributed networks in space. However, this is accompanied with the additional challenges stemming from a dynamic environment and tighter resource constraints. The critical challenge in beamforming is establishing phase synchronization with the required accuracy that is demanded for signal reinforcement. Traditionally, this would imply same order of time synchronization and localization as the required phase synchronization. For a simplistic femto-satellite, achieving such levels of time synchronization and localization may be extremely and even prohibitively demanding. This research question aims to explore novel and innovative approaches to synchronization that are feasible on resource-limited platforms.

A mathematical framework is developed for a general analysis of the proposed phase synchronization scheme. Sensitivity of achieved phase synchronization accuracy to spatial geometry and errors is analysed to define the operational boundaries for such schemes. This is followed by a software simulation to include effects of errors and to verify the performance.

1.6 Thesis structure

The contributions of this dissertation to the body of knowledge are presented through several chapters. There are three core chapters preceded by an introduction chapter (i.e. this chapter) and succeeded by a chapter on concluding remarks and recommendations. The structure of the chapters along with the associated research questions and key publications is shown in Figure 1-7.

Chapter 2 explores the dynamics of DSS. In this chapter, the orbital evolution of a cluster of uncontrolled satellites in LEO is investigated to provide insight into relative dynamics, deployment strategies and effect of perturbations on relative dynamics of DSS. Furthermore, quantitative measures such as a geometric cluster distribution index and a measure for overall collision probability for DSS are derived and discussed.

In **Chapter 3**, the communication capability is taken as a typical functionality and methods are identified to enhance the communication link between a distributed space segment, consisting of a number of simplistic, resource limited femto-satellites, and Earth.

Furthermore, a novel phase synchronization technique that enables beamforming with multiple resource limited spacecraft that capitalizes on their spatial geometry is proposed in **Chapter 4**. The challenging time synchronization problem is addressed through the proposed external beacon that obviates the need for explicit time synchronization. **Chapter 5** provides the conclusion and recommendation of the research presented in the different chapters and highlights the contribution

of this dissertation to enable and enhance DSS with miniature spacecraft. The chapter also presents a brief outlook on distributed space systems with miniature spacecraft.

	Chapters	Key Publications
Distributed Space Systems with miniature spacecraft	**Chapter 1** **Introduction**	**Sundaramoorthy, P.**, Verhoeven, C. (2010) Systematic Identification of *Applications for a Cluster of Femto-satellites*. 61st International Astronautical Congress. Verhoeven, C., Engelen, S., Noroozi, A., **Sundaramoorthy, P.**, Bentum, M., Meijer, R. (2011). Emerging Eco-system: Nano-satellite Swarms and Large Satellites. 62nd International Astronautical Congress. Angadi, C, **Sundaramoorthy, P.** (2012). Femto-Satellite System Architecture for LEO Applications. 63rd International Astronautical Congress.
	Chapter 2 **Spatial Distribution and Collision Probability in a DSS** **[RQ2]**	**Sundaramoorthy, P.,** Gill, E., & Verhoeven, C. (2010). *Relative Orbital Evolution of a Cluster of Femto-satellites in Low Earth Orbit.* Spaceflight Mechanics – Advances in the Astronautical Sciences. **Sundaramoorthy, P.**, Gill, E., Verhoeven, C., Reinhard, R., Asma, C. (2010). *Preliminary Orbit and Mission Analysis of the QB50 Satellite Cluster.* 4th International Conference on Astrodynamics Tools and Techniques. **Sundaramoorthy, P.**, Florijn, D., Gill, E., & Verhoeven, C. (2016). *A Spatial Distribution Measure and Collision Analysis Technique for Distributed Space Systems.* Acta Astronautica.
	Chapter 3 **Scalability of Distributed Space Systems** **[RQ1]**	**Sundaramoorthy, P.**, Gill, E., & Verhoeven C. (2013). *Enhancing Ground Communication of Distributed Space Systems.* Acta Astronautica. Verwilligen, J., **Sundaramoorthy, P.** (2013). A Novel Planar Antenna for CubeSats. Small Sats, Utah.
	Chapter 4 **Novel Phase Synchronization Technique** **[RQ3]**	**Sundaramoorthy, P.**, Gill, E., & Verhoeven, C. (2016). *Beamforming with Spacecraft under Reduced Localization and Clock Constraints.* IEEE Transaction on Aerospace and Electronic Systems.
	Chapter 5 **Conclusions and Recommendations**	**Speretta** et al. (2016). CubeSats to PocketQubes: Opportunities and Challenges. 67th International Astronautical Congress.

Figure 1-7 | Structure of the thesis showing the different chapters, associated research questions and key publications associated with corresponding chapters.

References

[1]   P. Sundaramoorthy, E. Gill and Verhoeven C., "Enhancing Ground Communication of Distributed Space Systems," *Acta Astronautica, Vol 84,* 2013.

[2]   D. Barnhart, T. Vladimirova and M. Sweeting, "Very-Small-Satellite Design for Distributed Space Missions," *Journal of Spacecraft and Rockets, Vol. 44, No. 6,* 2007.

[3]   E. Gill, *Together in Space – Potentials and Challenges of Distributed Space Systems; Inaugural speech; Delft University of Technology.,* 2008.

[4]   W. Morrow and T. Rogers, "The West Ford Experiment - An Introduction to this Issue," *Proceedings of the IEEE, pp. 461-468,* vol. 52, no. 5, 1964.

[5]   "GPS.gov," [Online]. Available: https://www.gps.gov/systems/gps/. [Accessed 01 03 2018].

[6]   "Information and Analysis Center for Positioning, Navigation and Timing," [Online]. Available: https://www.glonass-iac.ru/en/. [Accessed 01 03 2018].

[7]   "iridium," [Online]. Available: https://www.iridium.com/. [Accessed 01 03 2018].

[8]   NASA, "The Afternoon Constellation," [Online]. Available: https://atrain.nasa.gov/. [Accessed 01 03 2018].

[9]   D. Hutcheson, "SPECIAL REPORT: 50 Years of Moore's Law," 02 04 2015. [Online]. Available: http://spectrum.ieee.org/computing/hardware/transistor-production-has-reached-astronomical-scales. [Accessed 03 08 2017].

[10]   M. Day, "30 Years of Commercial Components In Space:Selection Techniques Without Formal Qualification," in *13th Annual AIAA/USU Conference on Small Satellites*, Utah, US, 1999.

[11]   D. Friedlander, "COTS/EEE parts in space: component engineering challenges," January 13 2017. [Online]. Available: http://www.intelligent-aerospace.com. [Accessed 9 10 2017].

[12]   D. Selva and D. Krejci, "A survey and assessment of the capabilities of Cubesats forEarth Observation," *Acta Astronautica,* vol. 74, pp. 50-68, 2012.

[13]   G. Brouwer and J. Bouwmeester, "From the Delfi-C3 nano-satellite towards the Delfi-n3xt nano-satellite," in *23rd Annual AIAA/USU Conference on Small Satellites, UTAH, US*, 2009.

[14]   J. Bouwmeester and J. Guo, "Survey of Worldwide pico- and nanosatellite missions, distributions and subsystem technology," *Acta Astronautica, Vol. 67, Issues 7-8, pp.854-862,* 2010.

[15]   A. R. C. M. F. C. Mission Design Division, "Small Spacecraft Technology State of the Art (NASA/TP–2015–216648/REV)".

[16]   "Nanosatellite Database by Erik," [Online]. Available: http://nanosats.eu/index.html#figures. [Accessed 01 09 2017].

[17]   "eoPortal Directory," 01 02 2015. [Online]. Available: https://directory.eoportal.org/web/eoportal/satellite-missions/f/flock-1.

[18]   NASA, 10 02 2015. [Online]. Available: http://www.nasa.gov/mission_pages/station/research/experiments/1326.html.

[19]   QB50. 05 02 2015. [Online]. Available: https://www.qb50.eu/index.php/project-description-obj.

[20]   D. Barnhart, T. Vladimirova, A. Baker and M. Sweeting, "A low-cost femtosatellite to enable distributed space missions," *Acta Actronautica, Vol. 64,* 2009.

[21]   G. McVittie and K. D. Kumar, "Design of a COTS Femtosatellite and Mission," in *AIAA SPACE Conference & Exposition*, 2007.

[22]   S. Janson and D. Barnhart, "The Next Little Thing: Femtosatellites," in *27th Annual AIAA/USU Conference on Small Satellites*, Utah, 2013.

[23]   A. Huang, W. Hansen, S. Janson and H. Helvajian, "Development of a 100 gm Class Inspector Satellite Using Photostructurable Glass/Ceramic Materials," *Proc. of SPIE,* vol. vol. 4637, p. pp. 297–304, 2002.

[24]   Z. Manchester, "KickSat -- Your personal spacecraft in space!," Kickstarter, [Online]. Available: https://www.kickstarter.com/projects/zacinaction/kicksat-your-personal-spacecraft-in-space. [Accessed 17 11 06].

[25]   B. Warneke, M. Last, B. Liebowitz and K. S. J. Pister, "Smart Dust: Communicating with a Cubic-Millimeter Computer," *IEEE Computer,* vol. 34, no. 1, p. pp. 44–51, 2001.

[26]   C. Enz, A. El-Hoiydi, J.-D. Decotignie and V. Peiris, "WiseNET: An Ultralow-powerWireless Sensor Network Solution," *IEEE Computer,* vol. 37, no. 8, p. pp. 62–70, 2004.

[27]   "Gunter's Space Page," [Online]. Available: http://space.skyrocket.de/doc_sdat/mitee.htm. [Accessed 07 11 2017].

[28]   A. Kyle, S. Vadali, P. Gurfil, J. How and L. Berger, Spacecraft Formation Flying: Dynamics, control and navigation, Elsevier, 2010.

[29]   Stanford, "Distributed Space Systems," [Online]. Available: https://aa.stanford.edu/research/distributed-space-systems. [Accessed 08 08 2017].

[30]   J. Wertz, Mission Geometry; Orbit and Constellation Design and Management, Kluwer Academic; 2001.

[31]   ESA, "Galileo: A Constellation of Navigation Satellites," [Online]. Available: https://www.esa.int/Our_Activities/Navigation/Galileo/Galileo_a_constellation_of_navigation_satellites. [Accessed 01 03 2018].

[32]   D. Scharf, F. Hadaegh and S. Ploen, "A Survey of Spacecraft Formation Flying Guidance and Control (Part II): Control," in *Proceeding of the 2004 American Control Conference, Boston, Massachusetts*, 2004.

[33]   J. Leitner, "Formation Flying - The Future of Remote Sensing from Space," in *Technical Report NASA-Techdoc-20040171390, NASA, Goddard Space Flight Centre*, 2004.

[34]   ESA, "LISA," [Online]. Available: http://sci.esa.int/lisa/. [Accessed 01 03 2018].

[35]   ESA, "DARWIN Overview," [Online]. Available: https://www.esa.int/Our_Activities/Space_Science/Darwin_overview. [Accessed 01 03 2018].

[36]   NASA, "TPF," [Online]. Available: https://science.nasa.gov/missions/tpf. [Accessed 01 03 2018].

[37]   "PROBA MISSIONS," 01 03 2015. [Online]. Available: http://www.esa.int/Our_Activities/Space_Engineering_Technology/Proba_Missions/Mission2.

[38]   O. Brown and P. Eremenko, "Fractionated Space Architectures: A Vision for Responsive Space," in *4th Responsive Space Conference April 24–27, Los Angeles, CA*, 2006.

[39]   "DARPA," 26 03 2015. [Online]. Available: http://www.darpa.mil/our_work/tto/programs/system_f6.aspx.

[40]   J.-L. Deneubourg, G. Theraulaz and R. Beckers, "Swarm made architectures," in *In Proceedings of the 1st European Conference on Artificial Life, Paris, MIT Press, Cambridge (Mass.)*, 1991.

[41]   S. Engelen, C. Verhoeven and M. Bentum, "OLFAR, A Radio Telescope based on Nano-satellites in Moon Orbit," in *24th Annual AIAA/USU Conference on Small Satellites, UTAH, USA*, 2010.

[42]   NASA, "March 16, 1966: Gemini's First Docking of Two Spacecraft in Earth Orbit," 16 03 2016. [Online]. Available: https://www.nasa.gov/image-feature/march-16-1966-geminis-first-docking-of-two-spacecraft-in-earth-orbit. [Accessed 09 03 2018].

[43]   NASA, "Cosmos 186," [Online]. Available: https://nssdc.gsfc.nasa.gov/nmc/masterCatalog.do?sc=1967-105A. [Accessed 07 11 2017].

[44]   A. Z., "Soyuz spacecraft dock in space," [Online]. Available: http://www.russianspaceweb.com/soyuz-7k-ok-kosmos-188.html. [Accessed 07 11 2017].

[45]   N. G. S. F. Center, "On-Orbit Satellite Servicing Study - Project Report," 2010.

[46]   NASA, "Gemini 11 Target," [Online]. Available: https://nssdc.gsfc.nasa.gov/nmc/spacecraftDisplay.do?id=1966-080A. [Accessed 07 11 2017].

[47]   M. Kruijff, Tethers in Space: A Propellantless Propulsion In-Orbit, PhD Dissertation, Uitgeverij BOXPress, Oisterwijk, Netherlands, 2011.

[48]   JAXA, "JAXA's Tether Technologies Rocket Experiment (T-REX)," [Online]. Available: http://spaceref.com/news/viewsr.html?pid=34856. [Accessed 07 11 2017].

[49]   M. Cartmell and D. McKenzie, "A review of space tether research," *Progress in Aerospace Sciences,* vol. 44, no. 1, pp. 1-21, 2008.

[50]   M. Cosmo and E. Lorenzini, Tethers In Space Handbook, 3/e, Cambridge, MA.: prepared for NASA/MSFC by Smithsonian Astrophysical Observatory, 1997.

[51]   T.-R. Hsu, "Miniaturization – A paradigm shift in advanced manufacturing and education," *A plenary speech delivered at the 2002 IEEE/ASME International conference on Advanced Manufacturing Technologies and Education in the 21st Century, Chia-Yi, Taiwan, Republic of China,* 2002.

[52] P. Sundaramoorthy and C. Verhoeven, "Systematic Identification of Applications for a Cluster of Femto-satellites," in *61st International Astronautical Congress*, Prague, Czech Republic, 2010.

[53] C. Angadi and P. Sundaramoorthy, "Femto-satellite System Architecture & Mission Design for LEO Applications," in *International Astronautical Congress*, Naples, Italy, 2012.

[54] S. Engelen, E. Gill and C. Verhoeven, "Systems Engineering Challenges for Satellite Swarms," *IEEE Aerospace Conference, Big Sky, MT, USA,* 2011.

[55] H. Schaub, S. Vadali, J. Junkins and K. Alfriend, "Spacecraft Formation Flying Control using Mean Orbit Elements," *Journal of the Astronautical Sciences,* vol. 48, no. 1, pp. 69-87, 2000.

[56] C. Sabol, R. Burns and C. McLaughlin, "Satellite Formation Flying Design and Evolution," *Journal of Spacecraft and Rockets,* vol. 38, no. 2, 2001.

[57] P. Sundaramoorthy, E. Gill and C. Verhoeven, "Relative Orbital Evolution of a Cluster of Femto-satellites in Low Earth Orbit," *Spaceflight Mechanics - Advances in the Astronautical Sciences,* vol. 136, 2010.

[58] J. Chu, J. Guo and E. Gill, "Fractionated space infrastructure for long-term earth observation missions," *IEEE Aerospace Conference,* 2013.

[59] S. Engelen, E. Gill and C. Verhoeven, "On the Reliability, Availability and Throughput of Satellite Swarms," *IEEE Transactions in Aerospace and Electronic Systems,* vol. 50, no. 2, 2014.

[60] C. Lafleur, "Table of Spacecrafts Launched in 2013," 15 01 2014. [Online]. Available: http://claudelafleur.qc.ca/Spacecrafts-Table-2013.html.

[61] ISRO, Feb 2017. [Online]. Available: https://www.isro.gov.in/update/15-feb-2017/pslv-c37-successfully-launches-104-satellites-single-flight. [Accessed 15 10 2017].

[62] S. Alfano, "A Numerical Implementation of Spherical Object Collision Probability," *The Journal of the Astronautical Sciences,* vol. 53, no. 1, pp. 103-109, 2005.

[63] K. Alfriend, M. Akella, J. Frisbee, J. Foster, D. LEE and M. Wilkins, "Probability of Collision Error Analysis," *Space Debris,* vol. 1, pp. 21-35, 1999.

[64] M. Akella, "Probability of Collision Between Space Objects," *Journal of Guidance, Control, and Dynamics,* vol. 23, no. 5, 2000.

[65] R. Patera, "Satellite Collision Probability for Nonlinear Relative Motion," *Journal of Guidance, Control, and Dynamics,* vol. 26, no. 5, 2003.

[66] O. E. Dictionary. [Online]. Available: https://en.oxforddictionaries.com/definition/synergy. [Accessed 04 11 2017].

[67] P. Sundaramoorthy, E. Gill and C. Verhoeven, "Beamforming with spacecraft under reduced localization and clock constraints," *IEEE Transactions on Aerospace and Electronic Systems,* vol. 52, no. 3, 2016.

1

Contents

Chapter 2

Spatial Distribution and Collision Probability in a Distributed Space System

"Some people see the glass half full. Others see it half empty. I see a glass that's twice as big as it needs to be."

— George Carlin, American stand-up comedian and social critic

quaquaversal /kweɪkwəˈvɜːsəl/

adjective **1** going off in all directions from the center. **2** (*astronomy*) dipping towards a center in all directions.

Language: English

This chapter is concerned with the temporal and spatial evolution of a satellite cluster in a low Earth orbit (LEO). After an initial foray into traditional methods for relative motion analysis between two spacecraft, the chapter then dives into the development of metrics that are suitable for a massively distributed system in space. Representation techniques, measure for spatial distribution and collision analysis between close-flying spacecraft are developed and discussed.

2.1 Introduction

Technology advances in contemporary space mission design and development allow for more and more miniaturized spacecraft which open up new application areas when deployed as distributed systems [1,2,3]. Miniature spacecraft could in the future be mass produced and hundreds to thousands of such spacecraft can be deployed as a cluster for example to enhance the monitoring capability of the Earth's environment [4,5,6]. Such mission concepts provide a suite of challenging problems, among them the orbital evolution of such a cluster and metrics to quantify distribution and collision risk. This paper investigates the temporal and spatial characteristics of a satellite cluster and proposes metrics to characterize the spatial distribution and the collision probability of such a cluster.

When we concern ourselves with the orbital evolution of a cluster of femto-satellites that are separated in space from a separation mechanism, then the distance between the satellites can vary from millimeters to thousands of kilometers over the mission lifetime [7]. The problem, therefore, cannot be categorized into either the domain of close satellite formations or conventional satellite constellations. This is the motivation to use analytical methods from both these domains to explore representations that can provide an intuitive picture over the entire mission.

For spacecraft dynamics, research on analysis and representation of relative dynamics has been restricted to, mainly dual spacecraft configurations [8,9]. Representations involving the Hill's frame, Eccentricity- Inclinations vectors and Analemmas are also primarily suited for dual spacecraft [10]. Although some of these methods can be extended to a larger number of spacecraft, the methods do not naturally scale and become extremely cumbersome when the number of spacecraft increase even moderately. Recent literature on DSS has focussed on applications and missions concepts involving multiple spacecraft, for example in the form of fractionated systems [11] and swarms [12], and not on representation or characterization of DSS. However, new approaches need to be investigated and new metrics need to be developed that are suitable and insightful for DSS design and characterization. The objective of this research is to define and develop metrics for DSS that can assist in characterizing the dynamics and distribution of DSS. To this end, two distinct DSS metrics are proposed and developed: A cluster distribution index (CDI) and a cluster collision probability (CCP).

CDI is a measure of the uniformity of the spatial distribution. Some of the key requirements for a space mission are expressed in terms of coverage, response time and resolution, and the extent to which these requirements are met cannot be determined in a straightforward manner for a DSS. The CDI can be used as a measure to assess the effectiveness of DSS in meeting these requirements. An n-dimensional grid-based numerical approach is used to evaluate the CDI.

CCP is a measure of the collision probability between spacecraft in a cluster. The number of spacecraft launched has been increasing steadily and a record 214 spacecraft were launched in 2013 alone [13]. Therefore, collisions not only with debris but between spacecraft has become a real and immediate concern. The collision probability analysis is, however, not straightforward and involves computationally intensive calculations. In this paper, a simplified model is proposed that exploits the deployment scenarios of a DSS to improve the computational efficiency of the probability analysis. The aim is to develop a measure of the collision probability between spacecraft in a DSS that can be efficiently computed. The Collisions Analysis using Line-Integral method (CALM) is proposed as an effective and efficient approach to analyzing the collision probability within a network of spacecraft.

This chapter will first introduce orbit propagation and some popular representations of relative motion. This will be followed by an extensive treatment on distribution measures and collision analysis within a cluster.

2.2 Analysis of Relative Motion

Missions with multiple spacecraft are envisioned as key enablers for innovative space applications. Depending on the particular space application we may want the network or cluster of spacecraft to evolve into specific configurations. For an earth monitoring mission that requires global coverage, the cluster would ideally spread in space in such a way so as to maximize spatial coverage, while for an application such as interferometry the cluster ideally maintains a tight configuration with the spacecraft relatively closer to each other. Either way, we need tools to analyze how these networks will evolve in time so that we can optimize mission design to enhance mission return.

In this chapter, the orbital evolution of a cluster of uncontrolled satellites in LEO is investigated to provide insight into relative dynamics, deployment strategies and effect of perturbations on relative dynamics between spacecraft. Furthermore, quantitative measures are derived to characterize clusters in space. Resource limited, simplistic femto-satellites are chosen as candidate spacecraft in the analysis. The chapter starts with a discussion on methods used for orbit determination and prediction in the presence of perturbations typical to a LEO environment. Cowell's method of special perturbations, the Gauss' variation of parameters and the Clohessy Wiltshire equations of relative motion are introduced. This is followed by a discussion on typical representations used for relative motion between two spacecraft and its usability for satellite clusters.

While a collision free and safe configuration is a prime concern, deriving parameters that can provide insight into the spatial and temporal evolution of these distributed systems in space can add additional value in mission design and operations. The last part of this chapter deals with the characterization of cluster evolution through quantitative parameters such as cluster distribution index and collision thresholds.

2.2.1 Orbit propagation

The objective of orbit propagation is to know the position of a spacecraft at a given instant of time and to gain insight into how the orbit of the spacecraft evolves when subject to gravity and other perturbations. The Keplerian two-body problem is a good representation, albeit an approximated one, for spacecraft orbiting planets. The gravitational force is the only force that is considered and the masses are treated as point masses. With this assumption, we already get a good insight into the behavior of a spacecraft in orbit about a planet.

Kepler's two-body equation of motion has been investigated quite rigorously and the properties of a Keplerian orbit are well understood to predict the trajectory of a spacecraft in such an orbit. However, the Keplerian two-body orbit is an idealized trajectory. In reality, there are several factors that we refer to as perturbations, which cause the actual motion to deviate from the Keplerian orbit. In practice, to predict the spacecraft motion with higher accuracy, these perturbations must be accounted for. For a geocentric orbit, these perturbations include:
- Asymmetrical nature of the Earth's gravity field arising due to the non-uniform mass distribution
- Atmospheric drag (significant at LEO where the atmospheric density is significant)
- Radiation pressure (solar, albedo and infrared)
- Third body attraction (influence of other bodies through their gravitational fields) eg: Sun, Moon
- Thruster operations in the space vehicle.

The most significant perturbations for spacecraft in LEO are the atmospheric drag and the asymmetrical gravity field of the Earth [14]. The influence of the velocity increment provided by deployment mechanisms, similar to CubeSat spring-based deployment mechanisms, can be analyzed either by propagating an orbit with a new set of initial conditions that includes the velocity increment or by treating the velocity increment as a perturbation. In this study, we treat the velocity increments from the deployment mechanisms as factors which change the initial conditions and the aspherical gravity field and atmospheric drag as perturbations. However, analytically the effect of the velocity increment can still be modeled as perturbation to get insight into the dynamics.

There are two approaches for dealing with perturbations referred to as the method of special perturbations and the method of general perturbations (Bate, Mueller and White, Fundamentals of Astrodynamics, Dover, 1971). In special perturbations, such as Cowell's method or Encke's method, some kind of numerical integration is involved to propagate and predict the orbit. While Cowell's method numerically integrates the equations of motion directly, Encke's method works by

numerically integrating only the deviation from the Keplerian orbit. It is referred to as "special", since the solution is only valid for one set of initial conditions and has to be repeated for every new set of initial conditions. In general perturbations, the solution is determined analytically and holds for any set of initial conditions.

To analyze the relative motion between spacecraft, the orbits of each spacecraft are propagated using Cowell's method, and then differenced to derive the relative trajectories. Analytical methods that model the relative motion such as Clohessy Wiltshire equations and Gauss variation of parameters that provides the variation of orbital parameters with time are used to gain insight into the relative dynamics.

2.2.1.1 Cowell's method

The equation of motion for the two-body problem including perturbations is given as [15],

$$\ddot{\mathbf{r}} + \frac{\mu}{r^3}\mathbf{r} = \mathbf{a}_d \qquad (2\text{-}1)$$

where r is the vector position of the spacecraft with respect to the centre of the main body, in this case Earth, μ is the gravitational parameter of the Earth, and a_d is the vector representing the accelerations due to perturbations. The above equation can be written in first order form appropriate for numerical integration as,

$$\dot{\mathbf{r}} = \mathbf{v}$$
$$\dot{\mathbf{v}} = -\frac{\mu}{r^3}\mathbf{r} + \mathbf{a}_d \qquad (2\text{-}2)$$

where $\mathbf{v}$ is the velocity of the spacecraft with respect to Earth. Cowell's method is a straightforward method for determining the position and velocity by direct numerical integration of the equation of motion. Given the initial conditions for $\mathbf{r}$ and $\mathbf{v}$, Eq. (2-2) can be numerically integrated for any time duration. This method is computationally expensive and has the drawback that the solution has to be redone for every new set of initial conditions. The advantage of this method, however, is that a_d can include any perturbation without modification to the method. Therefore, this method allows the use of numerical models for perturbations and the accuracy of these models, along with the round-off errors typical to numerical integration, determine the accuracy of the predicted orbits.

2.2.1.2 Gauss' variation of parameters

The Gauss' variation of parameters is a general perturbation method where the variation of the orbital elements with time is expressed analytically. In order to do so, it is convenient to first decompose the disturbing acceleration into three orthogonal directions: a radial component, a_{dr}, a component in the orbital plane perpendicular to the radius vector, $a_{d\phi}$, and a component normal to the orbital plane, a_{dz}. The set of variational equations can be summarized as [16,17],

$$\frac{da}{dt} = \frac{2a^2}{\sqrt{\mu a(1 - e^2)}}\left[e \sin \theta\, a_{dr} + (1 + e \cos \theta)\, a_{d\phi}\right]$$

$$\frac{de}{dt} = \sqrt{\frac{a(1 - e^2)}{\mu}}\left[\sin \theta\, a_{dr} + \frac{2 \cos \theta + e (1 + \cos^2 \theta)}{(1 + e \cos \theta)}\, a_{d\phi}\right]$$

$$\frac{di}{dt} = \sqrt{\frac{a (1 - e^2)}{\mu}}\ \frac{\cos(\omega + \theta)}{(1 + e \cos \theta)}\ a_{dz}$$

(2-3)

$$\frac{d\Omega}{dt} = \sqrt{\frac{a(1 - e^2)}{\mu}}\ \frac{\sin(\omega + \theta)}{\sin i (1 + e \cos \theta)}\ a_{dz}$$

$$\frac{d\omega}{dt} = \sqrt{\frac{a(1 - e^2)}{\mu}}\left[-\frac{\cos \theta}{e}\, a_{dr} + \frac{(2 + e \cos \theta) \sin \theta}{e(1 + e \cos \theta)}\, a_{d\phi} \right.$$
$$\left. - \frac{\sin(\omega + \theta)}{\tan i (1 + e \cos \theta)}\ a_{dz}\right]$$

where [**a e i Ω ω θ**] are the orbital elements representing the semi-major axis, eccentricity, inclination, right ascension of the ascending node, argument of perigee and the argument of latitude, respectively. A typical application of the Gauss' equations is analysis of small impulsive shots such as the ones delivered by the deployment mechanism to eject the spacecraft from the launcher. Therefore, we can apply the Gauss' equations to analyse the effect of the velocity increments from the deployment mechanism on the shape and orientation of the orbit that the spacecraft will follow.

Eq. (2-3) can be integrated to assess the change of an orbital element due to a small impulsive velocity increment. For this we treat, as a first approximation, the orbital parameters on the right hand side of the equations as a constant, and observing that the velocity increment ΔV over a time interval is given by,

$$\int a_{di} dt = \Delta V_i$$

where the index i takes on any of the indices r, ϕ, and z in the equations. This results in the following expressions for the change in the orbital element

$$\Delta a = 2\sqrt{\frac{a^3}{\mu(1 - e^2)}} \left[\Delta V_r \, e \sin \theta + \Delta V_\phi (1 + e \cos \theta)\right]$$

$$\Delta e = 2\sqrt{\frac{a(1 - e^2)}{\mu}} \left[\Delta V_r \, \sin \theta + \Delta V_\phi \left(\frac{2 \cos \theta + e(1 + \cos^2 \theta)}{1 + e \cos \theta}\right)\right] \qquad (2\text{-}4)$$

$$\Delta i = \sqrt{\frac{a(1 - e^2)}{\mu}} \, \Delta V_z \frac{\cos(\omega + \theta)}{1 + e \cos \theta}$$

$$\Delta \omega$$
$$= \sqrt{\frac{a(1 - e^2)}{\mu}} \left[- \Delta V_r \frac{\cos \theta}{e} + \Delta V_\phi \left\{\frac{\sin \theta(2 + e \cos \theta)}{e(1 + e \cos \theta)}\right\} - \Delta V_z \frac{\cot i \sin(\omega + \theta)}{1 + e \cos \theta}\right]$$

$$\Delta \Omega = \sqrt{\frac{a(1 - e^2)}{\mu}} \Delta V_z \frac{\sin(\omega + \theta)}{\sin i (1 + e \cos \theta)}$$

where, ΔV_r, ΔV_ϕ and ΔV_z are small impulsive velocity increments in the r, ϕ, and z directions.

2.2.1.3 Hill Clohessy Wiltshire equations

The first analysis of the relative motion between spacecraft started with the paper of Clohessy and Wiltshire in 1960 in which they derived the equations of motion of one spacecraft relative to another reference spacecraft that was in a circular orbit [18]. The relative motion between spacecraft, has since then, been extensively studied for spacecraft located close to each other using the Clohessy-Wiltshire equations. These equations describe the relative motion between two spacecraft as an effect of the difference in their initial conditions. The non-linear relative motion has been linearized and the approximation is valid only for small separation distances between the satellites relative to the reference orbit radius. They are also referred to as Hill's equations or Hill Clohessy Wiltshire (HCW) equations as the approach is the same as the one used by Hill to describe the motion of the moon relative to Earth [19]. When dealing with spacecraft, the spacecraft pair is commonly referred to as chief-deputy, leader-follower or target-chaser depending on the mission scenario. A useful frame for expressing the relative dynamics is a target-centred Local-Vertical Local-Horizontal (LVLH) reference frame, also referred to as the Hill frame. The HCW equations provide a simplified model of the dynamics of the chaser in this target-centred coordinate system.

With r, ϕ and z representing the motion in the radial, along-track and cross-track directions as shown in Figure 2-1, the equations describing the motion in the Hill's frame can be written as [20],

$$r = - A\cos(nt + \alpha) + 2(\frac{\dot{\phi}_0}{n} + 2r_0) \qquad (2\text{-}5)$$

$$\phi = 2A\sin(nt+\alpha) + \left(\frac{\dot{\phi}_0 - 2\dot{r}_0}{n}\right) - 3(\dot{\phi}_0 + 2nr_0)t \qquad (2\text{-}6)$$

$$z = A_z\sin(nt + \alpha_z) \qquad (2\text{-}7)$$

where,

$$A = \sqrt{\left(\frac{\dot{r}_0}{n}\right)^2 + \left(\frac{2\dot{\phi}_0}{n} + 3r_0\right)^2} \qquad (2\text{-}8)$$

$$\alpha = \operatorname{atan}\left(\frac{\dot{r}_0}{2\dot{\phi}_0 + 3r_0 n}\right) \qquad (2\text{-}9)$$

$$A_z = \sqrt{z_0^2 + \left(\frac{\dot{z}_0}{n}\right)^2} \qquad (2\text{-}10)$$

$$\alpha_z = \operatorname{atan}\left(\frac{nz_0}{\dot{z}_0}\right). \qquad (2\text{-}11)$$

Here, n is the mean motion and r_0, ϕ_0 and z_0 are the initial radial, along-track and cross-track separations of the spacecraft with respect to the reference spacecraft. It can be seen from Eq. (2-5) to (2-7), that along-track, radial and cross-track velocity increments result in a periodic motion around the reference satellite. However, it is only the along-track velocity increment that results in a secular drift leading to a growing satellite separation with time.

Hill's equations provide an easy and insightful peek into relative dynamics between spacecraft and is the starting point for most of the results using linearized gravitational acceleration models for circular reference orbits. The linearization error affects the long term accuracy in the solution and therefore, a number of solutions to the relative motion problem have been proposed to improve the accuracy of long-term prediction [21]. However, the complexity of these solutions increases as more non-linear factors are incorporated to improve the prediction accuracy.

2.2.1.4 Summary

Cowell's method to propagate orbits in the presence of perturbations is the chosen approach in this study to get orbits. Gauss's variation of parameters and the "Clohessy-Wiltshire" equations are the analytical approaches for relative motion analysis. Developing analytical relations that include all perturbations is cumbersome. For example, the J_2 effect, accounting for the Earth's non-homogeneous mass distribution and representing the equatorial bulge, can be incorporated with little complications, but including the higher order terms from the spherical harmonic expansion representing the Earth's gravity field is quite tedious. Readers are referred to the work of Alfriend

and Yan [22], where different solutions for relative motion such as Hill's solution is contrasted with other solutions that include for example, eccentric orbits of the chief orbit, J_2 effect and other nonlinearities. A brief survey and classification of work on linearized rendezvous can be found in the paper by Carter [23].
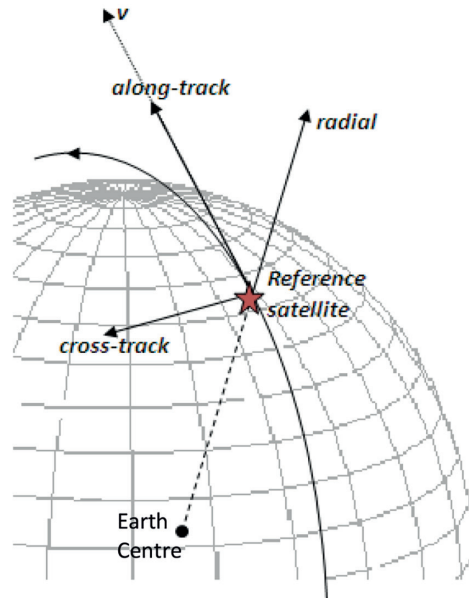

Figure 2-1 | The Hill's reference frame showing along-track (along the direction of the velocity vector), cross-track and radial directions with the reference satellite at the origin

2.2.2 Representations for Relative Motion

An important aspect is the representation of the spacecraft relative geometry. A number of representations have been used to represent relative motion between two spacecraft. It is essential to have an appropriate representation that will provide an intuitive and meaningful understanding of the spacecraft relative motion and evolution over the entire mission. To that end, four different representations for relative motion are explored:

- Differential orbital elements
- Hill's frame with along-track, cross-track and radial separations
- Eccentricity – inclination vectors
- Relative phase and relative inclination with analemmas to represent relative motion

In subsequent sections, the applicability of the above representations to assess the effect of perturbations is discussed. The effect of perturbations can be seen through the difference in select parameters between a reference unperturbed orbit and orbit perturbed with disturbances. The advantages and drawbacks of the different representations are highlighted. Moreover, the

applicability of the parameters introduced in this section for representing the motion of a cluster of spacecraft is discussed.

2.2.2.1 Differential Orbital Elements

An orbit can be defined by using the standard set of orbital parameters $[a, e, i, \Omega, \omega, \nu]$. One way to define the relative orbit between two spacecraft is to use the difference in the orbital elements. A differential orbital element vector is a straightforward difference between the orbital elements of the two spacecraft. In the absence of perturbations, five of the six differential orbital elements remain constant, only the differential mean anomaly changes with time. The differential orbital element is denoted by dk_q where k is the orbital parameter of interest and q denotes the individual spacecraft being analysed.

$$dk_q = k_q - k_0$$
$$k \in \{a, e, i, \Omega, \omega, \nu\}$$

(2-12)

In Eq. (2-12), k_0 is the array of osculating elements of the parameter k of the reference spacecraft S_0 and k_q is the corresponding array of osculating parameter k of the spacecraft S_q.

While dealing with circular orbits, and since ω is undefined for such orbits, the argument of latitude, θ defined as

$$\theta = \omega + \nu$$

(2-13)

is commonly used to specify the position of the spacecraft in orbit. Therefore, $d\theta$, the differential argument of latitude is a more convenient term, to represent differential position in the orbital plane for circular orbits.

A major benefit in using differential orbital elements for representation of relative motion is its direct link with the equations stemming from Gauss variation of parameters. The variation of orbital parameters with time and even under the influence of select perturbations can be analytically assessed through these equations. Since the orbital parameters themselves are well understood, relative motion as a function of differential orbital parameters is convenient for first analysis.

2.2.2.2 Hill's Frame

One of the most common and intuitive way to visualize relative motion is to express the motion in three dimensional space with Cartesian coordinates. The origin is the reference satellite and the relative dynamics of the satellite of interest is expressed through a three dimensional relative position vector and a three dimensional relative velocity vector with respect to the reference satellite. The axes of the Hill's frame are shown in Figure 2-1. This is distinguished from a Frenet frame where one axis is parallel to the orbit velocity vector. For circular orbits there is no major difference between the frames as the velocity vector is perpendicular to the position vector but for elliptical orbits with eccentricity , the Frenet's frame deviates from the Hill's frame.

Visualizing the relative motion through the Hill's frame provides a straightforward insight into the relative dynamics between the spacecraft. The solutions of the Clohessy-Wiltshire equations can be mapped directly onto this frame. However, the evolution and prediction of motion due to perturbations such as complex gravity field and approaches for control are not evident.

2.2.2.3 Eccentricity – Inclination Vectors

The concept of using *e/i* vectors for analyzing relative motion was developed for safe collocation of geostationary satellites [24] and has later been used for proximity analysis in LEO formations. Controlling relative motion through eccentricity-inclination vectors started in the late 1980s, with a change in the mindset and approach for operating geostationary satellites. With increasing demand to maximize the effective use of desirable longitudinal positions, satellite operators started to collocate multiple spacecraft within one longitudinal control box. Collision hazard between collocated geostationary satellites is quite substantial unless their orbit control is properly coordinated. The operators realized that individual satellite control strategy with collision avoidance maneuvers was reasonable when close approaches were rare events. However, limited orbit prediction accuracy makes even 1 km to be considered dangerous and necessitate an avoidance maneuver. Such distances occur quite frequently (about once a month) for uncoordinated station keeping. Therefore, coordinated strategies such as *e/i* based control, to optimally separate the satellites sharing the same window were introduced [25,26].

More recently, the German Aerospace Centre (DLR) has successfully employed *e/i* vector separations for low earth orbit proximity operations [27,28]. The *e/i* representation gives an insight into the relative geometry that is useful to establish safe or collision-free configurations. The idea is based on the phase difference between the radial motion (represented by the *e* vector) and the cross-track motion (represented by the *i* vector). Studying the *e/i* vector will enable us to determine the phase difference required between these two motions which will ensure that the radial separation is maximum when the cross-track separation vanishes and vice versa, leading to a collision free formation.

For near circular orbits, the Keplerian elements e (eccentricity) and w (argument of perigee) can be replaced by the eccentricity vector defined by [29]

$$\boldsymbol{e} = \begin{bmatrix} e_X \\ e_Y \end{bmatrix} = e.\begin{bmatrix} \cos \omega \\ \sin \omega \end{bmatrix}. \tag{2-14}$$

The relative eccentricity between two satellites S_2 and S_1 with respective eccentricity vectors $\boldsymbol{e}_2$ and $\boldsymbol{e}_1$ is given by

$$\Delta \boldsymbol{e} = \boldsymbol{e}_2 - \boldsymbol{e}_1. \tag{2-15}$$

The inclination vector, for small differences in i (inclination) and Ω (right ascension of ascending node), simplifies to

$$\Delta \boldsymbol{i} \approx \begin{bmatrix} \Delta i \\ \Delta \Omega \ \sin i \end{bmatrix} . \tag{2-16}$$

Maintaining a specific phase between the relative eccentricity and relative inclination vectors, along with sufficient amplitude for the two vectors, will ensure a minimum radial or cross-track separation between the two spacecraft at all times. This is also sometimes referred to as applying an *e/i* vector separation to maintain a minimum distance between the spacecraft.

2.2.2.4 Relative Phase and Relative Inclination

This representation scheme is used to visualize the large scale relative motion between co-altitude satellites in a constellation, where two variables – relative inclination i_R and relative phase ϕ_R are used to completely determine the relative motion of co-altitude satellites with circular orbits (see Figure 2-2). An instant drawback is the fact that it cannot represent variations in the radial direction. However, any change in relative orbital planes is easy to identify and analyze.

The variables i_R and ϕ_R are defined as [20],

$$\cos i_R = \cos i_1 \cos i_2 + \sin i_1 \, sin \, i_2 \cos \Delta N \tag{2-17}$$

$$\phi_R = (T_2 - T_1)n + \Delta\phi \tag{2-18}$$

where,

$$\Delta\phi = \phi_2 + \phi_R - \phi_1 \tag{2-19}$$

$$\cos \phi_1 = \begin{bmatrix} \dfrac{\cos i_2 - \cos i_R \cos i_1}{\sin i_R \sin i_1} \end{bmatrix} \tag{2-20}$$

$$\cos(\phi_2 + \phi_R) = - \begin{bmatrix} \dfrac{\cos i_1 + \cos i_R \cos i_2}{\sin i_R \sin i_2} \end{bmatrix} \tag{2-21}$$

In Eq. (2-17) to (2-19), ΔN is the angular separation between the ascending nodes, $T2 - T1$ is the time interval between the satellites crossing their respective ascending nodes, ϕ is defined as the arc length in degrees from the ascending node to the point of intersection of the two orbits and $\Delta\phi$ represents the difference in arc length from the point where the two orbits intersect to their respective ascending nodes.
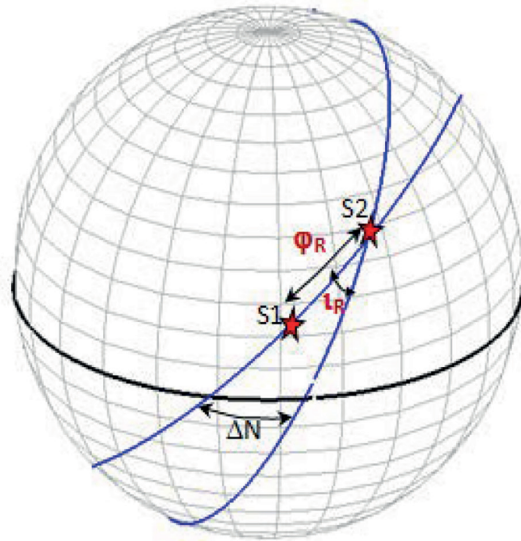
Figure 2-2 | S1 and S2 represent satellites 1 and 2 respectively at the instant of time when S2 crosses the orbit plane of S1. The critical parameters: Relative phase, ϕ_R and relative inclination i_R, for the two satellite orbits are shown
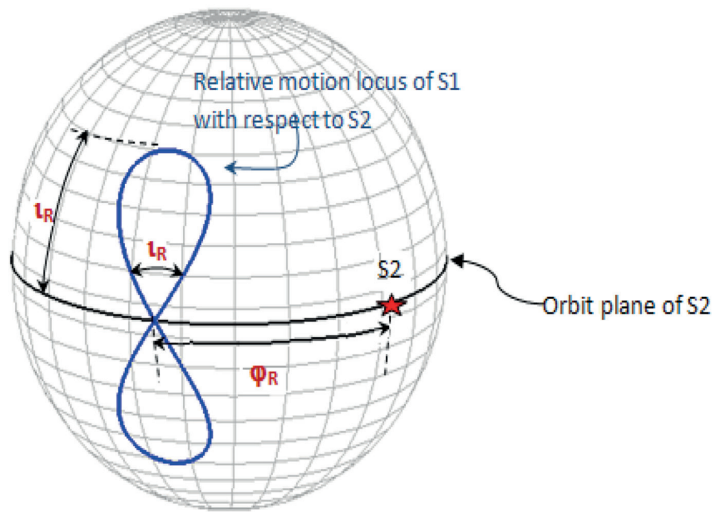
Figure 2-3 | The relative motion of satellite 1 with respect to satellite 2. The relative inclination i_R and the relative phase ϕ_R completely define the relative motion analemmas

Figure 2-3 shows the large-scale relative motion of one satellite with respect to another satellite indicating the role of i_R and ϕ_R in the geometry. The relative motion of the satellite forms a figure-

eight pattern or analemma. The figure clearly shows that i_R and $\phi_{R'}$ together completely define the relative motion geometry. The equations of motion for the analemma are given as [5]

$$\sin \delta = \sin i_R \sin nt \qquad (2\text{-}22)$$

$$\alpha = nt - \mathrm{atan}\,(\cos i_R \tan nt\,) \qquad (2\text{-}23)$$

where t is the time, n is the mean motion, δ and α are the elevation and azimuth components of the analemma respectively.

2.2.2.5 Summary

Different representations for relative motion between spacecraft can be used to draw meaningful and insightful information on relative dynamics between spacecraft. Some of these representations and their applicability were addressed in this section. These representations serve as an excellent tool to understand and model the effect of perturbations and can provide valuable pointers for prediction and control of dynamics. However, most of these representations are suitable for pairs (doublets) of satellites and although they can be applied with some increase in complexity for multiple satellites, these representation do not evolve naturally and intuitively for a network of spacecraft. Most of the parameters in the representation schemes that were discussed are not scalable for a network. For a spacecraft cluster, we require parameters that can characterize global trends of a network. In the next section such network parameters will be defined and developed.

2.3 Measure of Distribution

In a cluster with multiple satellites, it is important to have a measure that is representative of how these entities are distributed within this cluster. The aim is to have a quantitative indicator of the spatial distribution of satellites in such a cluster. This indicator can be used to assess, for example, parameters such as coverage, revisit time or resolution of the DSS.

A commonly used method for dealing with distribution of systems involving a large number of entities is based on the kinetic gas theory, where all entities are considered as particles which are in constant random motion. This method has been proposed for certain terrestrial 2-D applications involving robot swarms [30,31]. ESA's MASTER model [32] and NASA's EVOLVE model [33] to simulate collisions in space based on random motion of debris also employ the laws of kinetic gas theory. However, for a DSS with spacecraft deployed to achieve certain configurations, the motion cannot be assumed as random or non-correlated and the laws of kinetic gas theory cannot be applied.

There are classical approaches in statistics that involve hypothesis tests on homogeneity such as chi-squared tests to get a 'yes' or 'no' answer [34] on homogeneity, but these do not provide information on how uniform or non-uniform the system is. Metrics such as 'discrepancy' [35] have been used that

provide a quantitative measure of how non-uniform the distribution is. Schilcher et al. proposed a measure of inhomogeneity of node distribution for wireless networks that corresponded with human perception as well [34]. In this paper, a cluster distribution index (CDI) is developed that extends the concept of discrepancy and inhomogeneity to dynamic 3-D space networks.

In many space applications a uniform distribution is a desirable configuration, for example, to optimize re-visit time. Multiple spacecraft are typically used in Earth observation missions to increase revisit time. Assume a simplistic multi-satellite mission scenario where all the spacecraft are distributed around the same orbit. A typical mission objective for in-situ measurements could be to minimize the shortest interval between successive spacecraft visits to a spatial point that is sampled. The objective is achieved as long as the spacecraft distribution is uniform, and any deviation from uniformity implies a sub-optimal scenario. In this study we consider a uniform distribution and characterize how much the given configuration deviates from this uniform distribution. For some specific application scenarios, a custom distribution of the spacecraft may be required where the deviation from this specific configuration can be derived similarly to the CDI.

2.3.1 Cluster distribution index

To introduce the distribution index which will be developed in this section, imagine a swarm of birds in the sky and assessing the spatial distribution of this swarm. The idea proposed in this work, in a simplified version, involves overlaying a virtual cuboid that houses this swarm such that the sides of the cuboid represent the boundaries of the swarm. This cuboid is divided into equal-volume sub-cuboids in all three dimensions, keeping the number of these sub-cuboids as close to the number of birds in the swarm. The percentage of bird-occupied sub-cuboids is then a direct measure of the uniformity in the spatial distribution. When we add to this, features such as the ability to dynamically rotate this cuboid, resize and repopulate sub-cuboids, transform between reference frames, and extend it to toroidal shapes, it allows us to measure and analyse spatial distribution of massively distributed systems in space.

The Cluster Distribution Index (CDI) measures the instantaneous uniformity of the spatial distribution of the spacecraft within the cluster. The time-varying boundary of the satellite cluster is divided into equal sized grids in n-dimensional space. Depending on the application, n can take on any values from the set $n = \{1,2,3\}$. The three dimensions can correspond to, for example, the along-track, cross-track and radial dimensions when working with the Hill's frame or the dimensions could correspond to latitude, longitude and height when the geodetic reference frame is chosen. The cluster can be divided into grids along all the three dimensions to analyse the overall distribution or just in selected dimensions such as along-track and radial to analyse the in-plane spatial distribution of the cluster.

At each epoch, the cluster is divided into a number of equally sized grids. The CDI can be defined as,

$$\zeta = \frac{G_S}{N_S} \tag{2-24}$$

where G_S is the number of grids containing one or more spacecraft in it and N_S is the total number of spacecraft in the cluster.

At every epoch, the cluster is divided into a total of G_T equally sized grids. The value of G_T is critical and the procedure to estimate G_T is described below. The total number of grids in the cluster G_T is given as,

$$G_T = \prod_{k=1}^{n} G_k, \quad n = \{1,2,3\} \tag{2-25}$$

where G_k is the number of grid segments in dimension k. If we denote d_n as the length of the cluster in dimension n, then we define g_k as,

$$g_k = w_k \frac{d_k}{\sum d}, \quad k = 1 \text{ to } n. \tag{2-26}$$

where $\sum d$ is the sum of the lengths of the cluster in n dimensions. The number of grid points in each axis is proportional to the maximum cluster separation in that dimension and w_k is a factor that allows to weight a particular dimension based on its relevance. G_k is defined as,

$$G_k = \lfloor F \cdot g_k \rfloor \tag{2-27}$$

where F is the largest scaling factor that ensures

$$G_T \leq N_S. \tag{2-28}$$

For a single dimension, $n = 1$, G_T is equal to the number of satellites N_S. The constraint in Eq. (2-28) ensures that the CDI approaches unity for a homogeneous distribution.

The range of the distribution index is given as,

$$\frac{2}{N_S} \leq \zeta \leq 1 ; (\forall N_S \geq 2) \tag{2-29}$$

The higher the index, the greater is the uniformity of distribution. The lower limit of the distribution index implies that all the spacecraft in the cluster are confined to within two grids and the upper limit of unity implies a distribution that is uniform or very close to uniform. The above limits do not hold for the case when there are two satellites and both of them are collocated.

The Cluster distribution index can now be used as an effective measure of homogeneity in the spatial distribution of the network. CDI incorporates a dynamically changing envelope as the cluster evolves. This gives a better representation for the instantaneous distribution.

2.3.2 Simulation and Results

A software setup is established to simulate a cluster of spacecraft in a low earth orbit (LEO) that can include the effect of typical perturbations such as drag and aspherical gravity field. To illustrate the applicability of CDI, a scenario with 50 spacecraft with varying cross-sectional area, uniformly distributed in along-track is considered. The spacecraft are then subjected to drag for duration of 5 days. The effect of the differential drag on the spatial distribution of the cluster is then characterized through the CDI. The section concludes with a sample illustration of the applicability of CDI in a two-dimensional scenario using the GPS constellation as a case study.

The simulation parameters are shown in Table 2-1. The differential drag between the spacecraft is controlled through the drag coefficient, cross-sectional area and mass of the spacecraft. Two cases of 50% and 100% variation in differential drag between the spacecraft are simulated. For the 50% variation, each spacecraft in the cluster is randomly allocated a drag multiplication factor extracted from a uniform distribution between 0.5 and 1.5. The differential drag case of 100% is not a likely scenario, but represents an extreme case of one spacecraft experiencing a very high drag and another spacecraft with no drag, through drag compensation for example. The initial conditions of the reference spacecraft are shown in Table 2-2. The simulations are performed at two altitudes of 400 km and 500 km to investigate the effect of changing density, and hence drag conditions.

Table 2-1 | Cluster simulation parameters

Integration	ODE45 (MATLAB®)
	RelTol 10^{-13} AbsTol 10^{-6}
Reference system	True of Date
Central body	Earth
Gravity field	Central force without perturbations
Third body	None
Non-conservative forces	Atmospheric drag
Atmospheric density	Harris-Priester model
Drag coefficient, CD	2.2
Spacecraft Model	Box model (10cm x 5cm x 2cm)
Area of cross section	Nominal: 0.025 m^2
Mass	0.1 kg
Differential drag	Case 1) ±50% between spacecraft; uniform distribution
	Case 2) ±100% between spacecraft; uniform distribution
Attitude control	None
Solar array	Body Fixed
Number of satellites	50
Initial along-track separation	0.01 degree between each satellite
Duration of simulation	5 days

Table 2-2 | Initial conditions of reference spacecraft

Semi-major axis a (2 cases)	6778 km; 6878 km
Eccentricity e	0
Inclination i	90°
Right ascension of ascending node	0°
Argument of perigee ω	0°
Mean anomaly at epoch	0°
Epoch	January 1st 2016 00:00:00 UTC
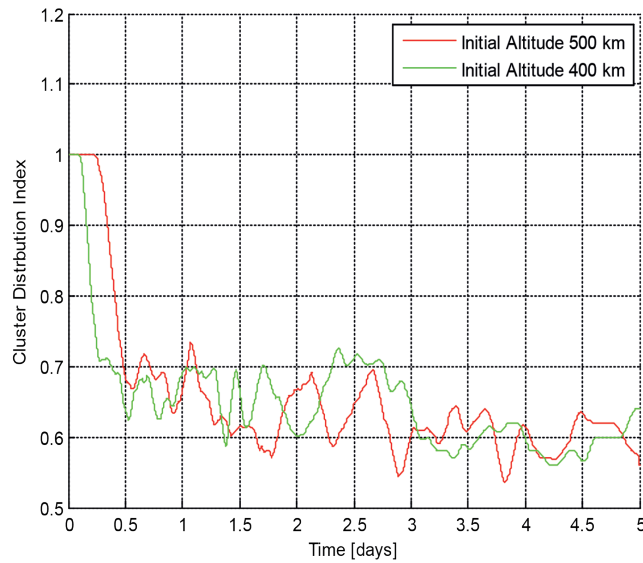
Figure 2-4 | CDI as a function of time for a differential drag variation of 50% between the spacecraft at 400 km and 500 km

The change in CDI with time for a differential drag variation of 50% between the spacecraft at 400 km and 500 km is shown in Figure 2-4. A moving average filter with a window size corresponding to one minute has been applied to the instantaneous CDI values to provide a more insightful trend in the behaviour of the CDI. The spacecraft are initially distributed uniformly in the along-track direction. The differential drag between the spacecraft causes the separation to deviate from this uniform initial configuration. Essentially, what the CDI represents for this 1-dimensional scenario, is the uniformity of the along-track separation. Figure 2-4 clearly shows the CDI for 400 km and 500 km dropping from unity to a lower value and then settling down at a value of around 0.6 by day 5. At 400 km, because of the higher atmospheric density and higher drag, the spacecraft spread faster than at 500 km and after just about one orbit, the uniformity is lost and the CDI starts to steeply fall from unity. The CDI for the 500 km orbit falls off from unity at a later point, at about the 4th orbit. The

time-scale of five days has been chosen to illustrate two key points. First, that the drop-off from unity is earlier for the 400 km orbit where the density is higher. The second point is that in both cases (400 and 500 km) the CDI converges to a value of around 0.6. Only the rate at which CDI approaches the steady state is different between the two cases. The along-track separation between the spacecraft for the two altitudes is shown in Figure 2-5. It is clear that the spacecraft spread in along-track is much faster at 400 km. Simulations that included higher order gravity terms up to degree and order 20, showed similar trend in CDI evolution for the along-track separated spacecraft.
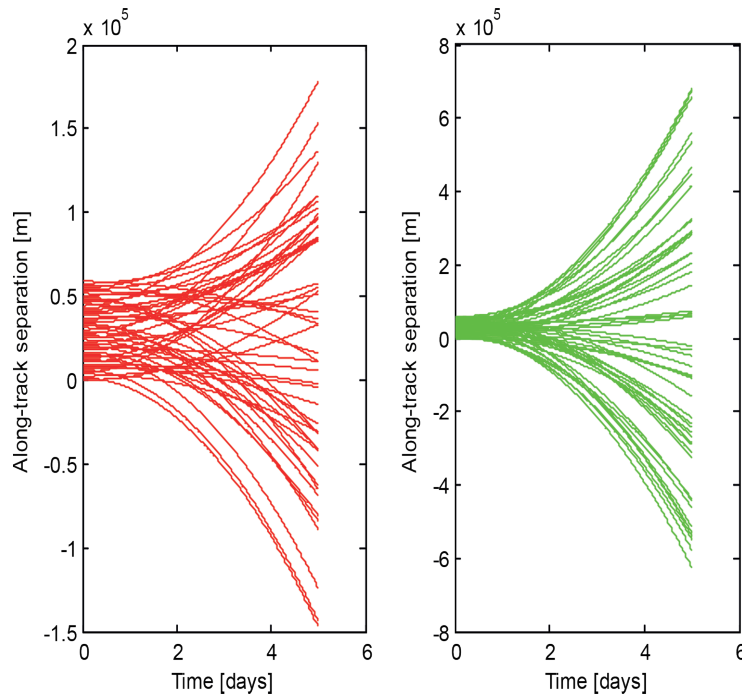

Figure 2-5 | Evolution of the along-track separation with time for a differential drag variation of 50% between the spacecraft in the cluster. (Left: Altitude of 500 km; Right: Altitude of 400 km)

In Figure 2-6, the trend in CDI for a differential drag variation of 50% and 100% at 400 km is shown. The corresponding along-track separations are shown in Figure 2-7. The CDI for 100% variation in differential drag drops off earlier to reach a steady state value close to 0.6.

The above analysis clearly shows that the differential drag can disturb the spatial uniformity of the cluster. The CDI for all cases drops from unity to a steady state value close to 0.6. The variation in altitude and magnitude of differential drag determine when the drop starts. The CDI changes rapidly from close to unity towards a value of around 0.6 and then hovers around this value. The same scenario was also simulated for a duration of 10 days for the orbit altitude of 400 km. The results

showed that once the CDI drops from unity to a value of around 0.65, it continued to hover around this value. The reason for the drop from unity is clear – the differential drag between the spacecraft leads to differential separations between the spacecraft. Therefore, starting from a uniform configuration, the spatial distribution changes once the differential drag comes into effect. The differential drag between the spacecraft is simulated through randomly assigning each spacecraft, a drag coefficient that varies between 1 and 3, deviating +/-1 from a nominal coefficient of 2. Ideally, if these drag coefficients varied uniformly between 1 and 3, then this would have resulted in a uniform difference in differential accelerations. A uniform difference in accelerations would then result in quadratic separations. For 50 spacecraft, the CDI for uniformly distributed drag coefficients, when computed as defined in section 2.3.1, would result in a value 0.76. From mission perspective, the CDI variation can provide valuable input to spacecraft structure design, necessity and accuracy of attitude control and other design drivers. The CDI can also be used as a control variable which needs to be maximized or minimized depending on the application.

The variation of the CDI in Figure 2-6 provides an indication of the effect of differential drag in along-track separations. High volatility in CDI would correspond to high volatility in parameters such as spacecraft cross-sectional area or attitude control that drive differential drag. Consider the example of a satellite mission for earth imaging where multiple satellites are used to increase revisit time. The objective is to minimize the shortest interval between successive revisits. Instead of monitoring the separation distances between all pairs of satellites, CDI can serve as a single global control variable that can be monitored and optimized.
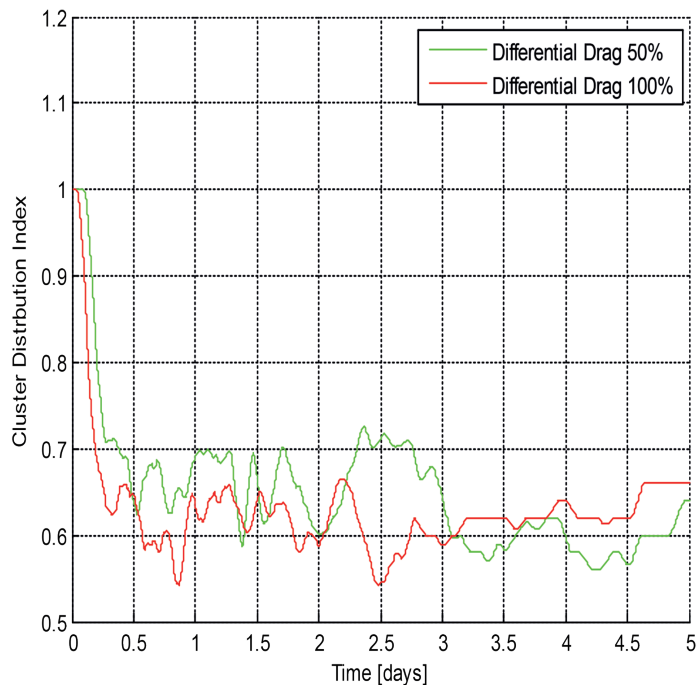

Figure 2-6 | CDI as a function of time for a differential drag variation of 50% and 100% between the spacecraft at 400 km altitude

The GPS constellation can be used to illustrate the applicability of CDI for a two-dimensional scenario. The positions of the spacecraft are based on the initial positions from the daily GPS broadcast ephemeris file brdc0010.18n [36] and the orbits are then propagated in a zero-perturbation environment. The behaviour of CDI for the GPS constellation for a chosen duration of 12 hours is shown in Figure 2-8. The top graph shows the instantaneous magnitude of the CDI, while the bottom graph displays a smoothed-out CDI, processed through a moving average filter with a 10-minute window size. The spatial distribution is based on the latitude and longitude of 30 GPS satellite ground tracks. The smoothed CDI can be seen to vary from a magnitude slightly higher than 0.7 to a maximum value close to 0.83. To get an intuitive idea of how the GPS constellation is spatially distributed at these low and high CDI instances, a 3D histogram that captures the GPS satellite distribution in latitude and longitude at epochs corresponding to lowest and highest values of CDI is shown in Figure 2-9. It is clear, that with respect to global coverage, the histogram on the right side of Figure 2-9, corresponding to a high value of CDI, is the more desirable one. The advantage of the CDI is that it captures the uniformity in the spatial distribution of the GPS constellation in a single variable.
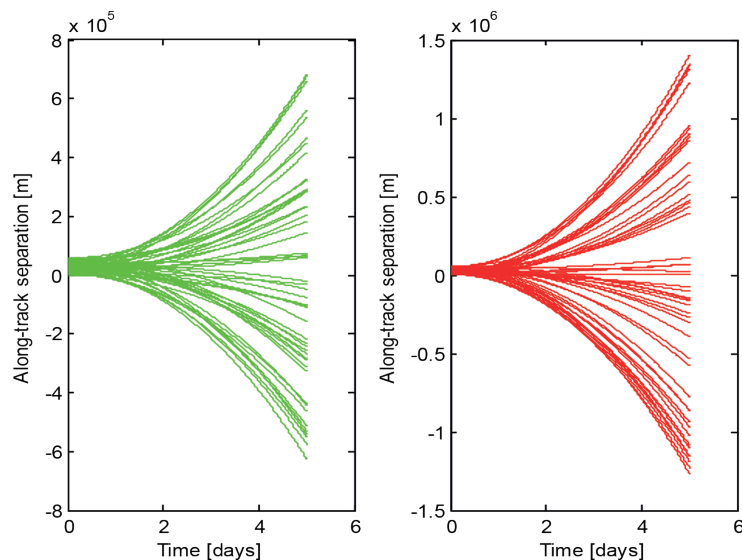
Figure 2-7 | Evolution of the along-track separation with time at 400 km altitude. (Left: Differential drag variation of 50%; Right: Differential drag variation of 100%)

2.3.3 Limitations and Recommendations

The current set of tools developed to evaluate the CDI allow the assessment of the spatial deviation of a distributed space system from a uniform distribution in 3D space. The software allows custom weighting of the different dimensions and the evaluation is based on a continuously changing envelope to capture the instantaneous spatial separations.
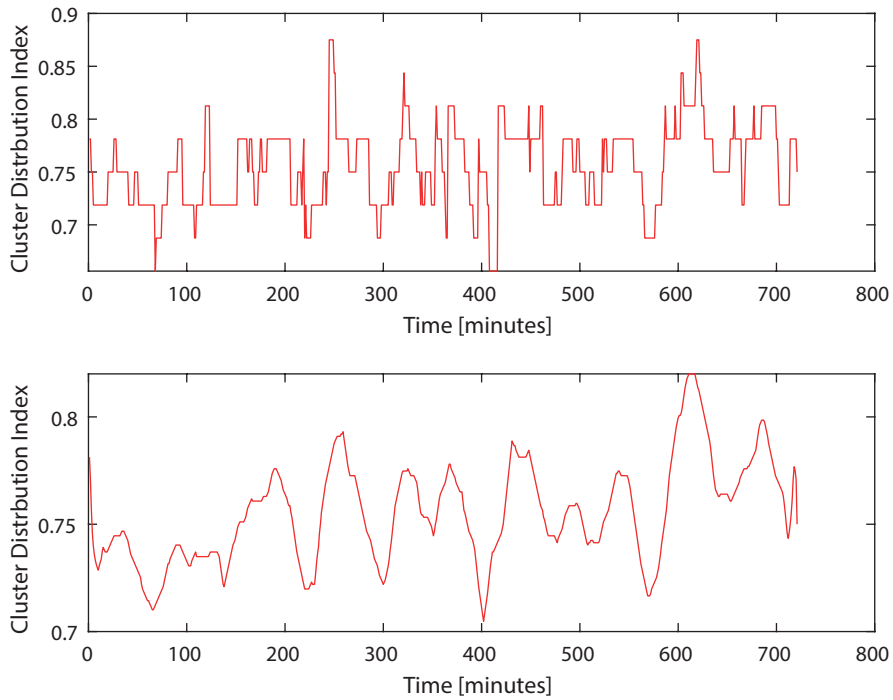
Figure 2-8 | Top: CDI for the GPS constellation (30 spacecraft) for a duration of 12 hours (1st January 2018 00:00 UTC to 12:00 UTC), based on latitude and longitude of the satellite ground tracks. The positions of the spacecraft are based on the initial positions from the daily GPS broadcast ephemeris file brdc0010.18n [36] distributed through the Crustal Dynamics Data Information System (CDDIS) [37]. Bottom: The CDI smoothed with a moving average filter with a window size corresponding to 10 minutes.

Figure 2-9 | 3D histogram representing the distribution of the satellites in the GPS constellation corresponding to the minimum CDI (left) and maximum CDI (right) shown in Figure 2-8.

However, the total number of grids is constrained by the total number of spacecraft. This poses a limit on the resolution of the discrepancy measure and becomes apparent when the number of spacecraft is not large.

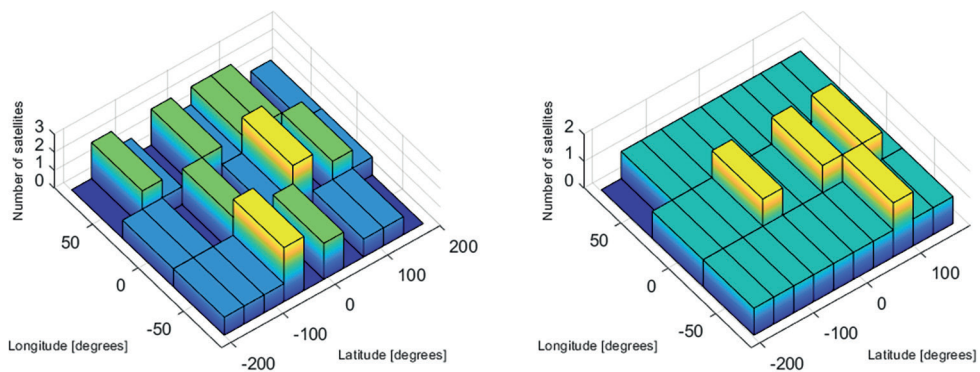Consider two sample configurations of a five-spacecraft system separated along one dimension as shown in Figure 2-10 to illustrate the importance of the grid size. The CDI in both cases is evaluated as unity, indicating a zero discrepancy from uniformity. This shows the limitation posed by the grid formation in this approach to evaluate CDI.

Case a)

| x | x | x | x | x | CDI = 5/5 = 1 |

Case b)

| | x | x | | x | x | | x | CDI = 5/5 = 1 |

Figure 2-10 | Two sample distributions of five spacecraft along one dimension of interest. 'x' indicates spacecraft

This can be overcome by introducing dummy spacecraft and artificially increasing the number of grids retaining the same envelope and boundaries. The lower limit of CDI increases but the sensitivity to small separations increase as shown in the computed CDIs in Figure 2-11. Clearly, the small separations which could not be captured earlier, represented through Figure 2-10, are now inducing a significant effect on the magnitude of CDI, shown in Figure 2-11. A similar approach can also be used to investigate scenarios where discrepancy with respect to non-uniform distributions need to be assessed.

Case c)

| o | x | o | o | x | o | o | x | o | o | x | o | o | x | o | CDI = 15/15 = 1.00 |

Case d)

| xo | | o | xo | | o | o | | xo | o | | xo | o | | xo | CDI = 10/15 = .67 |

Figure 2-11 | Two sample distributions of five spacecraft along one dimension of interest. 'x' indicates actual spacecraft and ten dummy spacecrafts are introduced and denoted by 'o'

2.4 Collision Probability

Determining the probability of collision is not straightforward and requires the integration of overlapping multi-dimensional probability distribution functions. Therefore, in most works on collision analysis, a number of assumptions are introduced to simplify collision probability analysis [38] which are summarized here. The objects are modelled as spheres and each object's positional

uncertainties are combined to create a unified error ellipsoid and the radii of both the objects are summed to form a larger hard body radius, R. The uncertainty in the relative position between the objects is then defined by a three-dimensional Gaussian distribution of the form [39].

$$\rho(\boldsymbol{X}) = \frac{1}{(2\pi)^{3/2} \ \sigma_x \ \sigma_y \ \sigma_z} \ e^{\left[-\left(\frac{x^2}{2\sigma_x{}^2}\right)-\left(\frac{y^2}{2\sigma_y{}^2}\right)-\left(\frac{z^2}{2\sigma_z{}^2}\right)\right]} \tag{2-30}$$

where $\boldsymbol{X}$ is the relative position vector with x, y and z as the individual components and σ_i represents the associated errors of the combined error ellipsoid. The collision probability, p_c for a given $\boldsymbol{X}$ is the volume integral of the uncertainty over the sphere of radius R,

$$p_c(\boldsymbol{X}) = \iiint\limits_V \rho(\boldsymbol{X}) \, \mathrm{d}x \ \mathrm{d}y \ \mathrm{d}z. \tag{2-31}$$

Evaluating the volume integral of the three-dimensional probability density function $\rho(\boldsymbol{X})$ is cumbersome and computationally intensive. The above problem can be reduced to a two-dimensional problem by projecting the error ellipsoid onto the plane perpendicular to the relative velocity and eliminating the dimension parallel to the relative velocity vector [40,41]. To further ease the computational load, Patera [39] proposed a formulation which reduced the problem to a one-dimensional integral where the integration is done around the perimeter of the area.

2.4.1 Collision Probability for Non-linear relative motion

The above simplified methods for determining collision probability assume a linearized motion. This is justified when the relative velocity between the objects is very high, as in the case of spacecraft and debris, and the time that the spacecraft spends in the encounter region is less than a few seconds. However, when we consider the dynamics between two spacecraft, especially when deployed together, the linearization assumption is not valid anymore.

For non-linear motion, Patera [42] proposed a method to calculate the instantaneous collision probability by transforming the problem into a scaled space, where the relative position error probability density is symmetric in three-dimension. The total collision probability for a given time is obtained by integrating the instantaneous probability over appropriate intervals that the non-linearity allows.

To summarize, the basic steps in determining the collision probability can be outlined in 3 key steps:
1. *Orbit propagation:* From point of closest approach, propagation of position, velocity and covariance is done backward/forward in time until a user limit is reached. The user limit can be based on the required accuracy of collision probability.
2. *Uncertainty ellipsoid calculation:* The ellipsoid is computed based on the covariance. When an orbit is propagated to determine the state vector, the associated covariance matrix contains

the uncertainty information. The individual error ellipsoids are then combined to form a unified error ellipsoid.

3. *Collision probability evaluation:* The uncertainty ellipsoids are projected on the plane perpendicular to relative velocity. This is done either by assuming linear relative motion and a constant relative velocity vector throughout the brief encounter or, for the non-linear case, a changing direction of the relative velocity that can be included by breaking the collision path into smaller nearly linear sections and then computing the collision probability. Collision potential is determined from the object footprint on the projected (and scaled in the case of non-linear motion) two-dimensional covariance ellipse.

2.4.2 Collision Analysis using Line-Integral Method [CALM]

In this thesis, we propose a simplified, computationally less-intensive approach to calculate the collision probability in a network of spacecraft that matches the results obtained from the non-linear approach of Patera to within one percent error. Collision Analysis using Line-Integral Method (CALM) exploits the following assumptions to simplify the problem:

a. The relative distance between the spacecraft is small compared with the semi-major axis of the satellite orbits, allowing the use of relative dynamics model such as the Hill-Clohessy-Wiltshire equations to determine the relative position between the spacecraft. In this study, we do not include the effect of orbital perturbations in the dynamics model.

b. Typical velocity increments, from deployment mechanisms to launch multiple spacecraft, are significantly smaller than the orbital velocity, enabling the error ellipsoids computed with respect to individual spacecraft body-frames to be directly combined to form the unified error ellipsoid with negligible error. The frame misalignment is less than 0.1° for velocity increments up to 10 m/s in LEO.

c. This is the third and the most significant assumption to reduce the computational load. The size of the error ellipsoid is significantly larger (in the order of hundreds of meters) than the combined hard body radius R (typically less than 0.5 m for nanosatellites). This allows the uncertainty in the relative position expressed in Eq. (2-30), to be treated as a constant throughout the volume of the combined hard body sphere. The collision probability in Eq. (2-31) can then be approximated as,

$$p_c(\boldsymbol{X}) = \iiint \rho(\boldsymbol{X})\, dx\, dy\, dz \;\approx\; \rho(\boldsymbol{X}) \cdot \frac{4}{3}\pi R^3. \qquad (2\text{-}32)$$

The volume integral is now reduced to a scalar multiplication to evaluate the instantaneous collision probability, which simplifies the computational load immensely. Eq. (2-32) computes the instantaneous collision probability. The overall collision probability within a pair of spacecraft using the line integral method P_c^{CALM} can be calculated by integrating $\rho(X)$ along the trajectory described by the relative motion,

$$P_c^{CALM} \;\approx\; \pi R^2 \int_L \rho(\boldsymbol{X}) \cdot dl\;. \qquad (2\text{-}33)$$

In Eq. (2-33), L represents the trajectory of the relative motion during the time of interest. If the trajectory would be a straight line, then the volume swept through would be a cylinder of radius R with hemispherical ends. The right hand side of Eq. (2-33) does not include these hemispherical extremities in evaluating the overall collision probability as their contribution is negligible. This is then repeated between all pairs of spacecraft in the network to assess the total collision probability within the network , referred to as the cluster collision probability (CCP).

2.4.3 CALM – Simulation and validation

This section investigates the validity of the line-integral method by comparing it with Patera's method for non-linear motion. Encounter trajectories with respect to a reference spacecraft are propagated in a zero-perturbation environment. Two encounter trajectories are chosen to represent different collision scenarios. The first trajectory is a close pass-by in along-track and radial plane, with a nominal miss distance of 500 m. The second trajectory is an oscillatory motion with, also, a nominal miss distance of 500 m. These two trajectories are depicted in Figure 2-12. The collision probability between the reference spacecraft and encounter spacecraft for both trajectories is evaluated with the proposed line-integral method, CALM and Patera's method for different combined error ellipsoids.

The implementation of Patera's method was verified by comparing the results for a linear trajectory with methods developed by Chan [43] and Foster [44]. The difference with Patera's linear method was found to be less than 0.075% and there was no visible difference between Patera's linear and non-linear results. A more elaborate discussion on comparing the results can be found in the thesis work on collision analysis by Florijn [45].

Three different scenarios are chosen for each trajectory: a) A homogeneous combined error ellipsoid with a standard deviation, $\sigma = 1000$ m in all the three dimensions; b) A non-homogeneous combined error ellipsoid with $\sigma_{at} = 5000$ m, $\sigma_{ct} = 2000$ m $\sigma_{rad} = 1000$ m where the subscripts at, ct and rad represent along-track, cross-track and radial dimensions respectively; c) A time varying homogeneous combined error ellipsoid with σ varying from to in the time span of the encounter.

For *case a*, different integration step sizes are chosen for the line-integral method to find whether an increase in the step size results in more accurate results. The step size for Patera's method is set to 200 steps for the duration of the encounter (100 minutes), a value for which the results have been verified to not change significantly.

Figure 2-13 shows the difference in the probability of collision in percentage between CALM and Patera's method for trajectory T1 for an encounter duration of 100 minutes. As can be clearly seen in the figures, the results is accurate until the ratio between the combined hard body radius to the size of the error ellipsoid, R/σ becomes too large.
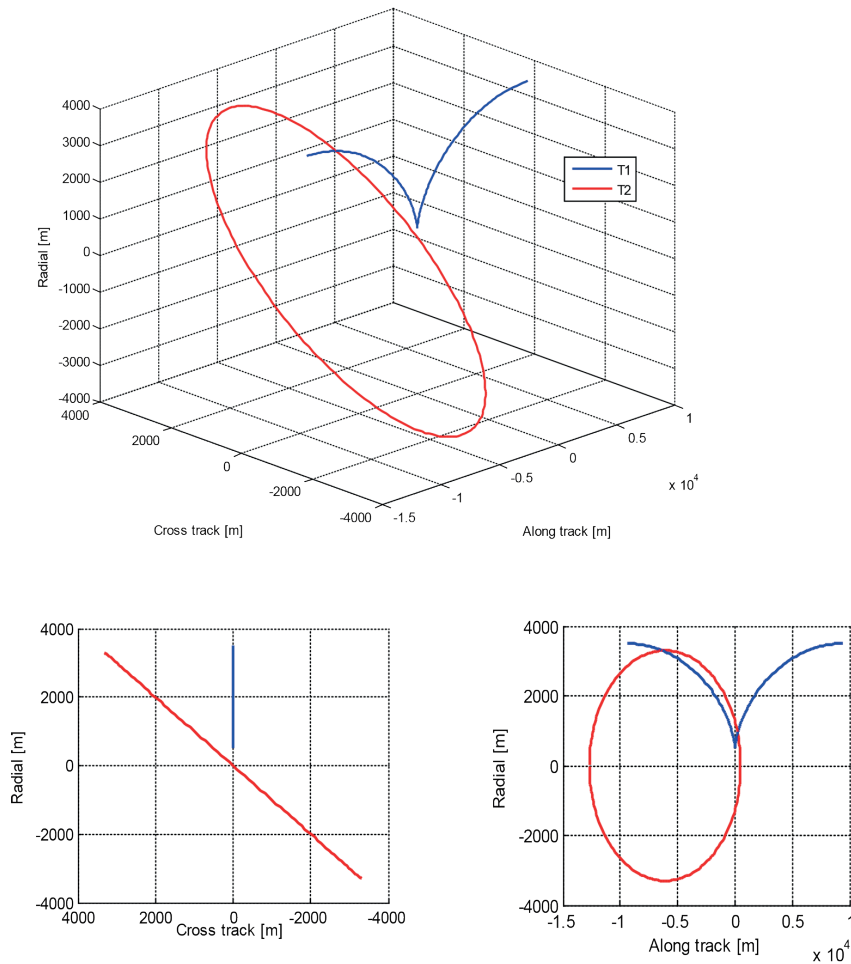
Figure 2-12 | The two encounter trajectories with nominal miss-distance of 500 m. T1 is a close pass-by in along-track and radial plane, T2 is an oscillatory motion about the reference spacecraft

The results for scenarios yield similar outcome as the homogenous case and are therefore not shown. The results of all scenarios and trajectories are tabulated in Table 2-3, in which CALM (10000 steps) is compared with Patera's method. The difference with Patera's method is smaller than 1% for R/σ values up to 0.2. Furthermore, the difference for the non-homogeneous scenario for the first trajectory is smaller than the other cases. This is due to the fact the non-homogeneous error ellipsoid is orientated in such a manner, that the value of R/σ is smaller in radial and along-track direction. The computational speed of the line-integral is, on average, 1850 times faster than Patera's method.
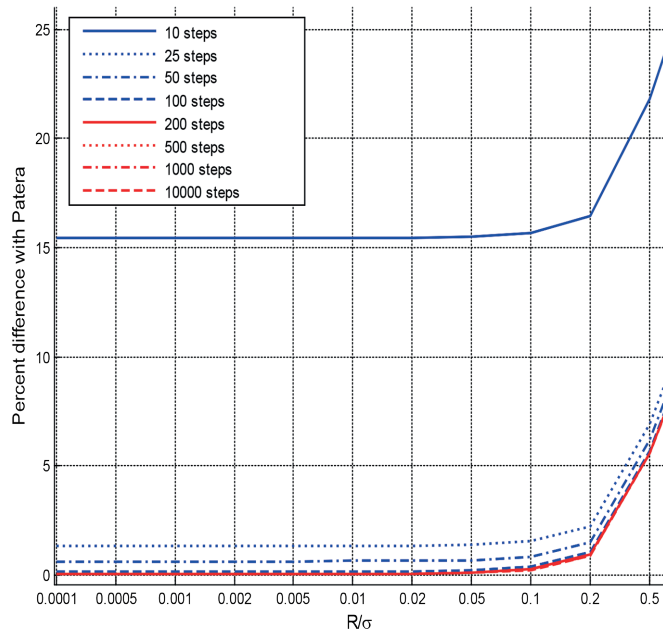
Figure 2-13 | Comparison of the collision probability between CALM and Patera's method for trajectory T1

Table 2-3 | Comparison of CALM (10000 steps) with Patera's method for non-linear collision probability. T1 and T2 indicate the first and second encounter trajectory respectively

R/σ	Case a) Homogeneous		Case b) Non-homogeneous 5000-2000-1000		Case c) Time varying	
	T1 [%]	T2 [%]	T1 [%]	T2 [%]	T1 [%]	T2 [%]
0.0001	0.0295	0.0166	0.0232	0.0166	0.0402	0.0166
0.0005	0.0295	0.0166	0.0232	0.0166	0.0402	0.0166
0.0010	0.0296	0.0166	0.0232	0.0166	0.0402	0.0166
0.0020	0.0296	0.0167	0.0233	0.0167	0.0403	0.0167
0.0050	0.0301	0.0171	0.0234	0.0171	0.0406	0.0170
0.0100	0.0317	0.0186	0.0237	0.0186	0.0416	0.0182
0.0200	0.0382	0.0244	0.0250	0.0244	0.0456	0.0227
0.0500	0.0834	0.0654	0.0337	0.0654	0.0741	0.0547
0.1000	0.2454	0.2117	0.0635	0.2117	0.1761	0.1690
0.2000	0.8953	0.7986	0.1799	0.7986	0.5851	0.6269
0.5000	5.5495	5.2491	1.0023	4.8379	3.5112	4.0206
0.7500	12.6833	11.3697	2.2183	11.3697	7.9173	9.7834
1.0000	23.1928	20.6701	3.9358	20.6701	14.3633	15.7302
2.0000	110.5356	98.3029	15.9848	98.3029	64.5315	71.3642

2.5 Conclusions and Recommendations

Two distinct metrics to characterize a DSS have been developed, analyzed and discussed: a cluster distribution index (CDI) and a measure for cluster collision probability (CCP) using the line-integral method (CALM). The metrics can be used either as an optimization variable in the mission design process for a DSS or as a control variable during operations. The CDI is an effective measure of spatial distribution within the network and a numerical n-dimensional grid-based method to derive the CDI has been developed. The applicability of CDI for a cluster of spacecraft under the influence of differential drag has been discussed. It has been shown that the CDI can be effective in capturing the influence of perturbations on spatial distribution.

The collision probability within a network is an important measure for DSS with a large number of spacecraft. The collision analysis using line-integral method (CALM) is proposed as a computationally efficient approach for collision analysis. The validity of the method is assessed by comparing results with existing non-linear methods which demonstrated an approximation better than one percent and a much lower computational load. The method for collision analysis has been developed in particular for DSS comprising of small spacecraft that are intended to be launched from a single deployment mechanism.

2

References

[1]   S. Engelen, C. Verhoeven and M. Bentum, "OLFAR, A Radio Telescope based on Nano-satellites in Moon Orbit," in *24th Annual AIAA/USU Conference on Small Satellites, UTAH, USA*, 2010.

[2]   D. Barnhart, T. Vladimirova and M. Sweeting, "Very-Small-Satellite Design for Distributed Space Missions," *Journal of Spacecraft and Rockets, Vol. 44, No. 6,* 2007.

[3]   C. Angadi and P. Sundaramoorthy, "Femto-satellite System Architecture & Mission Design for LEO Applications," in *International Astronautical Congress*, Naples, Italy, 2012.

[4]   P. Sundaramoorthy, E. Gill and C. Verhoeven, "Enhancing ground communication of distributed space systems," *Acta Astronautica,* vol. 84, pp. 15-23.

[5]   G. McVittie and K. D. Kumar, "Design of a COTS Femtosatellite and Mission," in *AIAA SPACE Conference & Exposition*, 2007.

[6]   T.-R. Hsu, "Miniaturization – A paradigm shift in advanced manufacturing and education," *A plenary speech delivered at the 2002 IEEE/ASME International conference on Advanced Manufacturing Technologies and Education in the 21st Century, Chia-Yi, Taiwan, Republic of China,* 2002.

[7]   W. Morrow and T. Rogers, "The West Ford Experiment - An Introduction to this Issue," *Proceedings of the IEEE, pp. 461-468,* vol. 52, no. 5, 1964.

[8]   H. Schaub, S. Vadali, J. Junkins and K. Alfriend, "Spacecraft Formation Flying Control using Mean Orbit Elements," *Journal of the Astronautical Sciences,* vol. 48, no. 1, pp. 69-87, 2000.

[9]   C. Sabol, R. Burns and C. McLaughlin, "Satellite Formation Flying Design and Evolution," *Journal of Spacecraft and Rockets,* vol. 38, no. 2, 2001.

[10]   P. Sundaramoorthy, E. Gill and C. Verhoeven, "Relative Orbital Evolution of a Cluster of Femto-satellites in Low Earth Orbit," *Spaceflight Mechanics - Advances in the Astronautical Sciences,* vol. 136, 2010.

[11]   J. Chu, J. Guo and E. Gill, "Fractionated space infrastructure for long-term earth observation missions," *IEEE Aerospace Conference,* 2013.

[12]   S. Engelen, E. Gill and C. Verhoeven, "On the Reliability, Availability and Throughput of Satellite Swarms," *IEEE Transactions in Aerospace and Electronic Systems,* vol. 50, no. 2, 2014.

[13]   C. Lafleur, "Table of Spacecrafts Launched in 2013," Jan. 2014. [Online]. Available: http://claudelafleur.qc.ca/Spacecrafts-Table-2013.html.

[14]   O. Montenbruck and E. Gill, Satellite Orbits - Models, Methods and Applications, Springer, 2000.

[15]   Bate, Mueller and White, Fundamentals of Astrodynamics, Dover, 1971.

[16]   R. Battin, An Introduction to the Mathematics and Methods of Astrodynamics, AIAA, 1987.

[17]   A. de Ruiter, C. Damaren and J. Forbes, Spacecraft Dynamics and Control : An Introduction, Wiley, 2012.

[18]   W. H. Clohessy and R. S. Wiltshire, "Terminal Guidance System for Satellite Rendezvous," *Journal of the Astronautical Sciences, Vol. 27, No. 9,1960, pp. 653–678.*

[19]   G. W. Hill, "Researches in the Lunar Theory," American Journal of Mathematics , Vol. 1, No. 1 (1878), pp. 5-26.

[20]   J. Wertz, Mission Geometry; Orbit and Constellation Design and Management. Kluwer Academic;, Vols. pp. 510 - 521, Kluwer Academic, 2001.

[21]   S. Vaddi, S. Vadali and A. K.T., "Formation Flying: Accommodating Nonlinearity and Eccentricity Perturbations," *JOURNAL OF GUIDANCE, CONTROL, AND DYNAMICS,* Vol. 26, No. 2, March–April 2003.

[22]   K. Alfriend and H. Yan, "Evaluation and Comparison of Relative Motion Theories," *JOURNAL OF GUIDANCE, CONTROL, AND DYNAMICS,* Vol. 28, No. 2, March–April 2005.

[23]   T. Carter, "State Transition Matrices for Terminal Rendezvous Studies:Brief Survey and New Example," *JOURNAL OF GUIDANCE, CONTROL, AND DYNAMICS,* Vol. 21, No. 1, January–February 1998.

[24]   L. Pattinson, "EUTELSAT Satellite Collocation," *Proceedings of the 16th International Communications Satellite Systems Conference,* AIAA Paper No. 96-1187, Washington DC, 1996.

[25]   M. Eckstein, C. Rajasingh and P. Blumer, Colocation Strategy and Collision Avoidance for the Geostationary Satellites at 19 Degrees West, DLR GSOC, Oberpfaffenhofen, Germany,1989.

[26]   A. Harting, C. Rajasingh and M. L. A. S. K. Eckstein, "On the Collision Hazard of Colocated Geostationary Satellites," *AIAA/AAS Astrodynamics Specialist Conference, Minneapolis, USA,* AIAA 88-4239, 1988.

[27]   O. Montenbruck, M. Kirschner, S. D'Amico and S. Bettadpur, "E/I-vector separation for safe switching of the GRACE formation," *Aerospace Science and Technology,* Volume 10, Issue 7, October 2006, Pages 628–635.

[28]   S. D'Amico and O. Montenbruck, "Proximity Operations of Formation-Flying Spacecraft Using an Eccentricity/Inclination Vector Separation," *JOURNAL OF GUIDANCE, CONTROL, AND DYNAMICS,* Vol. 29, No. 3, 2006.

[29]   O. Montenbruck and S. D'Amico, "Proximity operations of formation-flying spacecraft using an eccentricity/inclination vector separation," *Journal of Guidance, Control, and Dynamics,* Vols. Vol. 29, No. 3, 2006.

[30]   D. Spears, W. Kerr and W. Spears, "Physics-Based Robot Swarms for Coverage Problems," *International Journal on Intelligent Control and Systems,* vol. 11, pp. 11-23, 2006.

[31]   S. Jantz, K. Doty, A. Bagnell and I. Zapata, "Kinetics of Robotics: The Development of Universal Metrics in Robotic Swarms," in *Conference on Recent Advances in Robotics*, Florida, 1997.

[32]   ESA, "Micrometeoriods and Space Debris," [Online]. Available: http://space-env.esa.int/madweb/hmodels.php. [Accessed 15 11 2015].

[33]   K. Yates and F. Jonas, "Assessment of the NASA EVOLVE Long-term Orbital Debris Evolution Model," *ORION International Technologies, Inc.PL-TR-92-1030,* 1995.

[34]   U. Schilcher, M. Gyarmati, C. Bettsetter, Y.W. Chung and Y. Kim, "Measuring Inhomogeneity in Spatial Distributions," *Vehicular Technology Conference, 2008. IEEE 2008..*

[35]   L. Kuipers and H. Niederreiter, Uniform Distribution of Sequences, A Wiley-Interscience Publication, John Wiley and Sons, USA, 1974.

[36]   NASA, "CDDIS - NASA's Archive of Space Geodesy Data," [Online]. Available: https://cddis.nasa.gov/Data_and_Derived_Products/GNSS/broadcast_ephemeris_data.html. [Accessed 2018 10 30].

[37]   C. Noll, "The Crustal Dynamics Data Information System: A resource to support scientific analysis using space geodesy," Advances in Space Research, vol. 45, no. 12, pp. 1421-1440, 15 June 2010.

[38]   S. Alfano, "A Numerical Implementation of Spherical Object Collision Probability," *The Journal of the Astronautical Sciences,* vol. 53, no. 1, pp. 103-109, 2005.

[39]   R. Patera, "General Method for Calculating Satellite Collision Probability," *Journal of Guidance, Control, and Dynamics,* vol. 24, no. 4, 2001.

[40]   K. Alfriend, M. Akella, J. Frisbee, J. Foster, D. LEE and M. Wilkins, "Probability of Collision Error Analysis," *Space Debris,* vol. 1, pp. 21-35, 1999.

[41]   M. Akella, "Probability of Collision Between Space Objects," *Journal of Guidance, Control, and Dynamics,* vol. 23, no. 5, 2000.

[42]   R. Patera, "Satellite Collision Probability for Nonlinear Relative Motion," *Journal of Guidance, Control, and Dynamics,* vol. 26, no. 5, 2003.

[43]   F. Chan, "Improved analytical expressions for computing spacecraft collision probabilities," *Advances in the Astronautical Sciences,* vol. 114, pp. 1197-1216, 2003.

[44]   J. Foster and S. Herbert, "A parametric analysis of orbital debris collision probability and meneuver rate for space vehicles," *Technical Report, NASA Johnson Space Center,* 1992.

[45]   D. Florijn, "Collision Analysis and Mitigation for Distributed Space Systems," MSc. Thesis, TU Delft Repository, 2015. [Online]. Available: http://repository.tudelft.nl/assets/uuid:c57819ca-09c5-4cee-9846-29a13c121034/Master_Thesis_Diederik_Florijn_1317784.pdf. [Accessed 10 11 2015].

2

Contents

Chapter 3

Scalability of Distributed Space Systems

A set is a Many that allows itself to be thought of as a One.

— Georg Cantor, Russian born German mathematician and philosopher

sankofa /sʌn-ˋkəʊ-fɑː/

noun **1** go back and fetch it: *We must look back to the past so that we may understand how we became what we are, and move forward to a better future.* ○ *It is not wrong to go back for that which you have forgotten.* **2** Asante Adinkara symbol represented either with a stylised heart shape or by a bird with its head turned backwards while its feet face forward carrying a precious egg in its mouth

Language: Akan

The functionality of a distributed system [1,2] can be significantly enhanced by exploring non-traditional approaches that leverage on inherent aspects of distributed systems in space. Until now, the benefit of distributed systems in space has been limited to enhancing coverage, multipoint sensing, typically for creating virtual baselines (e.g. interferometry) or to enhance redundancy. Further benefits can be identified by understanding the nature of distributed systems and by productively incorporating it into mission and spacecraft design. For example, prior knowledge of the spatial evolution of such systems can lead to innovative communication architectures for these distributed systems. In this chapter, we explore the communication capability and identify methods to enhance the communication link between a Distributed Space Segment (DSS), consisting of a number of simplistic, resource limited femto-satellites, and Earth. The capability of a femto-satellite is explored through a preliminary estimate of the power budget and sample link budget for a femto-satellite. As a scenario, the concept of forming a dynamic phased array in space with a distributed space system of femto-satellites in Low-Earth Orbit (LEO) is investigated. We assume that the inter-satellite separations are small with respect to the distance to the ground station on Earth. Realizing such a phased array places strict accuracy requirements on time synchronization and knowledge of relative separation between the satellites with respect to the ground receiver.

3.1 Scalable Systems

Scalable systems are systems that are capable of operating over the entire scale of a dimension (mass, size, number). Similarly, scalable models are those that work effectively over the entire range of the dimension of interest.

Distributed systems and miniature systems are essentially systems that are scaled. While distributed systems are scaled up in quantity or units, miniature systems are scaled down with respect to size. Some systems are not scalable at all and some others scale over the entire range, but typically a number of systems are scalable within a specific range. While the efficiency* of some systems and functionalities are scale invariant (isometric systems), others show an increase or decrease in performance with scale (allometric systems). Identifying and classifying these systems accordingly is vital in recognizing which systems benefit from decreasing size (miniaturization) and increasing numbers (multiple entities). To this end, we broadly classify scalable systems into three kinds – systems that scale linearly; systems that scale sub-linearly; and ones that scale super-linearly with the dimension of interest.

---

* The ratio of the effective output to the total input in any system

If we define a metric for throughput[†] T related to a dimension D, such that

$$T \propto D^x \qquad\qquad (3\text{-}1)$$

then (see Figure 3-1 for trend in throughput and Figure 3-2 for trend in efficiency),

$x = 1$; leads to linear scaling
$x < 1$; leads to sub-linear scaling
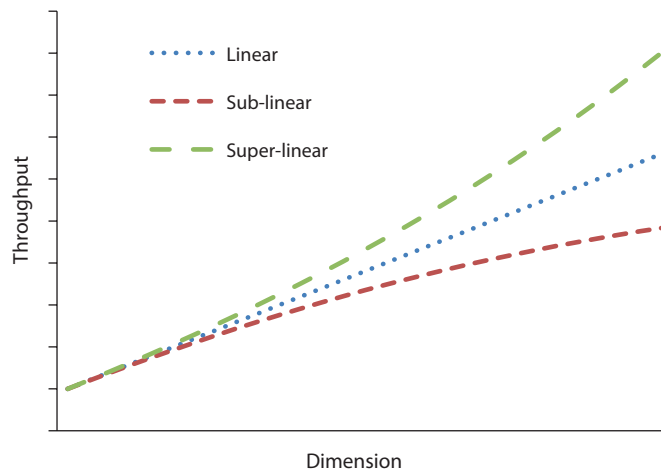$x > 1$; leads to super-linear scaling

Figure 3-1 | Throughput as a function of dimension, showing linear, sub-linear and super-linear scaling

Depending on the dimension of interest, inferences can be drawn on the trend lines. If the dimension is related to size (for e.g. volume or length), then a sub-linear trend implies a pro-micro system (systems whose efficiency benefits with miniaturization) and a super-linear trend implies a pro-macro system. On the other hand, if the dimension of interest is the number of units, then a super-linear trend indicates a pro-multiple configuration (configurations where multiple systems improve efficiency) and a sub-linear trend indicates pro-single configuration. Ideally, for massively distributed systems with miniature satellites we would use systems that scale sub-linearly with size and super-linearly with number. The trend lines can be used to identify systems that favor miniaturization and functionalities that benefit from multiple entities. Such laws can be established on a component level, but must be finally integrated to the sub-system and then system level to get the comprehensive overview of the scaling trend. These trends can be obtained through statistical data, physical principles or other established theories as shown in the following three examples.

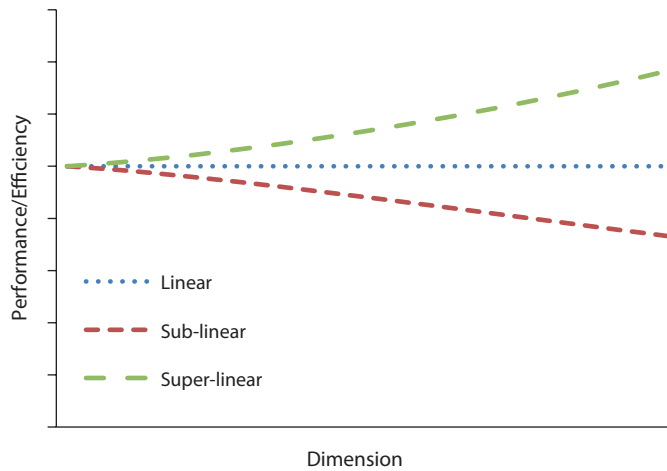[†] Output or production over a period of time.

Figure 3-2 | Efficiency as function of dimension showing linear (scale-invariant performance), sub-linear (pro-micro; pro-single) and super-linear (pro-macro; pro-multiple) trends
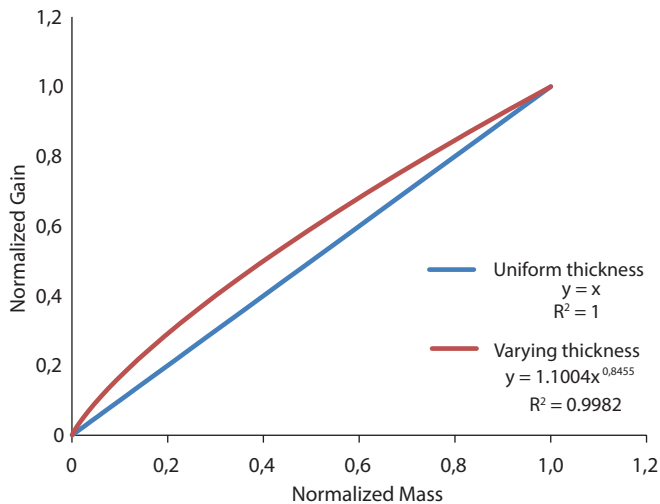
Figure 3-3 | Normalized Gain as a function of Normalized mass for a parabolic solid dish antenna (λ = 0.1 m; η = 0.55; ρ = 8000 kg/m³; for uniform thickness **t = 0.8 mm** and for varying thickness **t=0.375 to 0.8 mm**)

3.1.1 Mass of parabolic antenna vs. gain of the parabolic antenna

As an example of a physical model for a scalable system, we select a parabolic antenna, as this ground segment element plays an important role in spacecraft operations. The gain of a parabolic antenna G_r can be expressed as

$$G_r = \pi^2 D^2 \eta / \lambda^2 \tag{3-2}$$

where D is the diameter of the dish, λ is the wavelength used for transmission and η is the antenna efficiency.

Considering a solid dish antenna, the mass of the dish M_d can be expressed as the product of the dish surface area S, the thickness t of the dish which is a function of the mass, i.e. $t(M_d)$, and the density ρ of the material used.

$$M_d = S\, t(M_d)\, \rho \tag{3-3}$$

The surface area of a paraboloid is given by

$$S = \frac{\pi r}{6h^2} \left[(r^2 + 4h^2)^{\frac{3}{2}} - r^3 \right] \tag{3-4}$$

where r is the radius of the dish and h is the height (or depth) of the dish.

If we assume a constant density and thickness (thickness independent of M_d) of the dish then we see a linear increase in gain with respect to the mass. However, if we consider the thickness of the dish to increase with mass and hence size of the dish, we get a sub-linear trend line, indicating a pro-micro system. Hence, for a solid dish antenna, a smaller dish is more mass efficient with respect to gain compared to a larger dish.

3.1.2 Mass of reaction wheel vs. stored angular momentum

A power-law to establish the best fit curve based on statistical data relating reaction wheel mass (including wheel electronics) M in kg and stored angular momentum H in Nms is shown in Eq. (3-5) [3].

$$M = 2.018\, H^{0.4483} \tag{3-5}$$

The co-efficient 2.018 in Eq. (3-5) has a dimension of kg.Nms$^{-0.4493}$. This can be rewritten as Eq. (3-6).

$$H = 0.209\, M^{2.231} \tag{3-6}$$

This shows that the performance of the reaction wheel exhibits a super-linear trend with the mass of the reaction wheel (see Figure 3-4), favouring scaling up rather than scaling down.

3.1.3 Unit cost vs. production

Economies of scale [4] is a popular economic principle and refers to the reduction in unit cost as the number of units produced increases. Therefore, the cost efficiency against number of units will show a super-linear trend, with the degree of super-linearity varying according to each individual case.
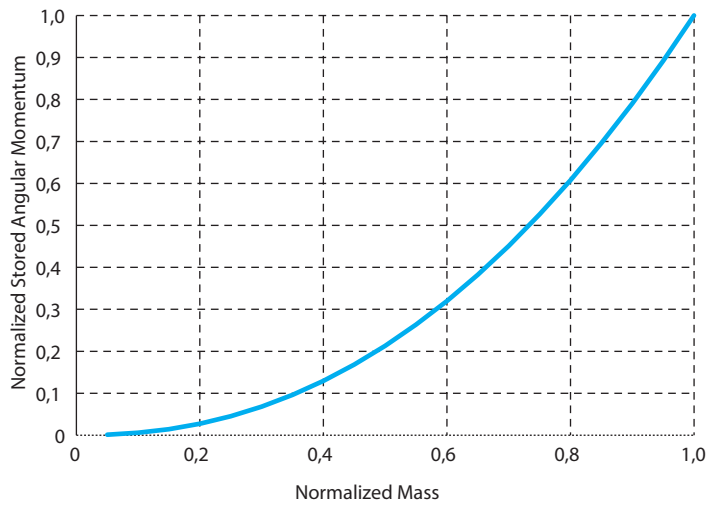
3

Figure 3-4 | Increase in the stored angular momentum against the normalized mass of the reaction wheel

3.2 Preliminary sizing of a femto-satellite

Femto-satellites, with a maximum mass of 100 g, have been chosen as candidate spacecraft to represent resource-limited miniature spacecraft. Basic spacecraft sizing rules are employed to get first estimates with respect to femto-satellite power and communication capabilities. To this end, a femto-satellite power budget and a sample downlink budget are estimated in this section.

3.2.1 Power budget of a femto-satellite

A femto-satellite is defined as having a mass range between 10 and 100 g. Using the 100 g upper limit, a power budget is derived for a femto-satellite. SMAD [6] has been used as the source for the typical values with respect to power allocation, mass allocation and performance of components. The actual values could deviate considerably based on advances in technology and implementation, so this approach provides conservative numbers to get a preliminary budget.

Table 3-1 and Table 3-2 show the mass distribution and power budget for a femto-satellite without battery and with battery respectively. The power budget is also worked out for the case with battery to assess the feasibility of having a battery in a femto-satellite and evaluate how much energy can be harvested in one orbit. Including a battery could be an attractive option for many mission scenarios.

Table 3-1 | Mass distribution and Power budget for a femto-satellite without battery (Orbit altitude = 500 km)

Parameters	Equations & Typical values	Mass [g]
Total mass of spacecraft [g]		100
Mass available for Power system, M_p [g]	28% of spacecraft mass	28
Power generation (solar array), M_s [g]	$M_p - M_b - M_c - M_r - M_d$	22.4
Power storage (battery), M_b [g]		0
Power control, M_c [g]	0.02 kg/W x P	0
Power regulation, M_r [g]	0.025 kg/W x P	3.5
Power distribution, M_d [g]	2% of spacecraft mass	2

Parameters	Equations & Typical values	Power [W]
Specific performance of solar array, S_{sa} (W/kg)	25	
Power output with planar solar array, P_{psa} [W]	M_s x S_{sa}	0.56
Power output with omnidirectional solar array, P [W]	1/4 th of P_{psa}	0.14
Orbital period, T_o [hr]	1.576	
Maximum possible energy in one orbit [W.hr]	P x T_o = 0.221	
Power available for communication subsystem, P_c [W]	21% of P	0.0294
Power available for transmission, P_t [W]	Assume 100% of P_c	0.0294
Transmitter efficiency, η	25%	
Output power to transmitting antenna [W]	**P_t x η**	**0.00735**

Table 3-2 | Mass distribution and Power budget for a femto-satellite with battery (Orbit altitude = 500 km)

Parameters	Equations & Typical values	Mass [g]
Total mass of spacecraft		100
Mass available for Power system	28% of spacecraft mass	28
Power generation (solar array), M_s [g]	$M_p - M_b - M_c - M_r - M_d$	17
Power storage (battery), M_b [g]	Through iteration	4
Power control, M_c [g]	0.02 kg/W x P	2.125
Power regulation, M_r [g]	0.025 kg/W x P	2.65625
Power distribution, M_d [g]	2% of spacecraft mass	2

Parameters	Equations & Typical values	Power [W]
Specific performance of solar array, S_{sa} (W/kg)	25	
Power output with planar solar array, P_{psa} [W]	M_s x S_{sa}	0.425
Power output with omnidirectional solar array, P [W]	1/4th of P_{psa}	0.10625
Orbital period, T_o [hr]	1.576	
Maximum Eclipse duration, T_e [hr]	(35.75 min) 0.596	
Maximum energy storage in one orbit [W.hr]	P x T_o = 0.168	
Battery performance [W.hr/kg]	40	
Battery capacity [W.hr]	M_b x Battery performance = 0.16	
Minimum energy available per orbit [W.hr]	P x ($T_o - T_e$) = 0.104	

The above approach, as shown in Table 3-1, results in an available power of 29 mW for the communication subsystem. The communication subsystem of the femto-satellite developed by Barnhart et al. [1] is based on commercially available products and has an estimated typical power consumption of 20 mW (for a much smaller range than 500 km). The 7.35 mW output power to the transmitting antenna established in Table 3-1 provides a starting point for the link analysis in the next section.

3.2.2 Downlink budget for a femto-satellite

A sample downlink budget for a femto-satellite is shown in Table 3-3. The starting value for the transmitted power is taken from the last row of the power budget in Table 3-1. The aim is to get an estimate of the down link margin.

$$\frac{E_b}{N_0} = \frac{P_t G_t G_r L_s L}{k T_s R}$$

(3-7)

Table 3-3 | Sample Downlink budget for a femto-satellite (f = 3 GHz; Max. range = 2000 km)

Parameter	Value	Value [dB]
Transmitted power [W]	0.0074	-21.34
Transmitter to antenna loss, L_l		(-) 1
Transmitting antenna gain, G_t	1	0
Receiving antenna gain, G_r (0.5 m diameter; efficiency 0.55)		7.35
Pointing loss		(-) 3
Connector loss		(-) 2
Free space loss, L_s	3x10^{-16}	(-) 168.00
Path loss, L_a		(-) 1
System noise, T_s [K]	135.0	(-) 21.30
Data rate, R [bps]	100	(-) 20.00
Boltzmann constant, k		228.6
Required E_b/N_0 (BPSK; $P_E = 10^{-5}$)		(-) 9.6
Margin		2.68

The link is sensitive to a number of parameters as shown in Eq. (3-7) [6]. The symbols are elaborated in Table 3-3. Additionally, mission scenario dependent parameters like the receiving antenna gain, data rate, maximum range and frequency of operation can vary considerably from what is shown in the sample downlink budget in Table 3-3. Eq. (3-7) gives a clear idea of the impact that these parameters have on the link. From Table 3-3, it is clear that the link, even with an extremely low data rate, just closes with a margin less than the typically required 3 dB margin. The sample link budget outlines the challenges for resource-limited spacecraft like femto-satellites in establishing a robust communication link individually. The next section explores scenarios where collective and cooperative communication can benefit a group of femto-satellites.

3.3 Scenarios for Enhanced Communication

In this section we will explore scenarios which may enhance downlink communication using multiple satellites. Enhancing the downlink implies either establishing a robust link through multiple satellites when individual satellites fail to establish the link or increasing the downlink data throughput of multiple satellites to more than the combined throughput of the individual satellites. For example consider multiple satellites in a 500 km LEO with each satellite capable of establishing a communication link that has a maximum range of 250 km with minimum required bitrate. In such a scenario, no ground communication can take place. The downlink can be enabled if there are enough satellites to cooperate and realize a link that has a range of at least 500 km. The downlink can be further enhanced if the number of satellites allows the range of the link to be extended for operation in optimal elevation angles that maximizes data throughput. The basic link equation is given as [6]

$$\frac{E_b}{N_0} = \frac{P_t G_t G_r L_s L}{k T_s R}$$

(3-8)

where E_b/N_0 is the received bit energy to noise ratio is, P_t is the transmitting power, G_t and G_r are the transmitting and receiving antenna gains respectively, L_S is the free space loss, L incorporates all other losses, k is Boltzmann's constant, T_S is the system noise temperature, and R is the data rate.

Figure 3-5 shows a typical graph of required E_b/N_0 against probability of error. Moreover three different regions are identified in Figure 3-5 based on the E_b/N_0 that is actually received from the satellite. In each region, the benefits of enhancing the downlink using DSS are explored.
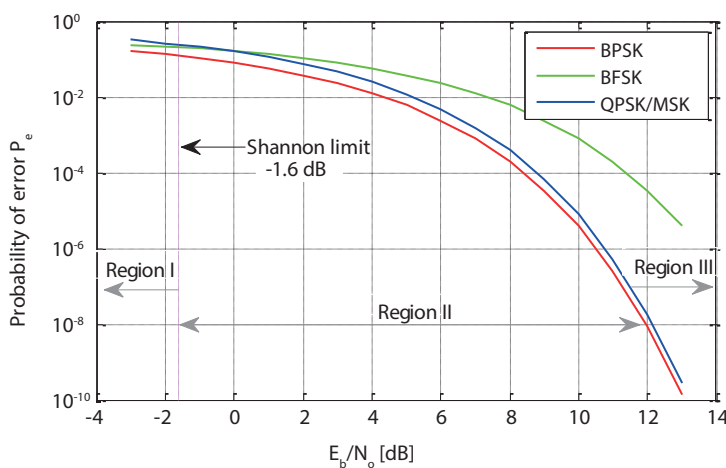

Figure 3-5 | Probability of error as a function of required E_b/N_o for simple modulation schemes

The first objective is to ensure that the received E_b/N_0 is sufficient to establish a link with the required error probability and the next objective is to maximize the throughput. The data throughput, T_d for a single pass is defined as the product of the data rate of the link, R, and the satellite time in view in a single pass, t_s.

$$T_d = R. t_s . \tag{3-9}$$

The throughput can be maximized for a pass by either increasing the satellite time in view in that pass or by increasing the data rate. From Eq. (3-8), for a given transmitting power a trade-off is possible between data rate and range to achieve the required E_b/N_0. The range of the communication link indirectly defines the satellite time in view and for a given link, there exists an optimum t_s that maximizes the data throughput. It is beneficial (for throughput considerations) to increase the range to approach this optimum t_s rather than increasing the data rate. This can be achieved, for example, by forming a phased array with multiple satellites to increase the received E_b/N_0 that increases the range of the link and hence allows the link to be established through a larger range of elevation angles. However, beyond the optimum t_s the throughput is maximized by increasing R rather than t_s.

Figure 3-6 shows throughput (downlink data volume in one satellite pass) as a function of elevation angle. It can be seen that maximum throughput is achieved for an elevation angle of around 45° for zenith pass and around 30° for a satellite pass which is 50° off zenith. A lower limit of 50 bps has been imposed on the data rate for these simulations. An analytical treatment of optimizing throughput for power constrained scenarios can be found in Gill et al. [7]. If the individual satellite link cannot achieve the required E_b/N_0 to operate in this region, then multiple satellites can increase throughput by cooperating to collectively operate in this optimal region.
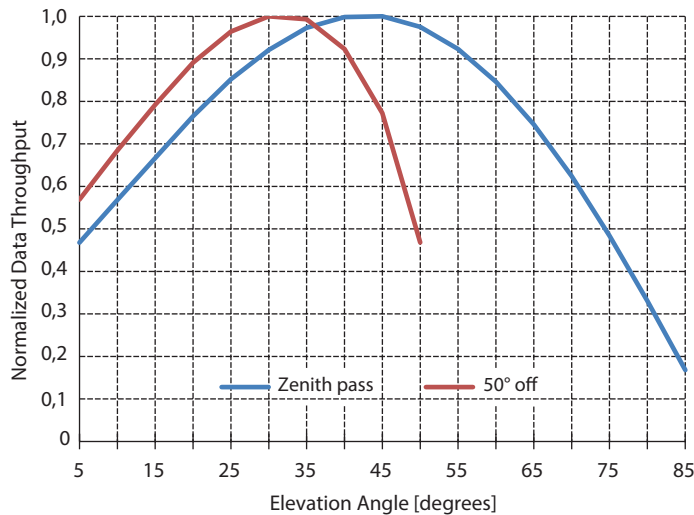

Figure 3-6 | Normalized throughput as a function of minimum elevation angle

3.3.1 Region I – Below the Shannon Limit

In this region, E_b/N_0 is less than -1.6 dB, which is the Shannon limit below which no error-free communication at any information rate can take place.

$$C = B \log_2(1 + SNR) \qquad (3\text{-}10)$$

Eq. (3-10) is the Shannon's channel capacity theorem [8], where C is the channel capacity, B is the channel bandwidth and SNR denotes the received signal-to-noise ratio. In the limiting case when the channel bandwidth is infinitely large, implying data rate to bandwidth is tending to zero, from Eq. (3-10), the corresponding limit on E_b/N_0 is -1.6 dB, which is referred to as the Shannon limit. In this power-limited region, no communication can take place with a single femto-satellite and no coding or shaping techniques can enable communication. When the link of a single satellite results in an E_b/N_0 that lies in this region, there is a clear need to explore schemes that will combine power resources from multiple satellites and shift the received E_b/N_0 to region II or region III.

3.3.2 Region II – Power Limited Region

In region II the E_b/N_0 is greater than -1.6 dB but less than the value required for receiving the signal with given probability of error (using simple modulation and coding schemes). Here, advanced and complex coding techniques and modulation schemes, supplemented with constellation shaping techniques, can reduce the requirement on E_b/N_0 and bring it closer to the ultimate Shannon capacity limit [9]. The implementation of such high performing codes and algorithms on simplistic femto-satellites will be a challenge. Therefore enhancement of the downlink with multiple femto-satellites becomes attractive in this region as well. The downlink can be enhanced in two aspects:

a. Basic improvement of E_b/N_0 to achieve required margin and ensure a communication link with sufficient range albeit for high elevation angles and short ground contact time.

b. Improvement of E_b/N_0 to increase throughput by ensuring operation at optimal elevation angles (i.e., increasing E_b/N_0 beyond what is required to achieve the margin and increasing the range of the link to operate with optimal ground contact time).

3.3.3 Region III – Power Abundant Region

In region III the received E_b/N_0 is sufficient to establish a basic communication link. The scope for enhancing communication with multiple satellites is to improve E_b/N_0 to ensure operation at optimal elevation angles, if existing link does not allow it. The challenge in this region will primarily be in handling multiple links from multiple satellites to a ground station leading to solutions such as FDMA (Frequency Division Multiple Access), TDMA (Time Division Multiple Access), CDMA (Code Division Multiple Access).

3

3.4 Phased Array with Multiple Satellites

One option to enhance the communication link is to combine the transmitter powers by realizing a phased array of multiple satellites. Cooperative transmission from multiple antennas has been investigated for terrestrial wireless sensors [10,11,12], but limited mainly to static configurations. In this section, the concept of phased arrays with multiple satellites will be explored.

A phased array is a group of antennas in which the relative phases of the respective signals feeding the antennas are varied in such a way that the effective radiation pattern of the array is reinforced in a desired direction and suppressed in undesired directions. With respect to the receiver, this implies constructive superposition of the signals coming from the different transmitters at the receiver. Realizing such an array will require effective phase synchronization.

Phase synchronization in its simplest explanation is a technique to synchronize the antennas to ensure the signals arriving or leaving the antennas have the required relative phases. Phase synchronization can be done with respect to a preferred direction or a point in space. When the array is used for transmission, the synchronization shall be such that the signals from all the spatially distributed antennas reach the desired receiver in phase, enabling constructive interference of the signals. Likewise, when the array is used for reception, the phase synchronization should ensure that the entire array is focused in the direction of interest.

The second pre-requisite for such a phased array is to exchange the data to be transmitted between the satellites, so that all satellites have the common data before they start transmitting in phase. In this research, we will not focus on approaches for inter-satellite data transfer, but recognize that this data transfer will require a finite energy. Furthermore, there are many network algorithms which can be employed to optimize the performance of data transfer between satellites constrained with low onboard power availability.

3.4.1 Theory of Superposition of Signals

Consider r_1, r_2, ..., r_n as the signals at the receiver from satellite transmitters defined as,

$$
\begin{aligned}
r_1 &= A_1 \sin(\omega t + \alpha_1) \\
r_2 &= A_2 \sin(\omega t + \alpha_2) \\
&\ \ . \\
&\ \ . \\
r_n &= A_n \sin(\omega t + \alpha_n)
\end{aligned}
\tag{3-11}
$$

where A, ω and α represent the amplitude, angular frequency and phase offset of the received signals. Then the superposition of these signals would result in,

$$
\sum_{i=1}^{n} r_i = A_1 \sin(\omega t + \alpha_1) + A_2 \sin(\omega t + \alpha_2) + \cdots + A_n \sin(\omega t + \alpha_3) .
\tag{3-12}
$$

This can be rewritten as,

$$\sum_{i=1}^{n} r_i = (A_1 cos\alpha_1 + A_2 cos\alpha_2 + \cdots + A_n cos\alpha_n)\ sin\omega t$$
$$+\ (A_1 sin\alpha_1 + A_2 sin\alpha_2 + \cdots + A_n sin\alpha_n)\ cos\omega t$$

(3-13)

The satellites are assumed to be located relatively close to each other and hence the signals from the different satellites suffer similar attenuation before reaching the receiver. If we assume that the transmission amplitude of the individual satellites is identical then the received amplitude of the signals from the different satellites will be of similar magnitude as well. Therefore to simplify the analysis we assume that the amplitude of the received signals are equal and establish Eq. (3-14).

$$A_1 = A_2 = \cdots = A_n = A .$$

(3-14)

The amplitude of this superposed signal in Eq. (3-13) can then be described as

$$\left|\sum_{i=1}^{n} r_i\right| = A\sqrt{(cos\alpha_1 + cos\alpha_2 + \cdots + cos\alpha_n)^2 + (sin\alpha_1 + sin\alpha_2 + \cdots + sin\alpha_n)^2} .$$

(3-15)

The normalized received signal amplitude with respect to A then takes the form as shown in *Eq. (3-16)*.

$$\bar{A} = \sqrt{(cos\alpha_1 + cos\alpha_2 + \cdots + cos\alpha_n)^2 + (sin\alpha_1 + sin\alpha_2 + \cdots + sin\alpha_n)^2} .$$

(3-16)

The above equation relates the phase differences α_i of the individual satellites to the received signal amplitude. In a distributed network of satellites that are transmitting simultaneously, the phase difference at the receiver arises due to the errors in clock synchronization and difference in the relative position of these transmitters with respect to the receiver.

Assuming we can compensate for these phase differences, then the accuracy with which we know the relative position of the transmitters with respect to the receiver and the accuracy of time synchronization will directly impact the amplitude of the received signal. To understand the criticality of the phase synchronization accuracy, a simulation setup was established and up to 50 identical satellite signals were generated to assess the magnitude of the superposed signal. A Monte Carlo approach was used to introduce the phase offsets that simulated the appropriate phase synchronization accuracy.

Figure 3-7 shows the normalized amplitude $\bar{A}$ of the superposed signal that is received as a function of the number of satellites for different accuracies of phase synchronization. The amplitude of the superposed signal is normalized with respect to the received amplitude of an individual satellite signal at the receiver which is assumed to be equal for all the satellites. Perfect phase synchronization

implies that there is no phase offset between the received signals at the receiver and therefore, the amplitude of the superposed signal is the summed amplitudes of the individual signals.

In Figure 3-7, we see that the normalized amplitude linearly increases with number of satellite for perfect synchronization reaching a value of 50 for 50 satellites. It can also be seen that as the accuracy of the phase synchronization deteriorates the amplitude of the superposed signal reduces consistently. As an example we can see that if the phases of the received signals can be synchronized to within one-third of the wavelength of the signal, then with 50 transmitted signals, the received superposed signal amplitude is 18 times the amplitude of an individual signal, while synchronization to within one-fifth the wavelength will result in a received signal that is 38 times the magnitude of an individual signal. The trends captured in Figure 3-7 allow us to determine the benefit of signal superposition for different levels of phase synchronization.
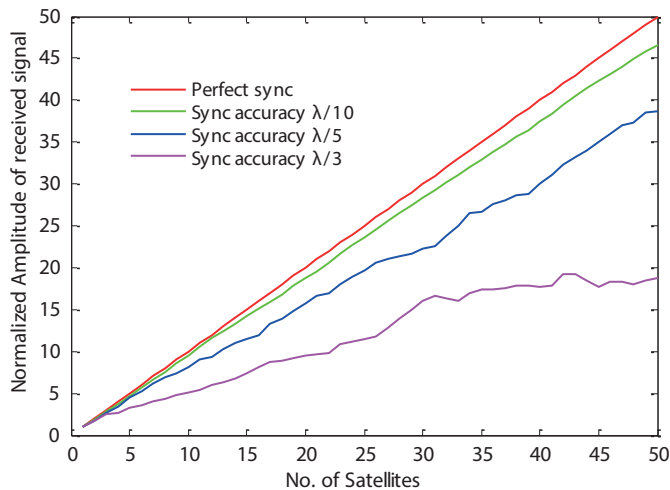

Figure 3-7 | Normalized amplitude of the received signal as a function of the number of satellite transmitters for different accuracies of phase synchronization (λ is the wavelength of transmission).

3.4.2 Enhancing Throughput with a Phased Array

In this section the benefits of forming a phased array with the elements of a DSS to enhance downlink data throughput is investigated. As candidate elements of the DSS we consider femto-satellites with constrained power and link budgets. The received E_b/N_0 from a sample femto-satellite link budget suggests that the scenario corresponds to region II of Figure 3-5. Therefore a single satellite cannot establish even a basic communication downlink and the link can be enhanced as suggested in Section 3.3.2.

Figure 3-8 shows the increase in throughput with increasing number of satellites for a satellite pass which is 50° off zenith. It is assumed there are no errors in phase synchronization and the transmitter powers of the individual satellites can be added up as the satellites increase. The link is not realized with a single femto-satellite which results in zero throughput. Two femto-satellites result in a throughput of around 1000 bits and three femto-satellites realize 6000 bits. Thereon, the throughput increases by around 2000 bits per additional satellite. A super-linear trend can be seen in the throughput increase from zero through 1000 to 6000 bits as the number of femto-satellites increase from one to two and then three. Further increase in the number of satellites results in a linear increase in throughput. The throughput of a system with optimal number of elements will be higher than the summed throughput of systems formed of elements less than the optimal number, given that the total number of elements in both cases is the same. The finite network overhead which has been neglected till now that increases with the number of elements is the motivation to keep the system size as low as possible making the transition point the optimal size. Figure 3-9 shows the increasing throughput with number of satellites for different accuracies of phase synchronization. In all three cases the trend is similar with a super-linear increase up to the transition point followed by a liner increase. The throughput increase with a phase synchronization accuracy of $\lambda/3$ is remarkably close to the perfect synchronization case. This suggests that in some scenarios achieving an accuracy of $\lambda/3$ maybe sufficient and the additional effort towards achieving perfect phase synchronization may not be worth the endeavor. Depending on what level of phase synchronization is achievable at a certain frequency of operation, the throughput can be derived from a graph as shown in Figure 3-9.
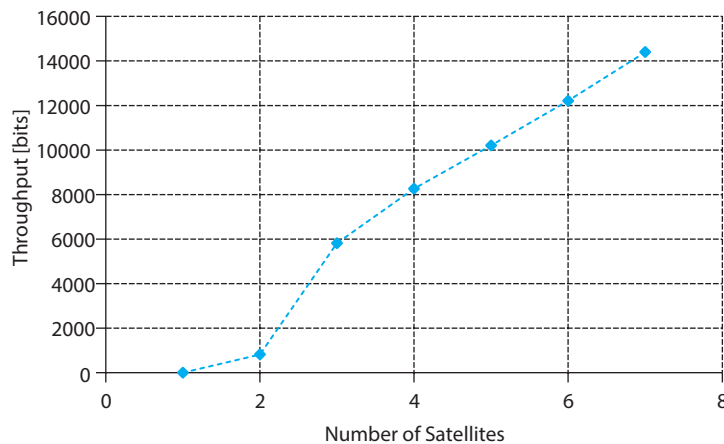
3

Figure 3-8 | Increase in throughput with increase in number of satellites, assuming perfect synchronization in the phased array, for a satellite pass which is 50° off zenith
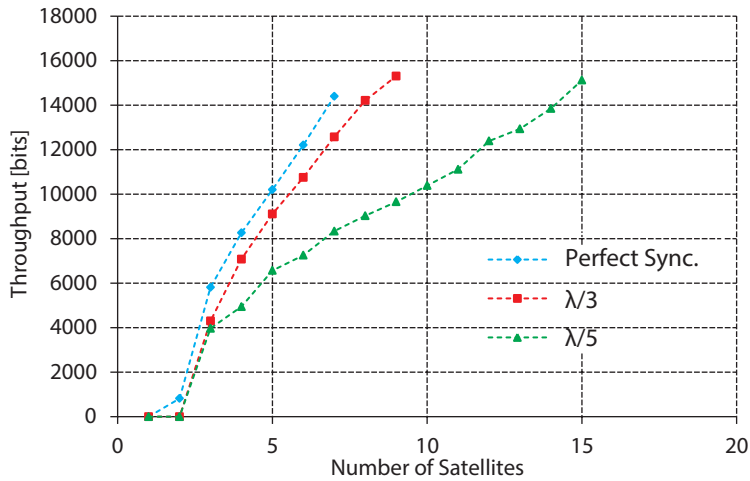
Figure 3-9 | Throughput increase with number of satellites for different accuracy levels of phase synchronization for a satellite pass which is 50° off zenith

3.4.3 Feasibility of the Phased Array

The main challenge to increase the throughput by increasing the number of satellites as shown in Figure 3-9, is achieving the required levels of phase synchronization. Phase synchronization accuracy has two components – the accuracy with which we can determine the relative positions of the satellites, referred to as localization; and the accuracy of time synchronization. The localization accuracy expressed in units of distance and the time synchronization accuracy expressed in units of time, together constitute the phase synchronization accuracy. Therefore, either by translating the time synchronization accuracy into equivalent distance or by translating the localization accuracy into equivalent time the two components can be combined to express the phase synchronization accuracy in distance or time. The translation between time and distance is effectuated by assuming that the speed of propagation is that of the velocity of electromagnetic waves in vacuum. The accuracy of the required phase synchronization can be expressed as a fraction of the transmission wavelength, in units of distance or in equivalent time as shown in Table 3-4.

For the case with transmission frequency of 3 GHz (wavelength 10 cm) and required phase synchronization accuracy of $\lambda/3$, the required phase synchronization accuracy is 3.3 cm in distance or 0.11 ns in time as shown in Table 3-4. This means that if the relative position accuracy is 1 cm, then the accuracy of time synchronization should be within 2.3 cm (when considered as correlated errors or within 3.15 cm for uncorrelated errors) or equivalently 0.076 ns.

Table 3-4 | Requirements on phase synchronization accuracy translated into equivalent distance (relative positions) and time

Frequency [GHz]	Wavelength [m]	$\lambda/10$		$\lambda/5$		$\lambda/3$	
		distance [cm]	time [ns]	distance [cm]	time [ns]	distance [cm]	time [ns]
3	0.1	1	0.033	2	0.066	3.3	0.11
1	0.3	3	0.1	6	0.2	10	0.33
0.3	1	10	0.33	20	0.66	33	1.1

Time synchronization and localization are standard concepts in terrestrial wireless sensor systems. Motivated by advances in large-scale highly distributed terrestrial wireless sensor systems, there has been a lot of effort in developing time synchronization methods that are mindful of the resource constraints of such systems [13]. Time synchronized COTS (Commercial Off The Shelf) platforms have also been considered for applications such as beam forming [14]. There are multiple ways to achieve localization within a sensor network. GPS based positioning and ranging are popular methods for localization. In ranging, the accuracy of relative range estimation is a fraction of the wavelength used for ranging. Currently there is considerable interest in miniaturized GPS receivers that can be used in small satellites. However, femto-satellites with current technology will barely be able to accommodate such systems and meet the phase synchronization requirements by achieving the necessary time synchronization and localization. Therefore, although conceptually the idea of beamforming could enable multiple spacecraft to increase their communication capability, practically, traditional approaches would place such high constraints on localization and time keeping accuracy that beamforming is not realizable with current and foreseen technologies in the immediate future. This is the motivation to explore other approaches to phase synchronization such as the one developed and discussed in Chapter 4

Another challenging aspect in localization is the prediction of the satellite dynamics, and in particular, relative orbital prediction. Once phase synchronization is established the prediction in relative dynamics between the spacecraft will play a crucial role in determining the duration for which the synchronization is valid. The prediction accuracy of relative positions of the spacecraft will determine update rate from sensors used for positioning. Advancing these methods and technologies to meet the stringent requirements of phase synchronization and adopting them for space applications with miniature satellites in a dynamic environment will be the key challenge with respect to achieving the required levels of time synchronization and localization. The stringency on these requirements can be reduced by choosing lower frequencies of operation. However, this will impact the bandwidth available and the antenna size employed.

3.5 Discussion

The scaling trend – linear, sub-linear or super-linear, dictates the benefit in increasing the number of entities to enhance a particular functionality. In the phased array example (see Figure 3-9), the

initial trend is super-linear followed by a linear increase in throughput. Depending on network implementation, the trend could be different if the energy expenditure to realize a distributed network is included in the analysis. This analysis assumed a zero overhead for network realization.

The transition point from super-linear to linear trend acquires significance as this defines the region where the benefit of combining multiple entities reaches saturation. In Figure 3-9 the transition occurs when the number of satellites reaches three. As discussed in Section 3-1, a super-linear trend implies improvement in efficiency with increasing elements, a linear trend implies constant efficiency and a sub-linear trend implies decrease in efficiency for distributed systems. Therefore, when we account for the finite network overhead that increases with the number of entities in the network, then optimal link performance is achieved by limiting the network to the number of satellites at the transition point, in this case three. In a massively distributed system of femto-satellites with the above established scenario, a conclusive implication of this result is that for enhancing ground communication, sub-groups of three femto-satellites communicating cooperatively is optimal. In general, the scaling trend identifies regions and subsequently number of elements that are optimal for distributed networks.

3.6 Conclusion

Highly miniaturized spacecraft such as femto-satellites are excellent candidates to realize massively distributed systems in space. Scaling rules which use the size of individual satellites and their number in a system are efficient to characterize the performance of highly distributed massively miniaturized space systems. Moreover, scaling trends can help identify optimal size and numbers of elements in a distributed network.

While the typical benefit of distributed systems in space originates from features as coverage, redundancy, baselines and multipoint sensing, the enhancement of the downlink communication capability of a distributed system of femto-satellites to a ground station was explored. To this end, the benefits of a phased array in space formed by multiple femto-satellites have been studied. It was shown that although individual satellites may not be able to communicate to the ground station, the phased array enables communication. The challenge of this approach, however, is to achieve phase synchronization between the satellites which necessitates a sufficient time synchronization and localization in a dynamic environment. For a simplistic femto-satellite, achieving such levels of time synchronization and localization may be extremely and even prohibitively demanding. Therefore, novel and innovative approaches to synchronization need to be explored that are feasible on resource-limited platforms. A phase synchronization strategy that obviates the need for high accuracy localization and clock synchronization, and enables realization of a phased-array with femto-satellites, is proposed and discussed in Chapter 4. Femto-satellites were chosen as candidates for resource limited spacecraft and LEO as a potential mission scenario. However, the concept and conclusion apply to all missions involving multiple satellites that aim to combine resources to extend or enhance the individual spacecraft capabilities.

References

[1]   D. J. Barnhart, T. Vladimirova, A. M. Baker and M. N. Sweeting, A low-cost femtosatellite to enable distributed space missions, Acta Actronautica, Vol. 64, 2009.

[2]   T.-R. Hsu, "Miniaturization – A paradigm shift in advanced manufacturing and education," A plenary speech delivered at the 2002 IEEE/ASME International conference on Advanced Manufacturing Technologies and Education in the 21st Century, Chia-Yi, Taiwan, Republic of China,August 10-15, 2002..

[3]   C. Aas, et al. SCALES – A System Level Tool for Conceptual Design of Nanoand Microsatellites, 7th IAA Symposium on Small Satellites for Earth Observation, Berlin, Germany,2009.

[4]   J. Downes and J. Goodman, Dictionary of Finance and Investment Terms, Barron's Educational Series Inc., 7/e, 2006.

[5]   W. J. James R. Wertz, Space Mission Analysis and Design 3e, pp 550 - 552, Microcosm Press and Springer,1999.

[6]   F. Dietrich and R. Davies, Communications Architecture; Space Mission Analysis and Design edited by J.R. Wertz and W.J. Larson, 3/e , Microcosm Press, CA, Springer, NY., 2008.

[7]   E. Gill, C. Verhoeven, K. Gill and M. d. Milliano, A New Approach for Enhanced Communication, SpaceOps 2010 Conference, Huntsville, Alabama., 2010.

[8]   S. Haykin, An Introduction to Analog and Digital Communication, John Wiley & Sons, Inc., 1994.

[9]   G. Forney and G. Ungerboeck, Modulation and Coding for Linear Gaussian Channels, Vols. Vol. 44, No. 6, October., IEEE Transactions on Information Theory., 1998.

[10]   A. Scaglione and Y.-W. Hong, Opportunistic Large Arrays: Cooperative transmission in Wireless Mutlihop Ad Hoc Networks to Reach Far Distances, IEEE Transactions on Signal Processing, Vol. 51, No. 8, August, 2003.

[11]   Y.-S. Tu and G. Pottie, Coherent cooperative transmission from multiple adjacent antennas to a distant stationary antenna through AWGN channels, Vehicular Technology Conference, 2002. VTC Spring 2002. IEEE 55th, 130 - 134 vol.1, 2002.

[12]   S. Sigg and M. Beigl, Collaborative Transmission in Wireless Sensor Networks by a (1 + 1)-EA, ASWN '08 Proceedings of the 2008 Eighth International Workshop on Applications and Services in Wireless Networks, 2008.

[13]   J. Elson and D. Estrin, Time Synchronization for Wireless Sensor Networks, 2001 International Parallel and Distributed Processing Symposium (IPDPS), Workshop on Parallel and Distributed Computing Issues in Wireless Networks and Mobile Computing, April 2001, San Francisco, CA, USA, pp. 1965--1970., 2001.

[14]   H. Wang, L. Yip, D. Maniezzo, J. Chen, R. Hudson, J. Elson and K. Yao, A Wireless Time-Synchronized COTS Sensor Platform : Applications to Beamforming, IEEE CAS Workshop on Wireless Communications and Networking, Pasadena, California. September, 2002..

3

Contents

Chapter 4

Novel Phase Synchronization Technique

"Unseen in the background,
Fate was quietly slipping lead into the boxing-glove."

— P.G. Wodehouse, Very Good, Jeeves!

kairos /ˈkʌɪrɒs/
noun **1** the perfect, delicate, crucial moment **2** the fleeting rightness of time and place that creates the opportune atmosphere for action, words, or movement. **3** weather
Language: Greek

The challenges with the traditional approach to phase synchronization and the associated prohibitive requirements that such an approach places on localization and clock accuracies have been derived and discussed in Chapter 3. In this chapter, a novel phase synchronization technique is proposed that enables beamforming with multiple resource-limited spacecraft in space and capitalizes on their spatial geometry. The proposed technique employs an external beacon to obviate the need for explicit time synchronization and reduces the accuracy requirements on localization. Results show that subcentimeter-level phase synchronization can be achieved with localization accuracy in the order of meters. The chapter starts with an introduction and need for phase synchronization. Following this, a mathematical formulation of the proposed phase synchronization technique is developed and discussed. The sensitivity of the achieved synchronization accuracy is analyzed with respect to key parameters and the design space of this synchronization technique is established. The chapter concludes with the simulation setup and the results of the achieved phase synchronization performance.

4.1 Introduction

Phased arrays in space can enhance the communication link between a network of spacecraft and the ground. A phased array is a group of antennas in which the relative phases of the respective signals feeding the antennas are varied such that the effective radiation pattern of the array is reinforced in a desired direction and suppressed in undesired directions. This cooperative technique that emulates a virtual array to steer the beam in a particular direction is also referred to as beamforming. In distributed beamforming, in contrast to conventional beamforming, the geometry of the sensor network is not known apriori and has to be acquired dynamically [1]. Beamforming is realized when nodes appropriately weight and forward the common signal to be transmitted [2].

Realizing such an array requires effective phase synchronization. Phase synchronization in its simplest explanation is a technique to synchronize the antennas to ensure the signals arriving or leaving the antennas have the desired phase offsets to ensure constructive interference. Phase synchronization can be done with respect to a preferred direction or a point in space. When the array is used for transmission, the synchronization shall be such that the signals from all the spatially distributed antennas reach the desired receiver in phase, enabling constructive interference of the signals. Likewise, when the array is used for reception, the phase synchronization should ensure that the entire array is focused in the direction of interest. Cooperative transmission from multiple antennas has been investigated for terrestrial wireless sensors [3-5], but has been limited mainly to static configurations.

This concept of beamforming can be extended and applied to distributed systems in space where the individual spacecraft form the nodes of a wireless dynamic network. The orbit and attitude dynamics of the nodes and mass and power restrictions of the spacecraft further increase the challenges involved in beamforming. The benefits of a phased array in space formed by multiple resource-

constrained spacecraft for enhanced communication has been investigated and highlighted in previous research work [6]. Time synchronization and localization were identified as key challenges to achieving the required accuracy of phase synchronization.

Phase synchronization accuracy has two components: the accuracy of the relative positions of the satellites, referred to as localization accuracy; and the accuracy of relative time synchronization. Time synchronization and localization are standard concepts in terrestrial wireless sensor systems. Motivated by advances in large-scale highly distributed terrestrial wireless sensor systems, there has been significant effort in developing time synchronization methods that are mindful of resource constraints of such systems [7]. Time synchronized COTS (Commercial Off The Shelf) platforms have also been considered for applications such as beamforming [8]. There are multiple ways to achieve localization within a sensor network. GPS based positioning and ranging are popular methods for localization. In ranging, the accuracy of relative range determination is a fraction of the wavelength used for ranging.

Miniature spacecraft with their small size, low individual cost and ability to be mass produced are key enablers of distributed space systems. A few of these advantages can be attributed to the usage of COTS [9]. However, these spacecraft also suffer from severe resource constraints that lead to limited functionalities. State of the art chip scale atomic clocks [10] needed for sub-meter phase synchronization would already take up more than 35% of the mass budget for a sub-100 g spacecraft. Localization systems are also resource intensive, and accommodating a localization subsystem that meets the mass requirements is an additional challenge. Therefore, miniaturized spacecraft with current technology will barely be able to accommodate the phase synchronization requirements for traditional beamforming.

Therefore, novel and innovative approaches to synchronization need to be explored that are feasible on highly resource-limited platforms like femto-satellites. In this chapter, a novel phase synchronization approach using an external beacon is presented that enables beamforming. The paper develops a mathematical framework and analysis of the synchronization scheme to assess feasibility and sensitivity of phase synchronization to key system components. An extensive simulation involving dynamics of beacon, receiver and satellites along with estimation of position and delay is performed to assess the characteristics of the proposed approach. The results of the simulation are analyzed followed by conclusions on performance.

4.2 Novel Phase Synchronization Technique

A novel approach to phase synchronization of multiple satellites is proposed that places minimal constraints and requirements on the satellites and achieves high levels of phase synchronization by exploiting the geometry of the system through an external beacon. High accuracy timing and localization are traditionally the most demanding elements to achieve high accuracy phase

synchronization. The proposed approach does not place stringent requirements on clock and localization accuracy and therefore, does not drive or constrain the spacecraft design. The satellites are typically in Low Earth Orbit (LEO) and they have to be synchronized with respect to a receiver located on ground.

The presence of an external beacon B for example a geo-stationary spacecraft above the ground receiver, as shown in Figure 4-1, can enable high levels of phase synchronization under favorable geometries. Let us assume that the reference satellite S^0 lies on the straight line that connects the beacon B to the receiver R. An arbitrary satellite S^n, at a distance L^n from B, h^n, from R, has an angular separation of θ^n at B with respect to S^0.

It is assumed that through prior data exchange, the satellites, S^0 and S^n, have common data which they intend to transmit to the ground receiver R. The beacon broadcasts a trigger signal to initiate signal transmission from the satellites to the receiver. The beacon serves just as a trigger and has no data component in its transmission. The most desired scenario is perfect synchronization where all the signals from the various satellites arrive at the receiver at the same time leading to maximum amplitude of the received signal. However, in practice there will be a finite difference in the time of arrival of the various signals which will be a measure of the level of achievable phase synchronization. Therefore, in this section we will formulate and develop a framework to determine the difference in the time of arrival of the signals from the satellites at the receiver. However, before we develop a general treatment of the time of arrival of the signals at the receiver, it is intuitive to consider first a simple limiting case where θ^0 approaches zero and the satellites are on the straight line connecting the beacon and receiver as shown in Figure 4-2 . This allows an insight into how the geometry can be exploited for synchronization. Let us assume that the positional difference between S^0 and S^n is the only reason for mismatch in phase synchronization. This implies that if S^0 and S^n were collocated, then a trigger from anywhere would initiate a transmission at the same instance from each of the satellites that will reach the receiver at the same instant in time. If there is a finite separation between the satellites, then the phase synchronization cannot be assured for general geometries, as the satellites will be triggered at different instances in time and the distance to the receiver is also different. However, if the beacon B is located as in Figure 4-2, then perfect synchronization is assured not only when the satellites are collocated but as long as the satellites lie on the line connecting B and R.

Moreover, if the satellites are not strictly on this straight line but have small angular separation θ_n, then, although perfect synchronization may not be possible, still the geometry is advantageous in that the sensitivity of the path difference to radial positional differences is very small. In the next section , a quantitative treatment follows to assess achievable phase synchronization and the sensitivity of the path difference to critical geometric parameters.

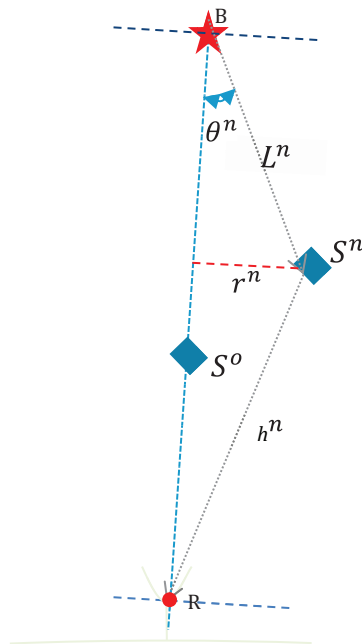**Figure 4-1 |** General geometry of beacon B, receiver R, reference satellite S^o, and arbitrary satellite S^n
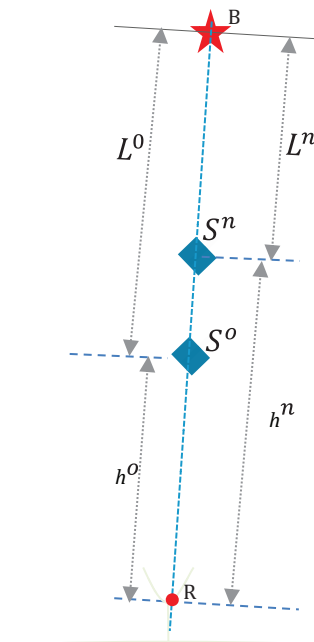

Figure 4-2 | Special geometry for satellites aligned on the straight line connecting the beacon with the receiver ($\theta_n = 0$)

4.3 Theory of proposed phase synchronization scheme

A timing diagram as shown in Figure 4-3 is developed based on the arrangement shown in Figure 4-1. The vertical arrows in Figure 4-3 indicate instances such as trigger or moment of reception and transmission. The green and red arrows are associated with satellites S^0 and S^n respectively. If we denote T_B as the absolute time at which the beacon transmits the trigger signal and T_R^n as the time of arrival of the data signal from S^n at the receiver R, then T_R^n can be expressed as

$$T_R^n = T_B + t_{BS_r^n} + t_{S_r^n S_t^n} + t_{S_i^n} + t_{S_t^n R} \tag{4-1}$$

where S_r^n and S_t^n denote the antennas of satellite S^n that receive the beacon signal and transmit the data signal respectively and t_{ab} refers to the travel time required to reach point b from point a.

The delay due to internal software and hardware latencies associated with S^n is absorbed in the time delay $t_{S_i^n}$. This delay may also include intentionally programmed delays.

Two terms on the right hand side of Eq. (4-1) can be combined as shown in Eq. (4-2) to introduce the satellite attitude dependent delay $\tau_{S_r^n S_t^n}$ representing the excess in path length with respect to the shortest distance between S_r^n and R. As shown in Figure 4-4, l_{rt}^n represents the length of a straight line connecting the receiving and transmitting antenna of S^n, and α^n is the angle between $S_r^n R$ and $S_r^n S_t^n$. The length of the physical path connecting the beacon receiving and data signal transmitting antenna of S^n is denoted by p_{rt}^n

$$t_{S_r^n S_t^n} + t_{S_t^n R} = t_{S_r^n R} + \tau_{S_r^n S_t^n}(p_{rt}^n, l_{rt}^n, \alpha^n). \tag{4-2}$$

Combining Equations (4-1) and (4-2), leads to

$$T_R^n = T_B + t_{BS_r^n} + t_{S_r^n R} + \tau_{S_r^n S_t^n}(p_{rt}^n, l_{rt}^n, \alpha^n) + t_{S_i^n}. \tag{4-3}$$
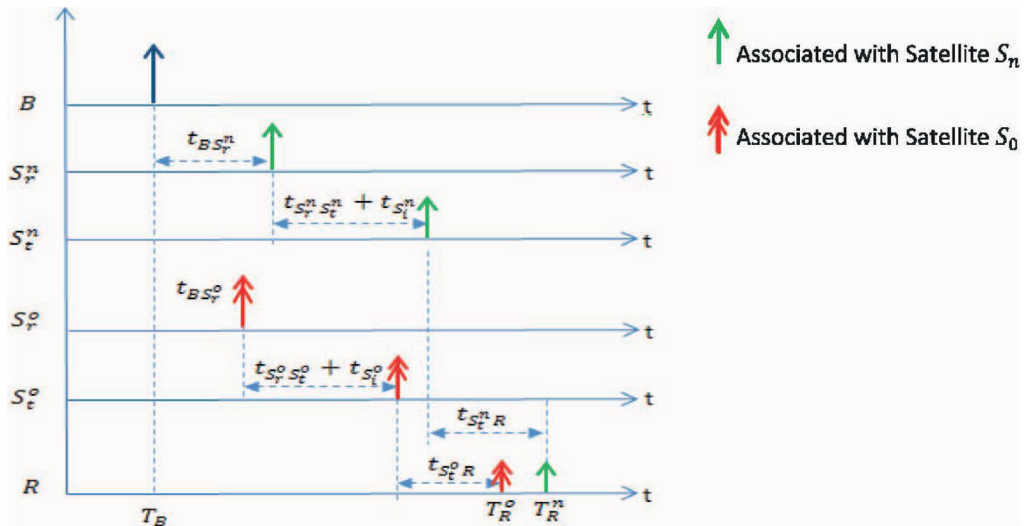

Figure 4-3 | Timing diagram for phase synchronization with external beacon.
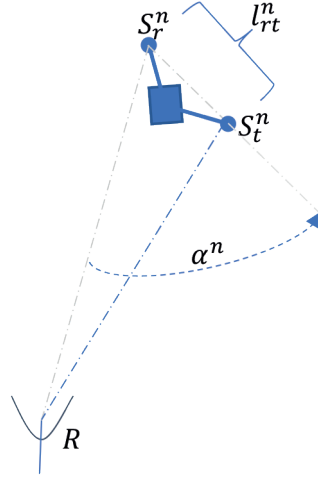
Figure 4-4 | Sketch showing the geometry to calculate the attitude induced delay.

Denoting X_p^k as the position of a point p at epoch k, and δ_{ab} as the media induced excess delay in travelling from point a to point b compared to travelling in vacuum, we can represent $t_{BS_r^n}$ and $t_{S_r^n R}$ as Equations (4-4) and (4-5) respectively, with c as the vacuum velocity of light. The media related delays are a function of the transmission frequency f, positions of the transmitter and receiver, abbreviated by X, and time t.

$$t_{BS_r^n} = \frac{\| X_B^{T_B} - X_{S_r^n}^{T_B + t_{BS_r^n}} \|}{c} + \delta_{BS_r^n}(f, X, t) \tag{4-4}$$

$$t_{S_r^n R} = \frac{\| X_{S_r^n}^{T_B + t_{BS_r^n} + t_{S_r^n S_t^n}} - X_R^{T_R^n} \|}{c} + \delta_{S_r^n R}(f, X, t) \tag{4-5}$$

Note that Equations (4-4) and (4-5) are implicit equations of $t_{BS_r^n}$ and $t_{S_r^n R}$, respectively. These equations are called light-time equations which are typically solved iteratively [11].

Combining Equations (4-3) to (4-5), we get the general expression for T_R^n as

$$T_R^n = T_B + \frac{\| X_B^{T_B} - X_{S_r^n}^{T_B + t_{BS_r^n}} \|}{c} + \frac{\| X_{S_r^n}^{T_B + t_{BS_r^n} + t_{S_r^n S_t^n}} - X_R^{T_R^n} \|}{c} \\ + \delta_{BS_r^n}(f, X, t) + \delta_{S_r^n R}(f, X, t) + \tau_{S_r^n S_t^n}(p_{rt}^n, l_{rt}^n, \alpha^n) + t_{S_i^n}. \tag{4-6}$$

We define the difference in the time of arrival of the signals from S^n and S^0 as $\Delta T_R^{n,o}$ given by,

$$\Delta T_R^{n,o} = T_R^n - T_R^o . \tag{4-7}$$

Defining as the delay due to the difference in the positions of the satellites, as the satellite attitude induced delay due to the finite transmission path between the receiving and transmitting antenna, as the media (non-vacuum) induced transmission delay and as the delay associated with internal latencies of the satellite receiver and transmitter, we arrive at

$$\Delta X^{n,o} = \left(\frac{\| X_B^{T_B} - X_{S_r^n}^{T_B+t_{BS_r^n}} \|}{c} - \frac{\| X_B^{T_B} - X_{S_r^o}^{T_B+t_{BS_r^o}} \|}{c} \right)$$

$$+ \left(\frac{\| X_{S_r^n}^{T_B+t_{BS_r^n}+t_{S_r^n S_t^n}} - X_R^{T_R^n} \|}{c} \right.$$

$$\left. - \frac{\| X_{S_r^o}^{T_B+t_{BS_r^o}+t_{S_r^o S_t^o}} - X_R^{T_R^o} \|}{c} \right) \tag{4-8}$$

$$\Delta M^{n,o} = (\delta_{BS_r^n} - \delta_{BS_r^o}) + (\delta_{S_r^n R} - \delta_{S_r^o R}) \tag{4-9}$$

$$\Delta \Omega^{n,o} = \tau_{S_r^n S_t^n}(p_{rt}^n, l_{rt}^n, \alpha^n) - \tau_{S_r^o S_t^o}(p_{rt}^n, l_{rt}^o, \alpha^o) \tag{4-10}$$

$$\Delta H^{n,o} = t_{S_i^n} - t_{S_i^o} \tag{4-11}$$

And can express $\Delta T_R^{n,o}$ as the sum of four components according to

$$\Delta T_R^{n,o} = \Delta X^{n,o} + \Delta M^{n,o} + \Delta \Omega^{n,o} + \Delta H^{n,o} . \tag{4-12}$$

The variable $\Delta T_R^{n,o}$ is a measure of the phase synchronization with respect to the time of arrival of the data signals at the receiver. It is noted that the data signals have a finite duration and the level of phase synchronization will change with time from the initially established $\Delta T_R^{n,o}$.

4.3.1 Effect and Sensitivity of Geometry on Phase Synchronization

The delay $\Delta X^{n,0}$ due to the differences in the positions of the satellites, is a significant hurdle towards perfect synchronization. If we define $\Lambda^{n,0}$ as the difference in the path length between $BS^n \, R$ and $BS^0 \, R$ shown in Figure 4-1, then $\Delta X^{n,0}$ can be expressed as

$$\Delta X^{n,0} = \frac{\Lambda^{n,0}}{c} . \tag{4-13}$$

Henceforth, we will omit the superscript 0, and arrive at an expression for $\Lambda^{n,0}$ as

$$\Lambda^n = L^n + h^n - d = L^n + \sqrt{d^2 + L^{n^2} - 2dL^n \cos\theta^n} - d \tag{14}$$

where the distance between the beacon B and the receiver R is represented by d. In the limiting case, with Θ^n approaching zero, Λ^n approaches zero. To gain further insight into how the geometry influences Λ^n, the sensitivity of this path length difference to critical parameters that define the geometry is analyzed.

To this end, the sensitivity of the path length difference with respect to the angle θ^n and length L^n, respectively, is derived from Eq (4-14) as

$$\frac{\partial \Lambda^n}{\partial \theta^n} = \frac{d L^n \sin \theta^n}{h^n} \qquad (4\text{-}15)$$

$$\frac{\partial \Lambda^n}{\partial L^n} = 1 + \frac{L^n - d \cos \theta^n}{h^n} \quad . \qquad (4\text{-}16)$$

The sensitivity of the path length difference to the lateral distance r^n can be approximately expressed for small angles of θ^n by

$$\frac{\partial \Lambda^n}{\partial r^n} \approx \frac{d \theta^n}{h^n} \quad . \qquad (4\text{-}17)$$

The distance r^n as shown in Figure 4-1, is the length of the perpendicular from S^n to the line BR. In Figure 4-5, the results from Equations (4-14) and (4-17) are depicted, showing that the approximation (4-17) is accurate to better than 10% for angles up to 25°. Equations (4-15) to (4-17) show a strong dependence of sensitivity on geometry. The sensitivity is minimized for small θ_n and the ratio h^n/d is crucial for the magnitude of the sensitivity.
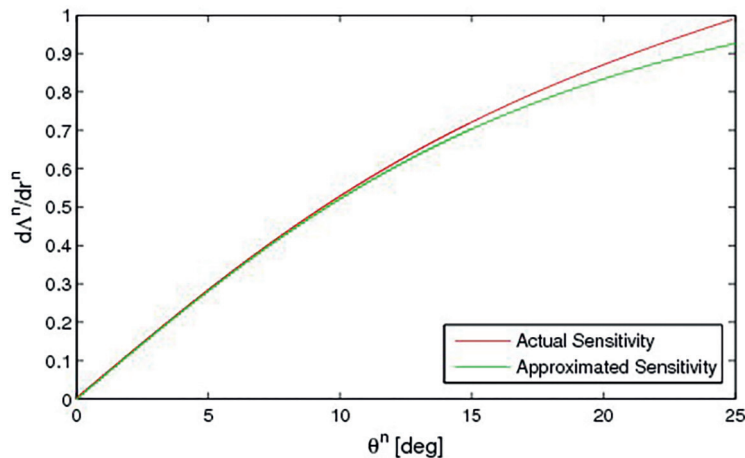
Figure 4-5 | A comparison of the analytically approximated sensitivity of the path length difference Λ^n to the lateral separation r^n against the actual sensitivity (d = 35,786 km)

To further analyze and quantify the sensitivity of the path length difference, a sample scenario of a geostationary satellite serving as an external beacon is used. This corresponds to a minimum distance of 35,786 km between the beacon and the ground-based receiver, when the receiver is

located on the equator at the same longitude as the beacon. An expression for h^n can be developed which is a function of L^n, d, and r^n instead of θ^n as

$$h^n = \sqrt{d^2 + L^{n^2} - 2d\sqrt{L^{n^2} - r^{n^2}}}. \qquad (4\text{-}18)$$

The expression in Eq. (4-14) for the path difference Λ^n, can then be rewritten as

$$\Lambda^n = L^n + \sqrt{d^2 + L^{n^2} - 2d\sqrt{L^{n^2} - r^{n^2}}} - d. \qquad (4\text{-}19)$$

Therefore, with d known, r^n and L^n need to be used onboard satellite S^n to determine Λ^n which can subsequently be compensated. The superscript n will be dropped in further discussions and r, L and h will refer to r^n, L^n and h^n respectively. If the sensitivity of the path difference to r and L is low then even a low accuracy estimate of r and L is sufficient to determine and compensate the path difference. For example, if $d\Lambda^n/dr^n = 0.1$ and L and d are error-free, then the estimation accuracy of the path difference is ten times better than the accuracy with which r can be estimated. If r can be estimated to within 1 m, Λ^n can be estimated to within 10 cm.

Figure 4-6 shows the variation of $d\Lambda^n/dr^n$ for different h^n/d ratios which corresponds to different orbital altitudes of S_n. It can be seen that a geometry with $h/d = 0.5$, corresponding to satellites orbiting midway between the beacon and the receiver, provides the least path difference sensitivity to r. The sensitivity of the path length difference to the length L is shown in Figure 4-7 for different lateral separations. The sensitivity gets extremely low as L approaches close to half the distance between the beacon and the receiver. The sensitivity is also significantly influenced by the lateral separation r, with decreased sensitivity for lower r. The information in Figure 4-6 and Figure 4-7 can be combined to produce a contour plot as shown in Figure 4-8.
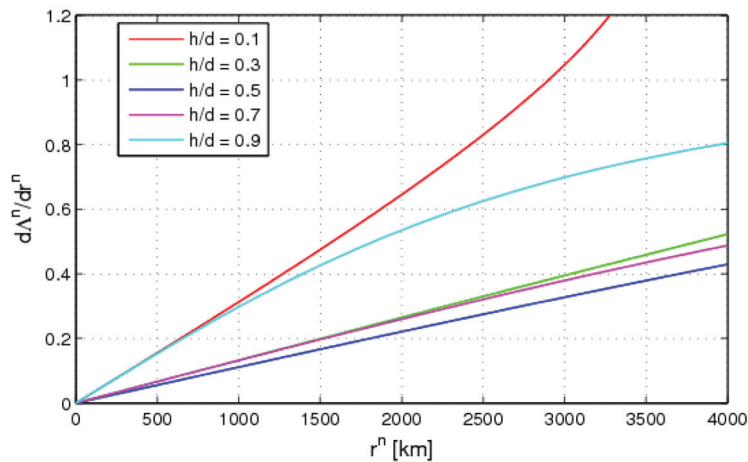

Figure 4-6 | Sensitivity of the path length difference as a function of the lateral separation r^n for different h/d ratios (d = 35,786 km)
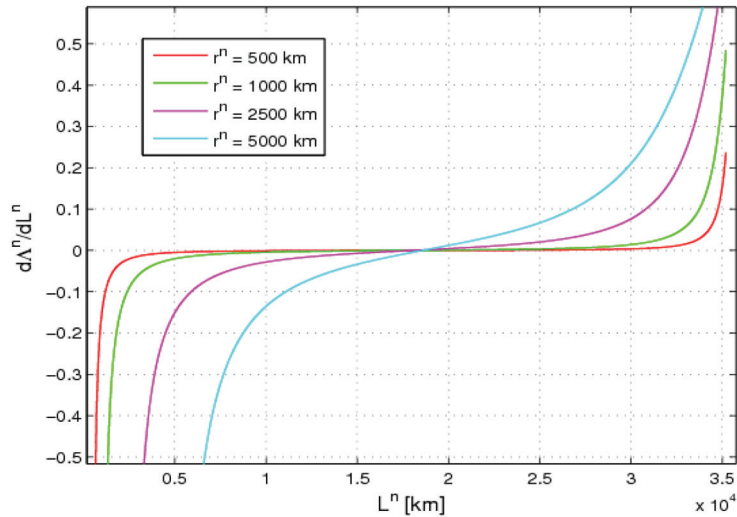
Figure 4-7 | Sensitivity of the path length difference as a function of the distance for different L^n lateral separations r^n (d = 35,786 km)

The black lines correspond to different sensitivity levels of $d\Lambda/dr$, starting from $d\Lambda/dr$ = 0.5 with the outermost line and moving to $d\Lambda/dr$ = 0.1 at the innermost line. The shaded blue and red regions correspond to areas where $d\Lambda/dr$ < 0.01 and $d\Lambda/dr$ < 0.001, respectively. For example, in the shaded red region an error of 1 m in the estimation of L, translates into an error of 1 mm in the path difference. Therefore, these contour lines represent the design space from which the geometric conditions can be chosen based on the required application and technical constraints. As is evident, the sensitivity to the lateral separation is much higher and therefore plays a crucial role in the selection of the geometric parameters. For example, with satellites capable of estimating r within tens of centimeters and L within tens of meters, we can restrict the geometry to lie within the contour line $d\Lambda/dr$ = 0.1, to achieve phase synchronization in the order of centimeters.
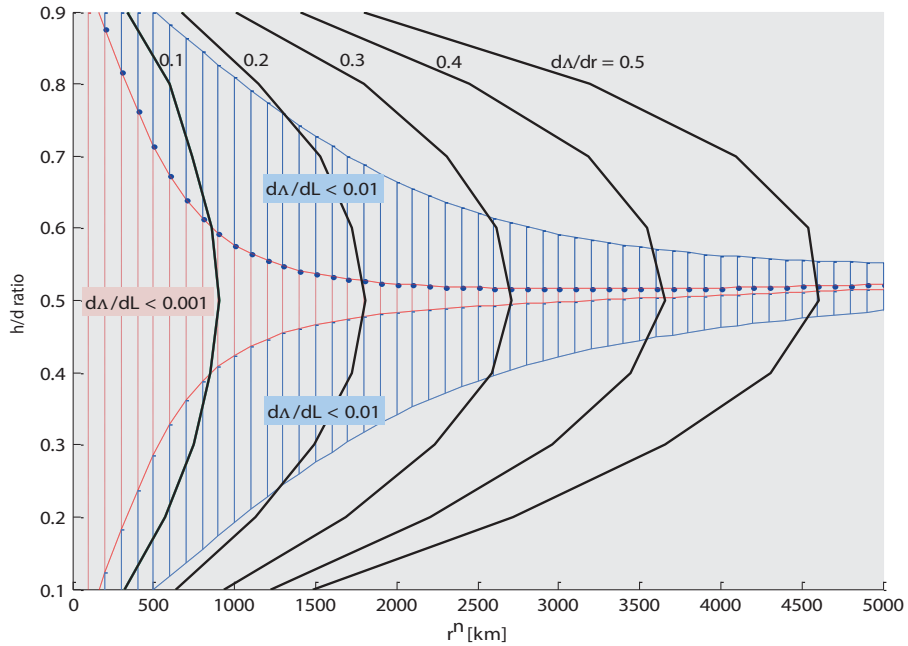
4

Figure 4-8 | Contour plots indicating path difference sensitivity to L^n and r^n as a function of h/d ratio and lateral separation r^n (d = 35,786 km)

In the above scenario, the geostationary altitude of 35,786 km was considered as the distance between the beacon and the receiver. In general, the phase synchronization improves as d increases. The reduced sensitivity Λ of to the relative position of the satellites is the prime advantage of this phase synchronization scheme.

4.3.2 Effect of Spacecraft Attitude on Phase Synchronization

The attitude induced delay component $\Delta\Omega^{n,o}$ of $\Delta T_R^{n,o}$ arises due to the finite transmission path between the receiving and transmitting antennas of the individual satellites as shown in Figure 4-4 and is given as

$$\Delta\Omega^{n,o} = \tau_{S_r^n S_t^n}(l_{rt}^n, \alpha^n) - \tau_{S_r^o S_t^o}(l_{rt}^o, \alpha^o) \,. \tag{4-20}$$

The delay due to the excess path length with respect to the shortest distance between S_r^n and R, $\tau_{S_r^n S_t^n}$ is expressed as

$$\tau_{S_r^n S_t^n}(l_{rt}^n, \alpha^n) = \frac{p_{rt}^n + \sqrt{\|\boldsymbol{S_r^n R}\|^2 + l_{rt}^{n\,2} - 2\|\boldsymbol{S_r^n R}\|\, l_{rt}^n \cos\alpha^n} - \|\boldsymbol{S_r^n R}\|}{c} \,. \tag{4-21}$$

The numerator in the right hand side of Eq. (4-21) is derived in the same lines as the path length difference Λ^n in Eq. (4-14). The approximate errors in phase synchronization from attitude induced

delays are shown in Table 4-1 for different attitude determination accuracies (with respect to the receiver) and different lengths between the receiving and transmitting antennas.

Table 4-1 | Phase synchronization error as function of attitude determination accuracy and distance between receiving and transmitting antennas

$\tau_{S_r^n S_t^n}$	Attitude determination accuracy		
	1^0	5^0	10^0
10 cm	0.015 mm	0.38 mm	1.5 mm
100 cm	0.150 mm	3.80 mm	15 mm

4.3.3 Effects of Media and Internal Latency

Atmospheric media such as troposphere and ionosphere introduce a time delay which is a function of transmission frequency, location and time. This delay can be quite considerable and can be of the order of nanoseconds, equivalent to tens of meters in path difference. However, only the differential delays associated with satellites forming the phased array contribute to errors in synchronization. The frequency of transmission is the same for all the satellites and the time scale is too small for temporal variations in the media to play a significant role. Therefore, the only source of the differential delay is the spatial separation of the satellites which, when considerable, can introduce a significant difference in the delay.

Signal delay models employed in GPS receivers on ground typically model the zenith signal delay above the receiver, and then scale the delay according to the elevation angle of the satellite [12]. For satellites that are relatively close together such that the elevation angles are not significantly different, the difference in the media induced delay will be considerably less. Expressions are available in literature to estimate the vertical or zenith delay. The delay associated with any other arbitrary elevation angle is referred to as slant delay and there are mapping functions that relate the slant delay with the vertical delay. For high elevation angles, a difference of one degree in the elevation angle results in a delay difference of around 0.01% of the atmospheric delay [13]. This corresponds to a sub-centimeter differential delay due to media effects.

The delay associated with internal latencies of the satellite receiver and transmitter will be significantly influenced by design and implementation of hardware and software. The internal latency will be limited by the onboard clock jitter. Chip clocks employ jitter minimization methods to reach jitter levels of picoseconds and even femtoseconds [14,15,16]. A jitter magnitude in the order of picoseconds corresponds to path delays of sub-millimeters.

4

4.4 Performance Summary of Phase Synchronization

The phase synchronization scheme presented employs an external beacon to achieve high levels of phase synchronization under favourable geometry. Four key delay components that affect the achievable accuracy of phase synchronization were identified and analysed. The contributions from these components are listed in Table 4-2 to form an error budget. The delay due to the positional difference is the most critical and also the one that is influenced the most by the geometric parameters. The geometric parameters have to be chosen such that this delay can be maintained within the required limits to achieve the desired phase synchronization. The attitude induced differential delay is very small and one order of magnitude smaller than the delay from the media. Differential delay from media is significant and can be a limiting factor in phase synchronization. The media induced differential delay can be reduced further by employing atmospheric delay models to compensate for the delays. Efficient hardware and software design can ensure that the differential delay from internal latencies is limited by the magnitude of the clock jitter, which can be made very small using jitter minimization techniques.

4.5 Simulation Analysis and Results

The analytical treatment of the proposed phase synchronization strategy in the previous section provides a theoretical assessment of the synchronization accuracy that is possible. In this section, the simulation setup and tools to include all relevant effects to get a realistic estimate of the feasible phase synchronization is developed and its results are discussed and analyzed.

Table 4-2 | Phase synchronization error budget

Delay components	Order of error	Remarks
Positional difference	Variable	Highly dependent on the geometry.
Attitude	< 2 mm	Assuming miniature satellites and a relaxed attitude determination accuracy of 10°.
Media	< 1 cm	Assuming 1° variation in elevation angle at high elevation angles.
Internal latencies	< 1 mm	Same order as the clock jitter of on board chip clocks.

The generic simulation setup to compute the true path length and the estimated length is shown in Figure 4-10. The required configuration for the beacon, satellites and receiver serve as fundamental inputs. The accuracy of the navigation filters can be pre-set to any required value. The main idea is to compare the true time of arrival of a signal at the receiver against the estimated arrival time for a given set of simulation parameters. This translates to the level of phase synchronization that is possible with the chosen simulation parameters. The error in phase synchronization is then computed as

$$\delta\Lambda^n = \|\Lambda^n_{truth} - \Lambda^n_{estimate}\|. \tag{4-22}$$

Table 4-3 | Simulation environment for orbit dynamics

Integration	ODE45 (Matlab®) RelTol 10^{-13}; AbsTol 10^{-6}
Reference system	True of Date
Central body	Earth
Gravity Field	JGM3 up to 20x20
Third body	None
Non-conservative forces	None

Table 4-4 | Simulation parameters and setup

Beacon location	Geostationary orbit	
Receiver location	On ground at Beacon footprint	
Satellites	Number	Variable (up to 50)
	Location	altitude; Reference satellite located on the line connecting Beacon and Receiver.
	Configuration	Train configuration, separated in along-track (≈ 6 km between each pair) on either side of reference satellite
	Size	Maximum distance of 10 cm between transmitting and receiving antenna
h/d ratio	0.42	
Beacon position estimation error	Maximum 1D error	1 m
	Distribution	Uniform with zero mean
Receiver position estimation error	Maximum 1D error	1 cm
	Distribution	Uniform with zero mean
Satellite position estimation error	Maximum 1D error	Variable (10, 20, 30, 50 m)
	Distribution	Uniform with zero mean
Error due to latency	Maximum error	1 mm
	Distribution	Uniform with zero mean
Error due to media effects	Differential Ionospheric and Troposheric delay are estimated as a function of elevation angle (Kaplan and Hegarty 2006).	
Error due to attitude estimation	Maximum error in attitude determination	10° (≡ 1.5 mm)
	Distribution	Uniform with zero mean

The chosen simulation environment and sample configuration for simulation is shown in Table 4-3 and Table 4-4, respectively. The simulation setup allows inclusion of latency, media and attitude

estimation effects. In this section, simulation results based on the simulation configuration in Table 4-4 are presented. Figure 4-9 shows the error in phase synchronization as a function of the lateral separation $\mathbf{r^n}$ for an error of 10 m in the estimated position of the satellite $\mathbf{S^n}$. An error of 10 m implies a 10 m error in the position estimation along each of the 3 principal axis of the Cartesian reference frame. The worst-case path length is identified through a 200-trial Monte-Carlo simulation run. In each trial the errors are varied within their respective intervals. The chosen number of 200 trials provides consistent results over many simulation runs and increasing this number does not capture additional worst case errors.

From Figure 4-9, we see that even with an error of 10 m in the satellite position estimate, at a lateral separation r^n of around 25 km, the phase can be synchronized to within 3 cm.
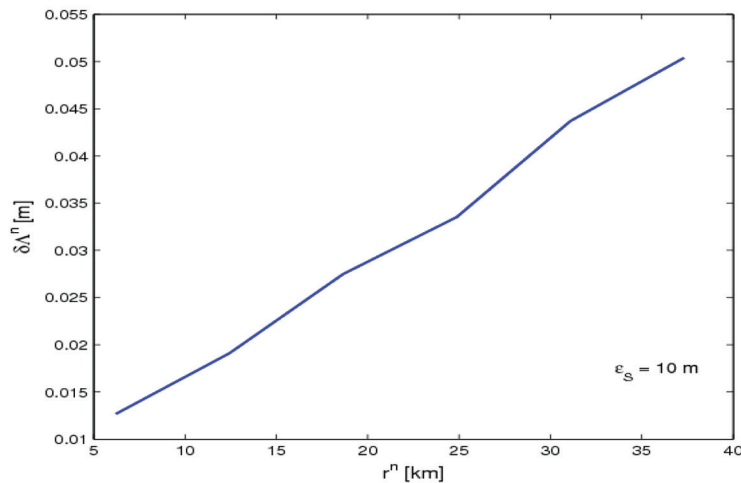

Figure 4-9 | Worst-case error in phase synchronization as a function of the lateral separation for an error of 10 m in the estimated position of the satellite .

The major contribution to the phase synchronization error comes from the uncertainty in the position of the satellites, especially in the lateral separation in the horizontal plane (along-track cross-track plane with respect to the reference spacecraft). The sensitivity of the path length difference to the lateral separation was discussed previously and was shown in Figure 4-6. Zooming in on this figure, we get Figure 4-11, where the sensitivity of the path length difference is shown for a lateral separation of up to 10 km. The h/d ratio of the simulation scenario is 0.42 and the sensitivity $\frac{d\Lambda^n}{dr^n}$ in Figure 4-11 lies between the trend lines of h/d ratio 0.3 and 0.5. As an example, for a lateral separation of 10 km, the $\frac{d\Lambda^n}{dr^n}$ sensitivity is around 0.0012, which translates to an error in path length difference of 0.012 m for an error of 10 m in lateral separation.

Since the error shown in Figure 4-9 incorporates more effects than just the one due to lateral separation, it is higher than 0.012 m. However, it is clearly seen that the major component of the phase synchronization error stems from the uncertainty in estimating the lateral separation.
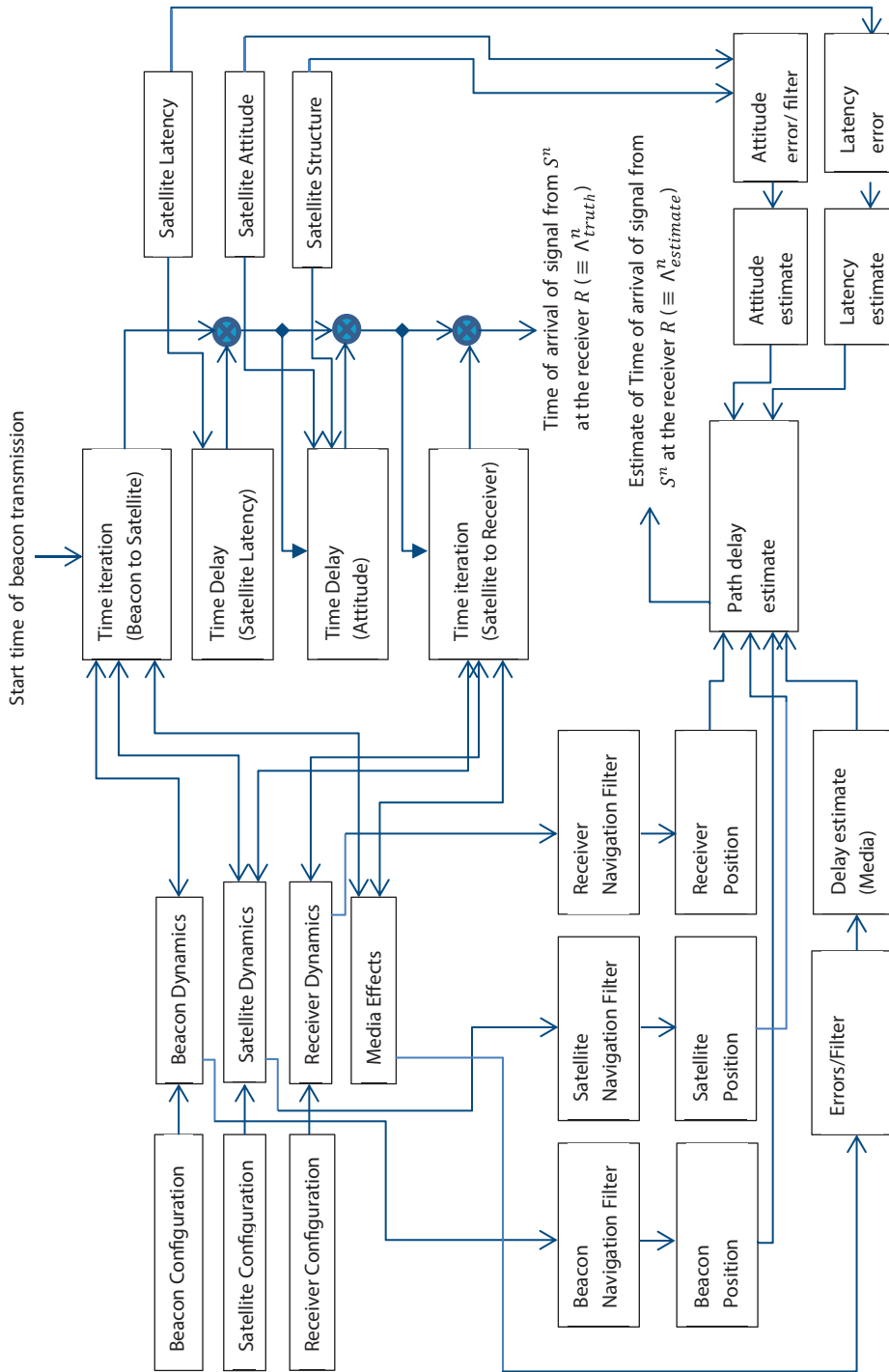
Figure 4-10 | Simulation setup to assess the performance of the beacon based phase synchronization.

The effect of the satellite position estimation error on phase synchronization is further elaborated through Figure 4-12 where the synchronization error is shown for different magnitudes of the satellite position estimation error. As expected, the achievable phase synchronization deteriorates as the error in satellite position estimate increases. The estimation of the total error in phase synchronization due to multiple spacecraft located at different distances from the reference spacecraft is treated in Section 3.4

In recent years, there has been significant progress in the performance of GNSS receivers leading to improved positioning accuracy, and reduced size and power consumption. Commercial GNSS receivers are available that are low-power with a mass of less than 5 g (without antenna), promising an in-orbit position accuracy of less than 10 m [17,18]. ESA has also initiated efforts to develop low-cost and low-profile GNSS antenna that are suitable for small satellite missions [19]. These developments suggest that femto-satellites, in the future, could accommodate systems to provide positioning accuracy in the order of meters. However, the mission requirements and the spacecraft design would strongly drive the budgets and hence determine if such a system could be housed in the spacecraft..
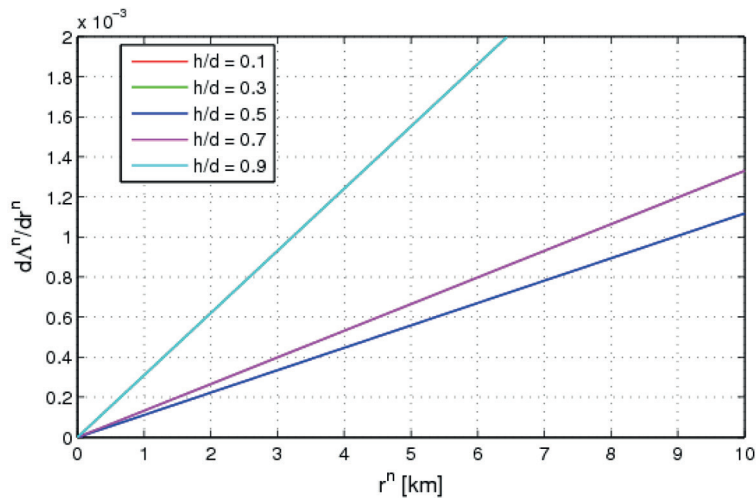

Figure 4-11 | Sensitivity of the path length difference as a function of the lateral separation r^n for different h/d ratios ($d = 35{,}786$ km). The sensitivity for the h/d ratios 0.1 and 0.9 overlap as do the sensitivities for the ratios 0.3 and 0.7
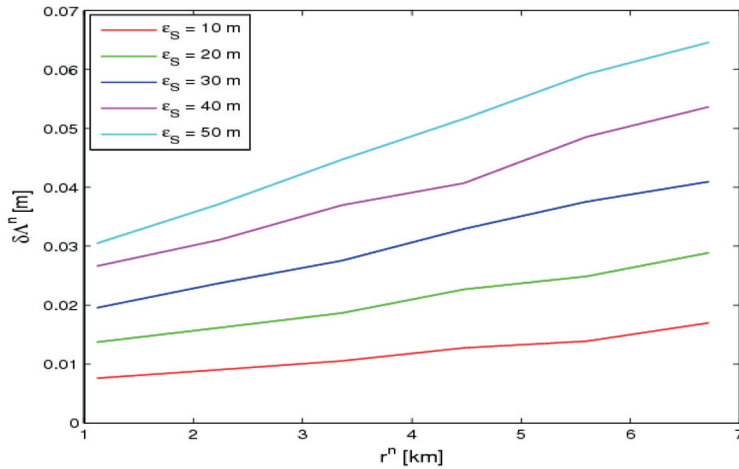
Figure 4-12 | Worst-case error in phase synchronization $\delta \Lambda^n$ as a function of the lateral separation r^n for different error levels in the estimated position of the satellite S^n

4.6 Conclusion

A phase synchronization strategy for distributed space systems has been developed and presented that exploits the favorable geometry created by employing an external beacon. Furthermore, this technique eliminates the need for time synchronization within the distributed space system and the accuracy requirements on relative position estimation are rather relaxed. Depending on the satellite and beacon altitude, the phases of the different transmitters can be synchronized to centimeters (nanoseconds) or even millimeters. It should also be kept in mind that the roles of the receiver and beacon can be interchanged and the satellites can be focused at B or any distant point for transmission or reception through a ground based beacon at R. This increases the range of applications that this strategy may be employed for.

The duration for which the phase synchronization is effective depends on the synchronization accuracy required, the relative dynamics between the satellites and the receiver, and the stability of the satellite clocks. The latency associated with each satellite (from receiving the beacon to transmitting the required signal) is a function of hardware and software implementation. The differences between individual satellite latencies and media induced differential delays will be a crucial factor on the achievable phase synchronization accuracy.

In conclusion, the proposed scheme offers the possibility of phase synchronization to form phased arrays with simplistic resource-limited satellites. Forming such phased arrays using distributed space systems can significantly enhance the link and communication capability of such systems leading to new applications with distributed systems.

4

References

[1]   I. Akildiz, W. Su, Y. Sankarasubramanium and E. Cayirci, "Wireless sensor networks: a survey," *Computer Networks,* pp. vol. 38, no. 4, pp 393-422, 2002.

[2]   I. Thibault, G. Corazza and L. Deambrogio, "Phase synchronization algorithms for distributed beamforming with time varying channels in wireless sensor networks," *7th International Wireless Communications and Mobile Computing Conference (IWCMC),* 2011.

[3]   A. Scaglione and Y.-W. Hong, Opportunistic Large Arrays: Cooperative transmission in Wireless Mutlihop Ad Hoc Networks to Reach Far Distances, IEEE Transactions on Signal Processing, Vol. 51, No. 8, August, 2003.

[4]   Y.-S. Tu and G. Pottie, Coherent cooperative transmission from multiple adjacent antennas to a distant stationary antenna through AWGN channels, Vehicular Technology Conference, 2002. VTC Spring 2002. IEEE 55th, 130 - 134 vol.1, 2002.

[5]   S. Sigg and M. Beigl, Collaborative Transmission in Wireless Sensor Networks by a (1 + 1)-EA, ASWN '08 Proceedings of the 2008 Eighth International Workshop on Applications and Services in Wireless Networks, 2008.

[6]   P. Sundaramoorthy, E. Gill and Verhoeven C., "Enhancing Ground Communication of Distributed Space Systems," vol. 84, 2013.

[7]   J. Elson and D. Estrin, Time Synchronization for Wireless Sensor Networks, 2001 International Parallel and Distributed Processing Symposium (IPDPS), Workshop on Parallel and Distributed Computing Issues in Wireless Networks and Mobile Computing, April 2001, San Francisco, CA, USA, pp. 1965--1970., 2001.

[8]   H. Wang, L. Yip, D. Maniezzo, J. Chen, R. Hudson, J. Elson and K. Yao, A Wireless Time-Synchronized COTS Sensor Platform : Applications to Beamforming, IEEE CAS Workshop on Wireless Communications and Networking, Pasadena, California. September, 2002..

[9]   M. Michelena, L. Arruego, J. Oter and H. Guerrero, "COTS-Based Wireless Magnetic Sensor for Small Satellites," *IEEE Transactions on Aerospace and Electronic Systems,* vol. 46, no. 2, 2010.

[10]   W. Jones, "Chip-scale atomic clock: The ultimate precission - the cessium clock - has been miniaturized," IEEE Spectrum , 16 March 2011. [Online]. Available: https://spectrum.ieee.org/semiconductors/devices/chipscale-atomic-clock. [Accessed 03 08 2018].

[11]   O. Montenbruck and E. Gill, Satellite Orbits - Models, Methods and Applications, Springer, 2000.

[12]   R. N. Thessin, "Atmospheric signal delay affecting GPS measurements made by space vehicles during launch, orbit and reentry," Thesis (S.M.)--Massachusetts Institute of Technology, Dept. of Aeronautics and Astronautics., 2005.

[13]   E. D. Kaplan and C. J. Hegarty, Understanding GPS: Principles And Applications, MA: 2/e, Artech House, 2006..

[14]   R. Farjad-Rad, W. Dally, H.-T. Ng, R. Senthinathan, M.-J. Lee, R. Rathi and J. Poulton, A low-power multiplying DLL for low-jitter multigigahertz clock generation in highly integrated digital chips, IEEE Journal of Solid-State Circuits, vol.37, no.12, pp. 1804- 1812, Dec, 2002..

[15]   Texas Instruments LMK04906, "Datasheet: LMK04906 Ultra Low Noise Clock Jitter Cleaner/Multiplier with 6 Programmable Outputs," [Online]. Available: http://www.ti.com/lit/ds/symlink/lmk04906.pdf. [Accessed 01 12 2012].

[16]   Linear technology, "Ultralow Jitter Clock Generation and Distribution LTC6950," [Online]. Available: www.linear.com/docs/45966. [Accessed 01 03 2015].

[17]   Hyperion Technologies, "Products," [Online]. Available: https://hyperiontechnologies.nl/products/gnss200/. [Accessed 30 10 2018].

[18]   Skytraq, "Products," [Online]. Available: https://www.skytraq.com.tw/homesite/home-product. [Accessed 30 10 2018].

[19]   ESA, "NAVISP - Navigation Innovation and Support Programme," [Online]. Available: https://navisp.esa.int/opportunity/details/32/show. [Accessed 30 10 2018].

Contents

Chapter 5

Conclusions and Recommendations

"We know what we are, but know not what we may be."

— William Shakespeare, Hamlet

People are crazy and times are strange
I'm locked in tight, I'm out of range
I used to care, but things have changed

— Bob Dylan, American singer-songwriter

pana po'o /ˈpɑːnɑː-ˈˌpəʊ-əʊ/
noun scratching your head in order to remember something you have forgotten.
Language: Hawaiian

The objective of this thesis, as outlined in the first chapter, is to advance the research in the field of Distributed Space Systems (DSS) of miniaturzed spacecraft in order to enhance and enable space applications with such systems. In this final chapter, the results of the research carried out during this study are summarised. The section begins with a highlight of key contributions of this study to the body of knowledge to enhance future DSS. The conclusions of this study are subsequently discussed as answers to the research questions that were defined in the introduction chapter. The chapter concludes with recommendations for further research in this area and an outlook on DSS with miniature spacecraft.

5.1 Key Contributions of Thesis

The main research contributions of this thesis are the development of metrics for spatial distribution and collision probability, analysis on the scalability of DSS and demonstration of the feasibility of beamforming with multiple miniature spacecraft. These contributions are discussed below.

a.   Cluster Distribution Index

In a cluster with multiple satellites, it is important to have a measure that is representative of how these entities are distributed within this cluster. The aim is to have a quantitative indicator of the spatial distribution of satellites in such a cluster. This indicator can be used to assess, for example, parameters such as coverage, revisit time or resolution of the DSS. The CDI, proposed and developed in this study, serves as a single parameter to characterize the spatial distribution of a network of spacecraft.

Ths CDI can be used as an effective measure of homogeneity in the spatial distribution of the network. CDI incorporates a dynamically changing envelope as the cluster evolves. This provides an insightful and instantaneous representation of the spatial distribution.

The variations in CDI provide an indication, for example, of the effect of differential drag in along-track separations between spacecraft. High volatility in CDI would correspond to high volatility in parameters such as spacecraft cross-sectional area or attitude control that drive differential drag. Consider the example of a satellite mission for earth imaging where multiple satellites are used to increase a revisit time. A typical mission objective could be to minimize the interval between successive revisits. Instead of monitoring the separation distances between all pairs of satellites, CDI can serve as a single global control variable that can be used to monitor and the revisit time for optimal performance.

In this work the applicability of the CDI has been illustrated with scenarios where a uniform distribution is required. The conformity for other spatial distributions can be analyzed with a small modification to the CDI method. Scenarios to illustrate the usefulness of the CDI can be extended to more dimensions. The GPS constellation is a good example to show the applicability for a 2-D case

and a constellation to monitor, for example, global variations in temperature at different layers of the atmosphere could be used to illustrate the 3-D case.

b. CALM

The number of spacecraft launched has been increasing steadily and a record 214 spacecraft were launched in 2013 alone [1]. In 2017 more than 100 spacecraft were deployed from a single launch [2]. Many space missions involving networks of small satellites have been proposed and initiated by companies such as Planet, Spire, Planetary Resources, GeoOptics and others [3]. Therefore, collisions not only with debris but between spacecraft have become a real and immediate concern. The CALM method, which is significantly faster than traditional methods is an excellent tool during design as well as operations to analyse and mitigate collisions.

The collision probability within a network is an important measure for DSS with a large number of spacecraft. The collision analysis using the line-integral method (CALM) is proposed as a computationally efficient approach for collision analysis. The method for collision analysis has been developed in particular for DSS comprising of small spacecraft that are intended to be launched from a single deployment mechanism or intended to be deployed in similar orbits.

c. Beamforming with resource constrained spacecraft

A high accuracy phase synchronization strategy has been proposed and developed in this thesis that can enable beamforming with a network of simplistic spacecraft. This phase synchronization, by exploiting geometry and employing an external synchronization source, removes the need for high accuracy time synchronization and localization between the individual spacecraft. The proposed scheme offers the possibility of phase synchronization to form phased arrays with simplistic resource limited satellites. Forming such phased arrays can significantly enhance the communication capability of DSS.

The communication capability, either through range or bandwidth or both, can be a limitation for small spacecraft and make them prohibitive for certain mission scenarios. Demonstrating that the individual limitation can be overcome by using multiple spacecraft is the key finding of this study. While the communication aspect was the core focus in this study, techniques to enhance other capabilities need to be investigated to fully enable and enhance DSS with miniature spacecraft.

5.2 Summary and Conclusions

Innovative space missions with miniature spacecraft that can be deployed as distributed systems in space have been considered as potential application scenarios in this thesis. A distributed network of miniaturized systems would ideally combine the advantages of miniaturization and distributed systems to realize an efficient and effective system. There, however, exist, significant gaps and hurdles in achieving this vision. The aim of this thesis was to identify and bridge some of these hurdles. In

an extensive exploration of the problem space, it was clear that certain critical questions needed to be addressed for this synergy to materialize. These were documented as Research Questions (RQ) in Chapter 1. The research questions and the findings from this thesis with respect to these questions are summarised in this section.

RQ1: When is scaling (in spacecraft size and number) beneficial for a DSS?

The conclusions of Chapter 3 provide answers to research questions RQ1. Highly miniaturized spacecraft, such as femto-satellites, are excellent candidates to realise massively distributed systems in space. Scaling rules which use the size of individual satellites and their number in a system are efficient to characterize the performance of highly distributed massively miniaturized space systems. Moreover, scaling trends can help identify optimal size and number of elements in a distributed network.

Until now, the benefit of distributed systems in space has been limited to enhancing coverage, multipoint sensing, creating virtual baselines (e.g. interferometry) or to enhance redundancy. The functionality of a distributed system can be significantly enhanced by exploring non-traditional approaches that leverage on inherent aspects of distributed systems in space. The enhancement of the downlink communication capability of a distributed system of femto-satellites to a ground station was explored. To this end, the benefits of a phased array in space formed by multiple femto-satellites have been studied. It was shown that although an individual satellite may not be able to communicate to the ground station, the phased array enables communication. The challenge of this approach is to achieve phase synchronisation between the satellites which necessitates a stringent time synchronization and localization accuracy requirement in a dynamic environment.

To summarize, a power law formulation has been proposed, where the magnitude of the coefficient indicates the benefit of scaling. Scenarios where scaling is beneficial have been identified and the feasibility of scaling the communication capability has been shown analytically.

RQ2: Are there quantifiable global metrics for a DSS that can aid in mission design and analysis? How can such metrics be defined, developed and used?

The work in Chapter 2 addresses RQ2. The conclusions are summarised here. A Distributed Space System (DSS) is an architecture with more than one spacecraft to achieve a common objective. A number of questions arise with respect to the characteristics and dynamics of distributed system in space. How fast is the system spreading? What is its size? How are the elements within the system distributed? Is it tightly or loosely packed? What is the effect of orbital perturbations on its absolute and relative dynamics? Perhaps more questions arise, depending on the specific mission scenario. One main contribution in this thesis is the definition and development of quantitative metrics that allow the spatial characterization of DSS.

Two distinct metrics to characterize a DSS have been developed and discussed – a cluster distribution index (CDI) and a cluster collision probability (CCP) measure. The CDI is a measure of the

how uniform the DSS is spatially distributed and the CCP provides an indication on the probability of collisions within the network. An n-dimensional grid-based numerical approach was developed to evaluate CDI. Furthermore, a collision analysis techniques that uses line-integrals instead of volume integrals was proposed as an effective and efficient approach to analyse collision probability within DSS. These two metrics have been derived and both metrics can be used either as an optimization variable in the mission design process for a DSS or as a control variable during operations. The CDI is an effective measure of spatial distribution within the network. The collision probability within a network is an important measure for DSS with a large number of spacecraft. The simplified Collision Analysis using Line-Integral method (CALM) is computationally much less intensive than other methods used for collision analysis. The validity of the method is assessed by comparing results with existing non-linear methods and the results match with an approximation better than one percent and the CALM approach has a significantly lower computational load. The method for collision analysis has been developed in particular for DSS comprising of small spacecraft that are intended to be separated from a single deployment mechanism.

The CDI or CCP could be introduced at the design phase as an optimization variable through a cost function that needs to be maximised. For example, a cost function which is proportional to $CDI_{mission}$ /Mp, where, Mp is the mass of the propellant needed for station keeping and $CDI_{mission}$ is the averaged CDI for entire mission duration, could be a useful function to maximize for a swarm of satellites. This would ensure an optimal uniform distribution of the spacecrafts in the network, keeping the propellant requirements under check. In station keeping during the operational phase, similar to maintaining the position of a satellite within a designated window for single satellites, station keeping for DSS could be centered, for example, on keeping the CDI and CCP within the required bounds.

RQ3: How can beamforming be achieved with highly resource constrained miniature spacecraft?
The phase synchronization strategy developed and discussed in Chapter 4 answers RQ3. A phase synchronization strategy for distributed space systems has been developed and presented that exploits the favourable geometry created by employing an external beacon. Furthermore, this technique eliminates the need for time synchronization within the distributed space system and the accuracy requirements on relative position estimation are rather relaxed. Depending on the satellite and beacon altitude, the phases of the different transmitters can be synchronized to centimetres (nanoseconds) or even millimetres.

The duration for which the phase synchronization is effective depends on the synchronization accuracy required, the relative dynamics between the satellites and the receiver, and the stability of the satellite clocks. The latency associated with each satellite (from receiving the beacon to transmitting the required signal) is a function of hardware and software implementation. The differences between individual satellite latencies and media induced differential delays will be a crucial factor on the achievable phase synchronization accuracy. In conclusion, the proposed scheme offers the possibility of phase synchronization to form phased arrays with simplistic resource-limited

satellites. Forming such phased arrays using distributed space systems can significantly enhance the link and communication capability of such systems leading to new applications with distributed systems.

5.3 Recommendations for Future Research

A summary of the contributions of this thesis in advancing DSS with miniature spacecraft has been presented in the previous section. In this section, key recommendations are proposed that can further strengthen the research in this field.

5.3.1 Collision Analysis

A collision analysis method was presented for objects with non-linear relative motion as is the case with spacecraft that are, for example, deployed together. In such cases, the time that the objects spend in the encounter region is considerable and assumptions for linear motion are not valid. Furthermore, a simplified Collision Analysis using Line-Integral method (CALM) was developed that greatly reduces the computational load.

Terrestrial scenarios also involve objects such as drones and automated cars that exhibit non-linear relative motion. Therefore, CALM can be modified to be applied for terrestrial distributed systems. Collision analysis between drones or micro-air vehicles in a warehouse would be a typical scenario where CALM could contribute for terrestrial applications. Efficiently porting the drone dynamics into the algorithm would be a very interesting topic for spin-off research.

5.3.2 Distribution index

The current set of tools developed to evaluate the CDI allows the assessment of the spatial deviation of a distributed space system from a uniform distribution in three-dimensional space. The software allows custom weighting of the different dimensions and the evaluation is based on a continuously changing envelope to capture the instantaneous spatial separations.

However, the total number of grids is constrained by the total number of spacecraft. This poses a limit on the resolution of the discrepancy measure and becomes apparent when the number of spacecraft is not large.

This can be overcome by introducing dummy spacecraft and artificially increasing the number of grids retaining the same envelope and boundaries. Then, the lower limit of CDI increases but the sensitivity to small separations increases. A similar approach can also be used to investigate scenarios where discrepancy with respect to non-uniform distributions need to be assessed.

5.3.3 Combined index for DSS

Two metrics, a measure for collision probability and a Cluster Distribution Index have been defined and developed in this thesis to characterize DSS. The Cluster Distribution Index (CDI) measures the instantaneous uniformity of the spatial distribution of the spacecraft within the cluster. The simplified Collision Analysis using Line Integral (CALM) method provides a computationally efficient means to assess the collision probability within the DSS.

Intuitively, it would appear that the collision probability and CDI are correlated. Further investigation is, however, required to establish a quantitative link between the two. A combined index which is a function of collision probability and CDI might be derived which could very well be a single performance indicator for a DSS.

5.3.4 Phase synchronization constraints

The proposed novel technique for phase synchronization achieves a remarkably high level of synchronization without accurate clocks. However, this synchronization is instantaneous and lasts only for a finite period of time. Methods for on-board short arc orbit prediction need to be investigated and applied to sustain this phase synchronization for a longer period of time.

5.3.5 Enhancing other capabilities

This thesis has mainly explored the enhancement of the communication capability of distributed system with miniature spacecraft. It would be interesting to explore further aspects where synergy could be demonstrated between the entities of a distributed space system.

5.4 Outlook

Over the years, the application potential of DSS has been showcased through space missions such as GPS, GLONASS and Iridium and the A-train where a number of high performing spacecraft work together to enable applications in diverse areas such as navigation, communication and Earth observation.

Planet, Skybox and Spire are examples of private start-ups entering the domain of satellite missions with multiple spacecraft. These companies have shown the commercial interest and proven the business case for space-based applications. The QB50 [4] and OLFAR [5] missions show the science potential of DSS with CubeSats. The Laser Interferometer Space Antenna (LISA) is an ESA project to detect gravity waves. LISA detects gravitational-wave-induced strains in space-time by measuring changes of the separation between three spacecraft 5 million kilometres apart [6]. Darwin was proposed as a four or five spacecraft constellation designed to search for Earth-like planets around other stars. The constellation was proposed to carry out high-resolution imaging of celestial objects with unprecedented detail using aperture synthesis [7]. The LISA and DARWIN mission show the

5

high science return that DSS can provide, which cannot be matched by single satellite missions. The above and more DSS missions clearly indicate the interest and potential of multi-satellite space missions. Figure 5-1 shows small satellite launches and projected launches. The number of multi-satellite missions is definitely on the rise and expected to increase even further.

Furthermore, most of the distributed missions being proposed are based on traditional DSS architectures such as constellation and formation flying. Table 5-1 provides a selected list of space companies in the current DSS landscape. The applications, launched and planned constellation numbers are provided along with the funding that has been secured. It is also interesting to note that most of these constellations involve a CubeSat configuration with a form factor ranging from 3U to 16U. There is significant research being done in swarm based architectures and fractionated systems to advance these concepts. Swarms are likely to involve a massive number of individual entities and fractionated systems will require continuous geometry control. The possibilities and potential of DSS will further increase when new architectures like swarm and fractionated systems are explored. The significance of collision analysis and characterizing DSS, addressed in this thesis, become even more pertinent in such missions.
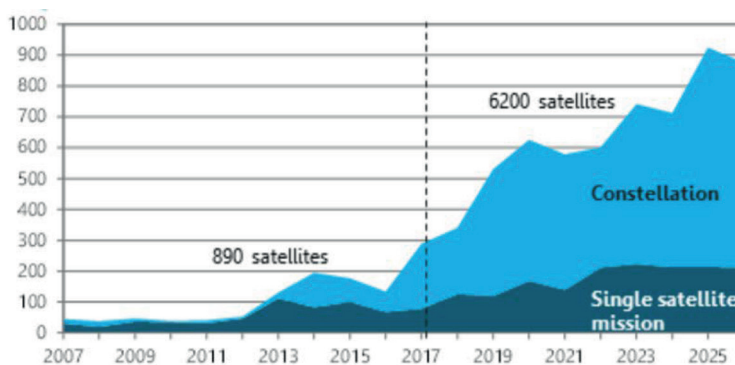

Figure 5-1 | Small satellite (< 500 kg) launches and projected launches [8]

In the terrestrial industry, the capability to size ratio has been improving consistently in the last decades, thereby allowing smaller systems with high performance. Progress, matching the Moore's law, in the semi-conductor industry and high levels of integration has enabled these high performing low form-factor components and systems. With spin-in of commercial technology, spacecraft can now enjoy low-cost, high performance miniature components and systems. Therefore, current miniature spacecraft can be equipped with adequate functionalities.

The true potential of miniature spacecraft will, however, lie in its application. Applications that benefit from innovative use of simplistic spacecraft or a network of simplistic spacecraft need to be identified. Although there will be niche applications with individual single miniature spacecraft, its true potential is envisioned through DSS.

Table 5-1 | List of organizations and their planned constellations. Selected and adapted from [3]

Organization	Launched / Planned Size	First Launch	Form Factor	Field	Funding
Planet	322/150+	2013	3U	Earth Observation	$183 million
Spire	71/100+	2013	3U	Weather/AIS/ADS-B	$149.5
Planetary Resources	2/10	2014	12U	Earth Observation	$50+ million
Astro Digital (Aquila)	4/10+	2014	6U/16U	Earth Observation	$16.7+ million
Sky and Space Global	3/200	2017	3U	IoT/M2M/Voice	$11.5 million
GeoOptics	4/6	2017	6U	Weather	$5.15 million

Advantages of miniaturized systems, in some cases, could be offset by the effort required to pack everything in a small volume. Moreover, at the extreme, where high integration is required, the advantages of modularization and standardization cannot be leveraged. This is the case in space as well as in terrestrial industry. In terrestrial applications, when it comes to integrated systems and solutions, mass production was seen as the only solution for low unit cost. An example of disruptive innovation in this paradigm, for terrestrial technologies, was 3D-printing which offered low-cost customized prototypes. Spin-in of such technology and thought process is essential in realizing efficient space missions with miniature spacecraft.

With increasing maturity levels of innovative DSS architectures like swarm on the one hand and rapid progress in performance density and prototyping of miniature spacecraft on the other, the fusion of these two domains to realize disruptive space applications is all but inevitable.

5

References

[1]   C. Lafleur, "Table of Spacecrafts Launched in 2013," 15 01 2014. [Online]. Available: http://claudelafleur.qc.ca/Spacecrafts-Table-2013.html.

[2]   ISRO, Feb 2017. [Online]. Available: https://www.isro.gov.in/update/15-feb-2017/pslv-c37-successfully-launches-104-satellites-single-flight. [Accessed 15 10 2017].

[3]   "Nanosatellite Database by Erik," [Online]. Available: http://nanosats.eu/index.html#figures. [Accessed 01 09 2017].

[4]   QB50. 05 02 2015. [Online]. Available: https://www.qb50.eu/index.php/project-description-obj.

[5]   S. Engelen, K. Quillen, C. Verhoeven, A. Noroozi, P. Sundaramoorthy, A. van der Veen, R. Rajan, A. Boonstra, M. Bentum, A. Meijerink and A. Budianu, "The Road to OLFAR - A Roadmap to Interferometric Long-Wavelength Radio Astronomy using Miniaturized Distributed Space Systems," in *64th International Astronautical Congress*, Beijing, China, 2013.

[6]   LISA. [Online]. Available: http://lisa.nasa.gov/ [Accessed 10 07 2015].

[7]   Darwin. [Online]. Available: http://www.esa.int/Our_Activities/Space_Science/Darwin_overview [Accessed 10 07 2015].

[8]   Euroconsult, "PROSPECTS FOR THE SMALL SATELLITE MARKET - Brochure," 2017.

Curriculum Vitae

Prem Sundaramoorthy was born on the 7th of August 1979 in Chennai, India. He did his schooling at Baldwin Boys' High School, Bangalore and his pre-university studies at Dr. Ambedkar College, Bangalore. In 1997, Prem enrolled in the Engineering program at M.S. Ramaiah Institute of Technology, Bangalore and received his undergraduate diploma in Telecommunication Engineering in 2001. Following this, Prem started as a Graduate Engineer Trainee working on network installations at Tata Teleservices Limited for a brief period before joining the Defence Research and Development Organization (DRDO), Government of India, as Scientist 'B' in 2002. During his term at DRDO, Prem was deputed at the Aeronautical Development Establishment in the Unmanned Air Vehicles (UAV) Systems Group, responsible for system integration and development of automated test equipment for UAVs.

In 2005, Prem enrolled for the MSc program at the Aerospace Engineering Faculty of TU Delft and received his MSc degree in 2007, specializing in Astrodynamics and Satellite Systems. His MSc. thesis was titled "Constellation control for the low-flying Swarm satellites". In 2008, Prem started pursuing research in the area of miniature spacecraft design through an employment as a PhD candidate at TU Delft. It was a collaborative project between the Microelectronics Department at the faculty of Electrical Engineering, Mathematics and Computer Science and the Space Systems Engineering Department at the Faculty of Aerospace Engineering.

From 2012 till 2018, Prem worked as a lecturer and researcher at the Space Systems Engineering group at the Faculty of Aerospace Engineering at TU Delft. Here, Prem developed, coordinated and conducted various courses and projects at the graduate and undergraduate level. He has also been the primary supervisor for many MSc theses. He has been involved in the in-house satellite projects Delfi-c3 and Delfi-n3xt at various stages. Prem has also participated and contributed to European and international research proposals and projects.

Between 2012 and 2017, Prem has also been actively involved in entrepreneurial activities. He co-founded Elpasys in 2012 to design and build innovative mobile applications. ElpaNav B.V., a company with a focus to develop and deliver high-accuracy real-time indoor localization and navigation systems, was co-founded by Prem in 2015.

At present, Prem is an Adjunct Professor at the University of Bologna, responsible for a graduate level course on Spacecraft Subsystems and Space Mission Design. He also delivers lectures on general systems engineering at the Faculty of Electrical Engineering, Mathematics and Computer Science at TU Delft. His research interests include systems engineering for small satellites, distributed space systems and space mission design.

Publications

Journals

Sundaramoorthy, P., Florijn, D., Gill, E., & Verhoeven, C. *A Spatial Distribution Measure and Collision Analysis Technique for Distributed Space Systems.* Acta Astronautica (In Press. Corrected Proof. Available online 3 May 2016).

Sundaramoorthy, P., Gill, E., & Verhoeven, C. *Beamforming with Spacecraft under Reduced Localization and Clock Constraints.* IEEE Transaction on Aersopace and Electronic Systems 52 (3) 1197-1209.

Sundaramoorthy, P., Gill, E., & Verhoeven C. (2013). *Enhancing Ground Communication of Distributed Space Systems.* Acta Astronautica, Vol 84.

Sundaramoorthy, P., Gill, E., & Verhoeven, C. (2010). *Relative Orbital Evolution of a Cluster of Femto-satellites in Low Earth Orbit.* Spaceflight Mechanics - Advances in the Astronautical Sciences, 136.

Gill, E., **Sundaramoorthy, P.,** Bouwmeester, J., Zandbergen, B., Reinhard, R. (2013). *Formation flying within a constellation of nano-satellites: The QB50 mission.* Acta Astronautica Vol 82.

Buist, P. J., Engelen, S., Noroozi, A., **Sundaramoorthy, P.,** Verhagen, S., & Verhoeven, C. (2011). *Overview of Pulsar Navigation: Past, Present and Future Trends.* Navigation, 58(2), 153-164.

Relevant Conferences

Sundaramoorthy, P., Gill, E., Verhoeven, C., Reinhard, R., Asma, C. **(2010).** *Preliminary Orbit and Mission Analysis of the QB50 Satellite Cluster.* 4th International Conference on Astrodynamics Tools and Techniques 3-6 May 2010, ESAC, Madrid, Spain

Sundaramoorthy, P., Gill, E., Verhoeven, C., Bouwmeester, J. **(2010).** *Two CubeSats with Micro-Propulsion in the QB50 Satellite Network.* 24th Annual Conference on Small Satellites, Logan, Utah, USA.

Sundaramoorthy, P., Verhoeven, C. **(2010).** *Systematic Identification of Applications for a Cluster of Femto-satellites.* 61st International Astronautical Congress, Prague, Czech Republic

Bouwmeester, J., Gill, E., **Sundaramoorthy, P.,** Kuiper, H. **(2011).** *Concept study of a LEO constellation of nanosatellites for near real time optical remote sensing.* Proceedings 62nd International Astronautical Congress (pp. 1-9). Cape Town, South Africa: IAF.

Engelen, S., Quillien, K., Verhoeven, C., Noroozi, A., **Sundaramoorthy, P.**, van der Veen, A., Rajan, R., Boonstra, A, Bentum, M., Meijerink, A., Budianu, A. (**2013**). *The road to OLFAR-a roadmap to interferometric long-wavelength radio astronomy using miniaturized distributed space systems.* Proceedings of the 64th International Astronautical Congress, Beijing, China.

Verhoeven, C., Engelen, S., Noroozi, A., **Sundaramoorthy, P.**, Bentum, M., Meijer, R. (**2011**). *Emerging Eco-system: Nano-satellite Swarms and Large Satellites.* Proceedings of the 62nd International Astronautical Congress, IAC 2011, Cape Town, Republic of South Africa.

Florijn, D., **Sundaramoorthy, P.** (**2014**). *Collisions Probabilities and Mitigation Strategies of the QB50 Network.* Proceedings of the 65th International Astronautical Congress, IAC 2014, Toronto, Canada.

Sundaramoorthy, P., Cervone, A. (**2013**). *How Can a Group of 3rd Year University Students Design a Nano-Satellite?* A Case Study at Delft University of Technology. In s.n. (Ed.), Proceedings of the 64th International Astronautical Congress (pp. 1-12). Beijing, China: IAF.

Angadi, C, **Sundaramoorthy, P.** (**2012**). *Femto-Satellite System Architecture for LEO Applications.* Proceedings of the 63rd International Astronautical Congress, IAC 2012, Naples, Italy.

Angadi, C.1, Chaimori, H., **Sundaramoorthy, P.**, Bhattacharya, S., Senesky, D.G. (**2013**). *Characterization of Wide Bandgap Microsystems Components for Nano, Pico & Femto-Satellite Applications.* Proceedings of the 64th International Astronautical Congress (IAC 2013), Beijing, China.

Speretta, Stefano & Perez Soriano, Tatiana & Bouwmeester, Jasper & Carvajal-Godínez, Johan & Menicucci, Alessandra & Watts, Trevor & **Sundaramoorthy, Prem** & Guo, Jian & Gill, Eberhard (**2016**). *CubeSats to PocketQubes: Opportunities and Challenges.* Proceedings of the 67th International Astronautical Congress (IAC): Guadalajara, Mexico

Verwilligen, J., & **Sundaramoorthy, P.** (**2013**). A Novel Planar Antenna for CubeSats. In Pre-Conference CubeSat Developers' Workshop. [SSC16-WK-08]